

ABRASION ASSISTED
WIRE ELECTRICAL DISCHARGE MACHINING

ABRASION ASSISTED
WIRE ELECTRICAL DISCHARGE MACHINING

MASTER OF APPLIED SCIENCE
Department of Mechanical Engineering
McMaster University
Hamilton, Ontario

By

TITLE: Abrasion Assisted Wire Electrical Discharge Machining
AUTHOR: Ian T. Menzies, B.Eng. (McMaster University)
SUPERVISOR: Dr. Philip Koshy
NUMBER OF PAGES: 126

A Thesis
Submitted to the School of Graduate Studies
in Partial Fulfillment of the Requirements
for the Degree
Master of Applied Science

MASTER OF APPLIED SCIENCE (2007)
(Department of Mechanical Engineering)

McMaster University
Hamilton, Ontario

TITLE: Abrasion Assisted Wire Electrical Discharge Machining
AUTHOR: Ian T. Menzies, B.Eng. (McMaster University)
SUPERVISOR: Dr. Philip Koshy
NUMBER OF PAGES: xiii, 126

Abstract

The adoption of Electrical Discharge Machining (EDM) technologies to mainstream manufacturing saw dramatic advances in the process starting in the 1980's. Wire Electrical Discharge Machining (WEDM) in particular achieved enhancements in cutting speed of over 800% between 1980 and 1992 due to improvements in generator and wire technology. Since then, increases in cutting speed have been gradual. To achieve dramatic improvements to the process once again, a paradigm shift, from improving upon existing technologies to introducing and developing new ones is required.

In this light, an investigation into the proof-of-concept and development of a novel hybrid machining process based upon Wire Electrical Discharge Machining (WEDM) and abrasive technologies is presented. In the process termed Abrasive Wire Electrical Discharge Machining (AWEDM), material removal is shown to occur by the simultaneous action of electrical erosion and abrasion. Through experimental evaluation, this combination is shown to bring about a manyfold improvement in the material removal rate and to generate machined surfaces with minimal recast layer, in comparison to conventional WEDM processes.

To understand the operation of the process and to control the proportion of abrasion and EDM taking place, the effect of varying the process conditions is studied. The servo-reference voltage and peak discharge current, in particular, provide effective means to control the process.

Practical implementation of the process presents several challenges, such as accurately guiding an abrasive wire; a discussion of some of these issues and possible solutions is included. The need for a wire that is specially suited to AWEDM is demonstrated with a discussion of the requirements and possible designs for such a wire.

Whether or not a manufacturing process sees practical industrial use is chiefly dictated by economics. By considering the increase in both productivity and wire cost, AWEDM is shown to be economically feasible and offer potentially substantial benefits.

This work ultimately serves as the basis for future work with respect to AWEDM. The work herein covers a broad range of topics in hopes of guiding future areas of research.

Acknowledgments

The author would like to take a moment to recognize all of the people who have in one form or another aided in making this work possible.

I would first like to thank my supervisor, Dr. Philip Koshy, who has been a mentor for me since having him as a professor in a second year undergraduate Mechanics course. He has provided countless hours of support, whether it be discussing projects over a coffee, playing squash or helping me to establish my future career goals. I am indebted.

Second, I would like to acknowledge all of my friends and family, who have been there to both help with my project when needed, as well as to have a beer when trying to forget about work altogether. Thanks to the members of our research group, who are always insightful and fun to talk with. Thanks to the GSA league softball and all my teammates, who made the summers exciting and entertaining. Thanks to all of you, who have made my stay at McMaster an enjoyable and memorable one.

Thanks to Thomas Puthanangady and his colleagues from Saint-Gobain Abrasives for their support and generous donation of materials used in this work.

Finally, I would like to acknowledge the McMaster faculty and staff who too provided invaluable support along the way. Special thanks to Dave Schick, Ron Lodewyks, Jim McLaren, Warren Reynolds, Mark McKenzie, Doug Culley and Steve Koprach who's technical support and patience in the machine shops, materials sample preparation lab or SEM lab enabled much of this work.

*Dedicated to my friends and family who have supported me
throughout my life and made this possible.*

Table of Contents

Abstract	iii
Acknowledgments	v
List of Figures	x
List of Tables	xiii
Chapter 1 Introduction	1
1.1 The Constituent Processes.....	2
1.1.1 Electrical Discharge Machining.....	2
1.1.2 Wire Electrical Discharge Machining.....	4
1.1.3 Abrasive Wire Saw Machining.....	6
1.2 Hybrid Machining Processes.....	7
1.3 Abrasive Wire Electrical Discharge Machining.....	9
1.3.1 Why use AWEDM?.....	10
1.3.2 Implementation.....	11
1.4 Scope and Organization of Present Work.....	12
Chapter 2 Literature Review	14
2.1 Electrical Discharge Machining.....	14
2.1.1 Process Fundamentals.....	14
2.1.2 Process Control.....	15
2.1.3 Recast Layer Formation.....	16
2.1.4 Developments in WEDM.....	19
2.2 Abrasive Wire Saw Machining.....	20
2.2.1 Wire Saw Technology.....	20
2.2.2 Free Abrasive Wire-Saw Machining.....	22
2.2.3 Fixed Abrasive Grain Wire-Sawing.....	24
2.3 Hybrid Machining Processes.....	28
2.3.1 Hybrid EDM Processes.....	29

Chapter 3	Experimental Details	42
3.1	Experimental Apparatus.....	42
3.2	Experimental Procedure.....	45
3.2.1	Machine Characterization and Process Modeling.....	45
3.2.2	Abrasion Assisted WEDM Testing.....	48
3.3	Other Procedural Techniques	52
3.3.1	Diamond Wire Characterization	52
3.3.2	Sample Preparation.....	54
3.3.3	Measurement of the Recast Layer.....	55
3.3.4	Debris Collection and Surface Examination.....	55
Chapter 4	Results and Discussion	57
4.1	Experimental Assessment of the Conventional WEDM Process.....	58
4.1.1	Linear Modeling	58
4.1.2	Expanded Analysis.....	60
4.1.3	Modeling of the material removal rates	61
4.1.4	Modeling of the Machining Gap.....	64
4.1.5	Modeling of the Recast Layer Thickness.....	67
4.1.6	Discussion of Model Results	69
4.1.7	The Effect of the open circuit voltage.....	70
4.2	Characterization of Fixed Abrasive Wire.....	72
4.2.1	SEM Inspection of the Diamond Wire	72
4.2.2	White Light Interferometry of the Wire Surface	76
4.3	Preliminary Testing and Process Refinement.....	79
4.3.1	Wire Effectiveness after Repeated Usage.....	79
4.3.2	Preliminary Testing.....	81
4.3.3	Wire Breakage Analysis.....	82
4.3.4	Process Refinement	83

4.4	Results from Abrasive Wire EDM Testing	85
4.4.1	Effect of Varying the Abrasive Engagement.....	86
4.4.2	Forces in the AWEDM Process	94
4.4.3	Recast Layer Formation.....	98
4.4.4	Current and Voltage Waveform Analysis.....	102
4.5	Related Discussion	104
4.5.1	Mechanism for the Increase of material removal rates in AWEDM.....	104
4.5.2	Economic Feasibility	109
 Chapter 5 Conclusions and Future Work		113
5.1	Conclusions.....	113
5.2	Future Work	115
5.2.1	Practical Implementation.....	115
5.2.2	Areas for Future Research.....	118
 References		120

List of Figures

Figure 1.1:	Schematic of Die-Sinking EDM.....	2
Figure 1.2:	Schematic voltage and current waveforms in EDM.....	3
Figure 1.3:	Schematic of WEDM.....	4
Figure 1.4:	Example of a single spark discharge crater and recast layer in EDM.....	5
Figure 1.5:	Schematic of abrasive wire sawing.....	6
Figure 1.6:	SEM micrograph of fixed abrasive wire.....	7
Figure 1.7:	Process condition scheme for hybrid machining.....	8
Figure 1.8:	Abrasive Wire EDM schematic.....	9
Figure 1.9:	Trends in WEDM.....	10
Figure 1.10:	Schematic of the abrasive protrusion and gap width in AWEDM.....	11
Figure 2.1:	Schematic of the servo-controlled feed system in EDM.....	16
Figure 2.2:	Defects in the recast layer of EDM.....	17
Figure 2.3:	Micrograph showing columnar and dendrite structures in the recast layer.....	18
Figure 2.4:	Micrograph of the material structures in the recast layer.....	18
Figure 2.5:	Schematic illustration of the WEDG process.....	19
Figure 2.6:	Schematic of multi-wire sawing.....	22
Figure 2.7:	Schematic illustrating three-body abrasion.....	23
Figure 2.8:	Schematic of the abrasive wire manufacturing process.....	25
Figure 2.9:	Schematic of EDM-USV.....	30
Figure 2.10:	MMR comparison with EDM, EDMUS.....	31
Figure 2.11:	Schematic of the AEDG process.....	33
Figure 2.12:	Time evolution of normal force in AEDG.....	34
Figure 2.13:	Effect of wheel speed and current on MRR in AEDG.....	35
Figure 2.14:	Effect of time on MRR in machining PCD by AEDG and Grinding.....	36
Figure 2.15:	Micrographs of chips collected from AEDG.....	37
Figure 2.16:	Micrographs of AEDG machined surfaces.....	38

Figure 2.17:	Schematic of the relationship between gap and abrasive size.....	39
Figure 2.18:	Schematic of combined Sawing - WEDM process.....	41
Figure 3.1:	Agietron Impact 2 EDM system.....	42
Figure 3.2:	3-D rendering of the wire-feed apparatus	44
Figure 3.3:	Illustration of DOE with three parameters.....	47
Figure 3.4:	Geometric interpretation of the cutting force calculation.....	51
Figure 3.5:	3-D optical images of fixed abrasive wire after gold sputtering.....	53
Figure 3.6:	3-D surface map of abrasive wire obtained using white light interferometry.....	54
Figure 4.1:	Flow chart outlining the experimental work presented in Chapter 4.....	57
Figure 4.2:	Contour plot for MRR response, $\log(I) - \log(T)$	62
Figure 4.3:	Contour plot for MRR response, $DF - \log(I)$	62
Figure 4.4:	Contour plot for MRR response, $\log(I) - DF$	63
Figure 4.5:	Contour plot for gap response, $\log(I) - \log(T)$	65
Figure 4.6:	Contour plot for gap response, $DF - \log(T)$	65
Figure 4.7:	Contour plot for gap response, $\log(I) - DF$	66
Figure 4.8:	Contour plot for recast response, $\log(I) - \log(T)$	68
Figure 4.9:	Contour plot for recast response, $DF - \log(T)$	68
Figure 4.10:	Contour plot for recast response, $\log(I) - DF$	69
Figure 4.11:	SEM micrographs of abrasive wire.....	73
Figure 4.12:	Close-up SEM micrographs of abrasive wire	74
Figure 4.13:	SEM micrographs of wire cross-sections	75
Figure 4.14:	Surface map of Manufacturer B –Wire 2,.....	76
Figure 4.15:	Protrusion height distribution for Manufacturer B - Wire 1.....	77
Figure 4.16:	Protrusion height distribution for Manufacturer B - Wire 2.....	77
Figure 4.17:	Effect of repeated use of abrasive wire on MRR.....	80
Figure 4.18:	SEM micrograph showing the condition of used wire	80
Figure 4.19:	SEM micrograph of the wire showing the location of discharge.....	81
Figure 4.20:	Comparison of wire core hardness	82
Figure 4.21:	WEDM material removal rates within stable operating regime	85

Figure 4.22:	Variation in removal rate with servo-reference voltage for AWEDM	86
Figure 4.23:	Percent increase in removal rate with AWEDM over WEDM	87
Figure 4.24:	Variation in removal rate with peak discharge current for AWEDM.....	88
Figure 4.25:	Percent increase in removal rate with AWEDM over WEDM	89
Figure 4.26:	Contour plot showing the variation of AMRR in AWEDM.....	90
Figure 4.27:	Micrograph of AWEDM Debris ($I=8A$, $V_{Ref}=162V$).....	91
Figure 4.28:	Micrograph of AWEDM Debris ($I=8A$, $V_{Ref}=144V$).....	91
Figure 4.29:	Micrograph of AWEDM Debris ($I=8A$, $V_{Ref}=108V$).....	91
Figure 4.30:	Micrographs of WEDM Machined Surface ($I=8A$, $V_{Ref}=126V$)	92
Figure 4.31:	Micrograph of AWEDM Machined Surface ($I=8A$, $V_{Ref}=162V$).....	93
Figure 4.32:	Micrograph of AWEDM Machined Surface ($I=8A$, $V_{Ref}=144V$).....	93
Figure 4.33:	Micrograph of AWEDM Machined Surface ($I=8A$, $V_{Ref}=108V$).....	93
Figure 4.34:	Normal force variation with servo-reference voltage.....	95
Figure 4.35:	Normal force variation with peak discharge current.....	95
Figure 4.36:	Contour plot showing the Normal Force in AWEDM.....	96
Figure 4.37:	Contour plot showing the AMRR and normal force in AWEDM	97
Figure 4.38:	Micrograph of the recast layer in steel after WEDM	99
Figure 4.39:	Micrograph of the recast layer in steel after AWEDM.....	100
Figure 4.40:	Micrograph of the recast layer in Inconel 600 alloy after WEDM	101
Figure 4.41:	Micrograph of the recast layer in Inconel 600 alloy after AWEDM.....	101
Figure 4.42:	Waveforms analysis for WEDM ($I=2.4A$).....	102
Figure 4.43:	Waveform analysis for AWEDM ($I=2.4$).....	103
Figure 4.44:	Arcing frequency in AWEDM.....	104
Figure 4.45:	Schematic of a simplified abrasive surface	106
Figure 4.46:	AWEDM job saving with abrasive wire at \$0.80/metre	110
Figure 4.47:	AWEDM job savings with abrasive wire at \$0.40/metre.....	111
Figure 5.1:	Schematic of fully coated abrasive wire with rotational wire guides.....	116
Figure 5.2:	Schematic of partially coated abrasive wire with stationary wire guides	117

List of Tables

Table 2.1:	Wire saw related US patents.....	21
Table 2.2:	Typical free abrasive wire saw machining parameters.....	23
Table 2.3:	Basic specification of resin bonded fixed abrasive wire.....	24
Table 2.4:	Parameters and typical values in fixed abrasive wire sawing machining.....	26
Table 3.1:	Agietron Impact 2 specifications.....	43
Table 3.2:	Wire feed apparatus specifications.....	44
Table 3.3:	Experiemental parameters and their levels as used in the DOE.....	47
Table 3.4:	Constant parameters used in DOE testing.....	48
Table 3.5:	Current sensor specifications.....	49
Table 3.6:	Data acquisition system specifications.....	50
Table 3.7:	Parameters and levels used in AWEDM testing.....	52
Table 3.8:	Constant machine settings used in AWEDM testing.....	52
Table 3.9:	Details on the sample preparation procedure.....	54
Table 4.1:	F and P statistics from ANOVA results for MRR.....	59
Table 4.2:	F and P statistics from ANOVA results for Gap.....	59
Table 4.3:	F and P statistics from ANOVA results for Recast.....	60
Table 4.4:	Model terms, regression coefficient and 't' statistics for MRR.....	61
Table 4.5:	Model terms, regression coefficient and 't' statistics for Gap.....	64
Table 4.6:	Model terms, regression coefficient and 't' statistics for Recast.....	67
Table 4.7:	Change in the average voltage with open circuit voltage.....	70
Table 4.8:	Variation in the average voltage with the compression setting.....	71
Table 4.9:	Manufacturers and details on fixed abrasive diamond wires.....	72
Table 4.10:	Machining parameter limitations of AWEDM.....	83
Table 4.11:	Final AWEDM testing conditions.....	84
Table 4.12:	Description of the factors included in the economic analysis.....	109

Chapter 1

Introduction

With the surge of technological developments over the past several decades, the limitations of existing manufacturing methods have become very apparent. Evolving engineering requirements and corporate economics have initiated a significant amount of research into various manufacturing methods. Improvements in precision, surface quality and efficiency are all measures of progress in the manufacturing industry. These improvements come from better machine tool design and deeper understanding of the processes themselves.

Advanced engineering materials play an increasingly important role in modern manufacturing, especially in the aerospace, automotive, tool, die and mould making industries. While having provided economic benefits through improved product performance and product design, the ability to efficiently machine these materials using traditional processes has become difficult and in some cases almost impossible. With the limitations of cutting and grinding, the once termed non-traditional machining processes have become standard. Electrical Discharge Machining (EDM), for example, is one of the most employed machining processes. To further expand current machining capabilities, the development of hybrid machining processes has been an area of recent development. In combining aspects of different machining processes, the limitations of the constituent processes can be reduced or eliminated. These new machining processes rarely, however, replace the traditional ones; instead, they are new tools that allow for the manufacture of the next generation of engineering designs and materials. The topic of discussion is henceforth aimed towards the development of a novel hybrid machining process: Abrasive Wire Electrical Discharge Machining (AWEDM).

1.1 The Constituent Processes

The use of EDM is vast across many areas of manufacturing. This process offers significant benefits over conventional machining techniques, though it also has some limitations. In an effort to overcome these limitations, a machining process based upon Wire Electrical Discharge Machining (WEDM) and abrasive grinding is developed in a process termed Abrasive Wire Electrical Discharge Machining (AWEDM). The following sections outline the fundamentals of the EDM process and various aspects of WEDM. In addition, an abrasive wire sawing process is introduced. These introductions provide a basis for discussion and comparison with regard to AWEDM.

1.1.1 Electrical Discharge Machining

EDM is a non-traditional machining process in that material is not removed by mechanical interactions such as in cutting; instead, the mechanism of material removal is electrical erosion. A schematic of the EDM process is shown in Figure 1.1.

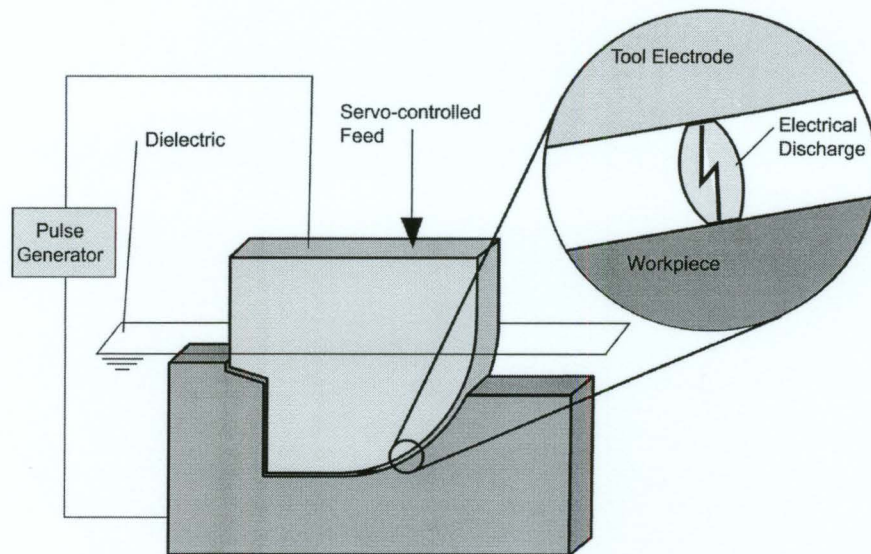


Figure 1.1: Schematic of Die-Sinking EDM

In general, EDM is achieved by applying a pulsed voltage between a conductive tool and workpiece. The electrode is positioned extremely close to the workpiece (5-50 μm) and the gap is filled with an insulating dielectric fluid such as de-ionized water or dielectric oil. When the voltage is pulsed on and the breakdown strength of the dielectric is exceeded, the current flows across the gap to the workpiece in the form of a discharge. Figure 1.2 shows schematic voltage and current waveforms with the different characteristics noted.

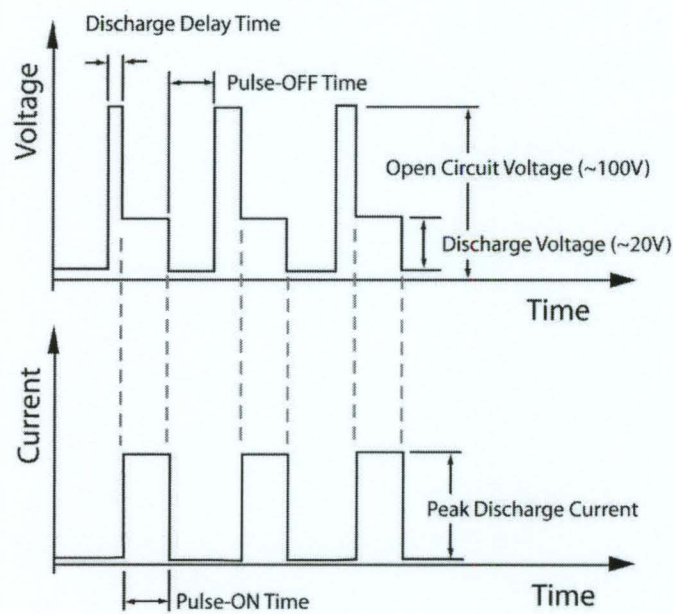


Figure 1.2: Schematic voltage and current waveforms during EDM

Thermal energy from the discharge generates a channel of plasma between the tool and workpiece. Temperatures in the plasma are reported to be in excess of 8000-12000°C, high enough to vaporize or melt any workpiece material [1]. High pressures are exerted on the surface by the plasma causing the workpiece material to superheat. When the voltage is switched off, and the plasma channel breaks down creating rapid reduction in pressure and temperature, the superheated material evaporates explosively into the gap. The dielectric fluid then flushes the channel to re-solidify the molten material and remove it in the form of microscopic debris. The amount of material removed from one discharge is typically between

10^{-6} - 10^{-4} mm³ and occurs at frequencies typically around 50-500 kHz providing material removal rates between 2 and 400mm³/min [2].

1.1.2 Wire Electrical Discharge Machining

Wire Electrical Discharge Machining is the most widely used variant of EDM. This process employs a fine, continually traveling wire electrode and is generally combined with Computer Numerical Control (CNC) to generate complex, swept shapes and geometries. This eliminates the need for the complex and costly electrodes as used in Die-Sinking EDM. Figure 1.3 shows a schematic of a typical WEDM system.

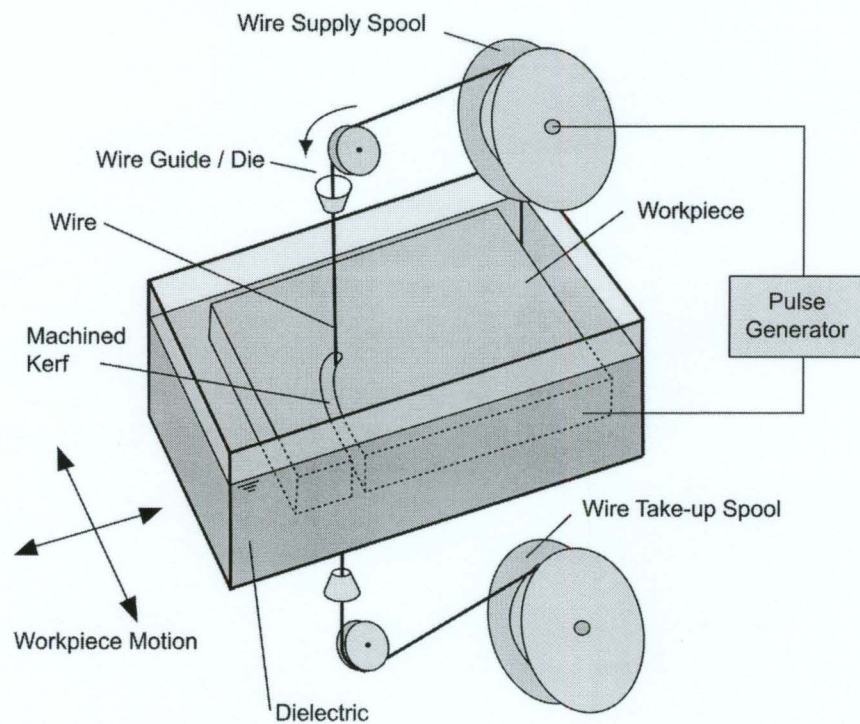


Figure 1.3: Schematic of WEDM

In WEDM, a wire of diameter 0.02–0.3 mm is fed through the workpiece in a dielectric medium while electrical discharges occur between the wire and workpiece. De-ionized water as

a dielectric typically provides higher cuttings speeds with greater tool wear, since the tool is continually renewed in WEDM, tool wear is not an issue, and thus de-ionized water is typically used. The wire is often made of brass, though stratified wires with a zinc layer for increased breakage protection are becoming more common. A significant benefit of WEDM over competing processes is that surface roughness as low as 0.04 to 0.25 R_a is achievable [3]. Further, the process is characterized by high accuracy, which is mainly attributed to the low, if not negligible forces generated by the process.

Limitations of EDM

As in any process, both advantages and disadvantages exist. The main advantages with the EDM process are its ability to machine materials regardless of hardness and to create intricate geometries. The most significant disadvantages or limitations are the comparably low removal rates when compared to conventional processes and the quality of the machined surface. Though EDM is capable of generating surfaces with extremely low roughness, the re-solidification of molten material that is not removed creates a recast layer on the surface. Figure 1.4(a) shows a discharge crater from a single spark experiment where much of the melted material remains on the surfaces, in fact only 10-15% of the melted material is removed [1]. In practical machining, this material forms a semi-continuous layer with micro-cracks as shown in the cross section image of Figure 1.4(b). Upon etching the sample, the layer is clearly distinguished, hence, the layer is often referred to as the ‘white layer’.

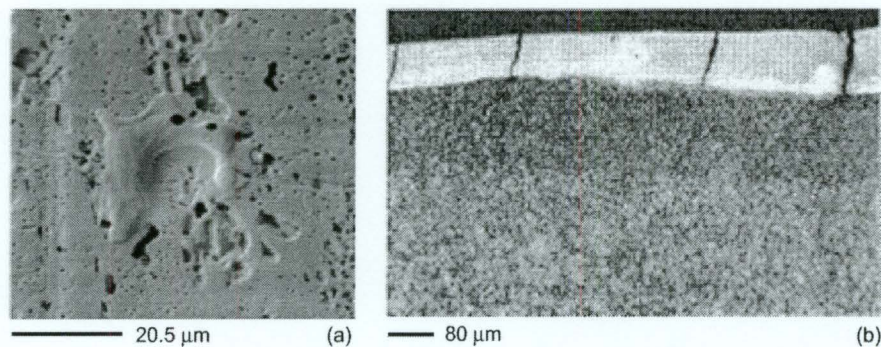


Figure 1.4: a) Example of a single spark discharge crater [4] and
b) re-cast layer on an EDM machined surfaces [5]

This layer is known to have high hardness and good resistance to corrosion; however, as shown in Figure 1.4(b), it contains micro-cracks that can be very undesirable. Many applications require that further processing such as polishing or abrasive flow machining (AFM) be done.

1.1.3 Abrasive Wire Saw Machining

The wire sawing process as shown in Figure 1.5 was developed in the early 1990's and was later applied to the manufacture of thin Silicon and Silicon Carbide wafers. Wire sawing is a more efficient method to manufacture wafers, when compared to existing processes such as Inner Diameter (ID) diamond saw cutting. These advantages are mainly due to the lower kerf losses associated with the process.

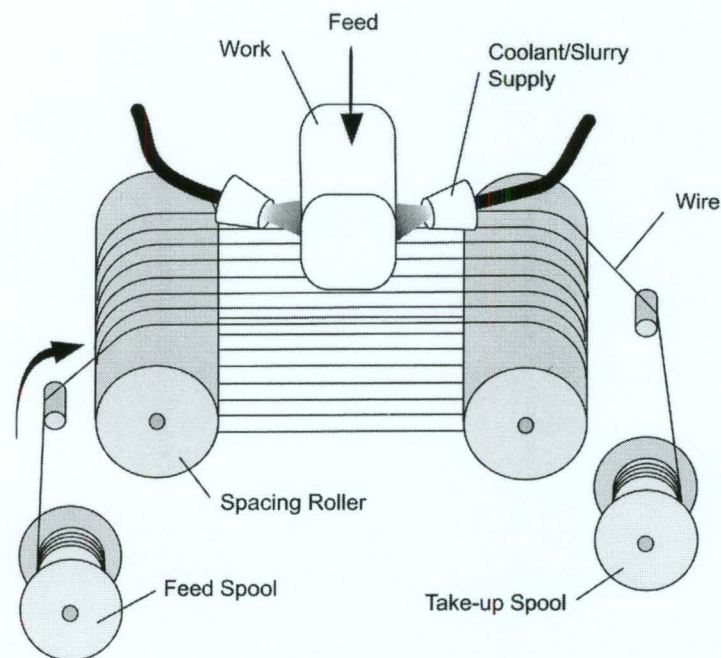


Figure 1.5: Schematic of abrasive wire sawing

Initial developments in wire saw technology utilized a plain steel wire with the application of an abrasive slurry solution to the cutting zone. Technological drawbacks such as

slow cutting speeds and variation of wafer thickness due to wire wear are limitations of this process [6]. To overcome these limitations, much of the recent progress in wire saw machining has been with regard to the development of fixed abrasive wires. As fixed abrasive wire sawing is more efficient than the slurry methods, a fixed abrasive wire, as shown in Figure 1.6, is used in the development of AWEDM.

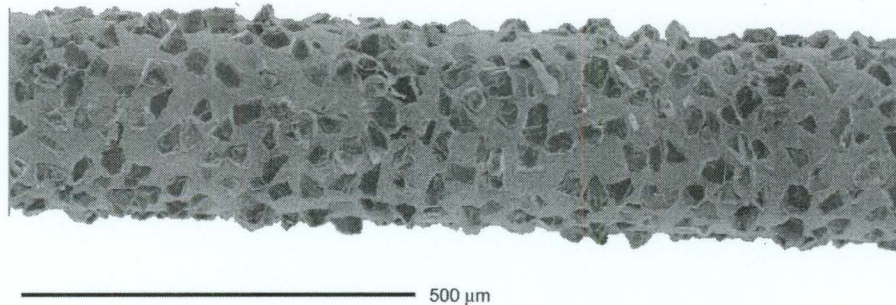


Figure 1.6: SEM micrograph of fixed abrasive wire

1.2 Hybrid Machining Processes

In combining different mechanisms of material removal, technological improvements in machining can be achieved. Hybrid Machining Processes (HMPs) synergistically combine aspects from different machining processes in order to exploit combined or mutual advantages and to avoid or reduce negative effects of the individual processes. There are two types of hybrid machining processes; one where each element contributes to material removal such as in Abrasive Electrical Discharge Grinding (AEDG), and the other where only one element contributes to material removal while others assist by altering the process conditions such as in Laser Assisted Turning [7]. Figure 1.7 presents a Process Condition Scheme (PCS) for AEDG.

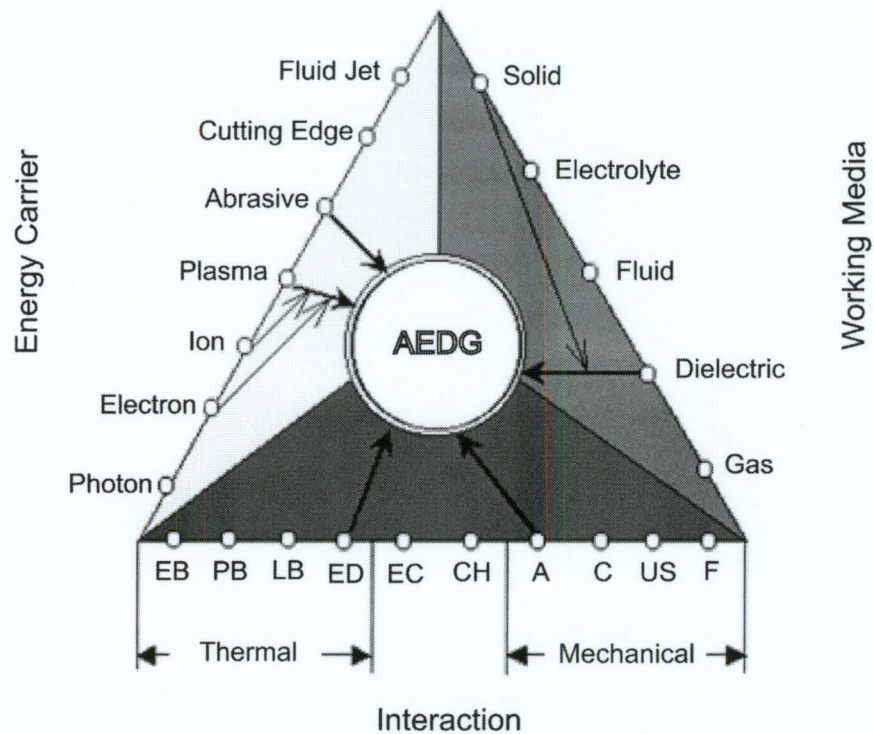


Figure 1.7: Process condition scheme for hybrid machining processes (adapted from [8])

The process condition scheme is used to identify the interactions, the working media and the energy carriers responsible for material removal. Similar PCSs can be created for processes such as Laser Assisted Cutting or Abrasive Electrochemical Machining. These charts can also be used to develop new hybrid processes.

Despite offering certain advantages, most HMPs have not seen widespread use and are used only when no other options are available. This is in part due to insufficient research efforts and lack of understanding of the process. The work herein is aimed towards developing and establishing a basis of understanding for a new HMP based upon electrical discharges and abrasive interactions.

1.3 Abrasive Wire Electrical Discharge Machining

Having a process condition scheme identical to that of AEDG, as shown in Figure 1.7, Abrasive Wire Electrical Discharge Machining (AWEDM) is a hybrid process combining the effect of abrasion and electrical erosion in a form comparable to both WEDM and wire saw machining. To realize the process, a fixed abrasive wire is used in place of the plain metallic wire that is conventionally used in WEDM. In this configuration, as shown in Figure 1.8, the electrical discharges occur between the conductive core of the wire and the workpiece to remove material by spark erosion, while the abrasives simultaneously abrade the work material that is molten, recast, or thermally softened by the heat from said electrical discharges.

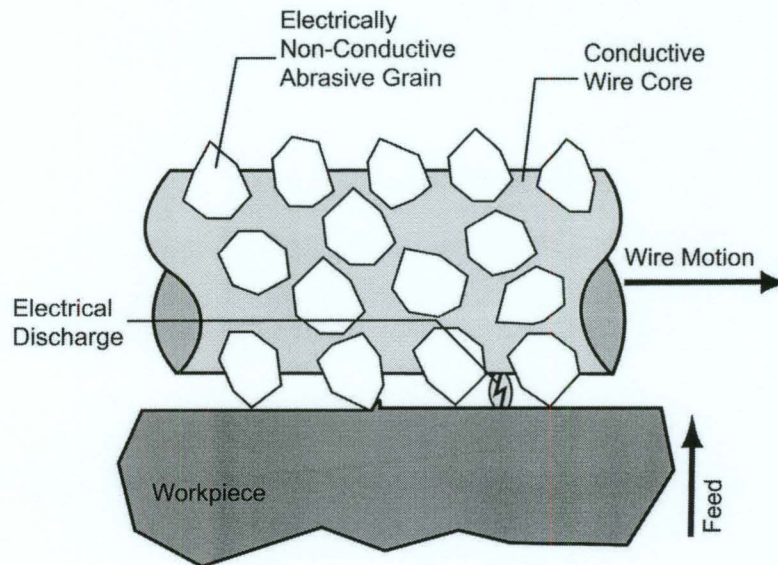


Figure 1.8: Abrasive Wire EDM schematic

In conventional WEDM processes, high removal rates and good surface quality are mutually exclusive, with one response obtained at the expense of the other. Since material removal in AWEDM occurs by the combination of abrasion and melting/vaporization, where the abrasion removes the unwanted recast layer, an increase in both removal rate and surface quality can be obtained.

1.3.1 Why use AWEDM?

The change in WEDM machine tool prices, maximum workpiece size (axes travel) and cuttings speed over time are shown in Figure 1.9. Advances in electronics and wire technology saw marked improvements in machining rates beginning around 1988. After about 1992, the machining speeds in WEDM appear to have stagnated. Improving the process through improved generator technology can only do so much, as there is a fundamental problem in EDM: material ejection efficiency is very low, where only 10% of the melted material is removed [1]. With flushing pressures at their limits, a new approach is required. The concept of combining WEDM and abrasion is one that serves to improve upon that fundamental problem by removing the non-ejected, but thermally softened material.

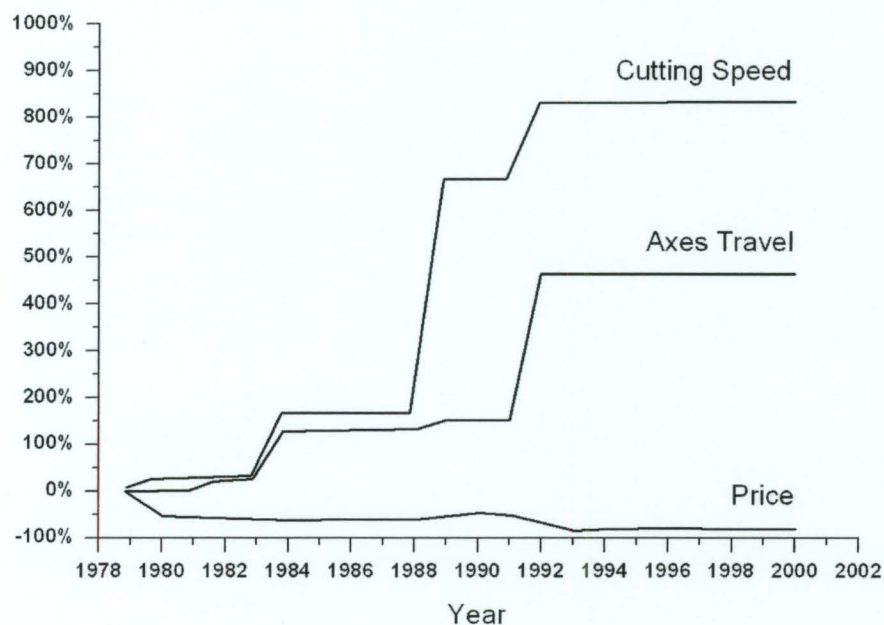


Figure 1.9: Trends in WEDM (adapted from [9])

The potential uses for AWEDM are almost unlimited. Regardless of the application, the goal in combining WEDM and abrasion is to improve the efficiency of the process. This improvement can be brought about directly by an increase in MRR or indirectly by reducing

the number of subsequent machining operations. In order to implement the process properly, it is crucial to understand how the two processes work together.

1.3.2 Implementation

Practically, the process can be carried out using a conventional wire electrical discharge machining apparatus of the kind represented in Figure 1.2. Some modifications, as are discussed in Chapter 5, would be required in order to accept an abrasive wire with an electrically conducting core and non-conductive abrasives embedded along the periphery, as shown in Figure 1.6

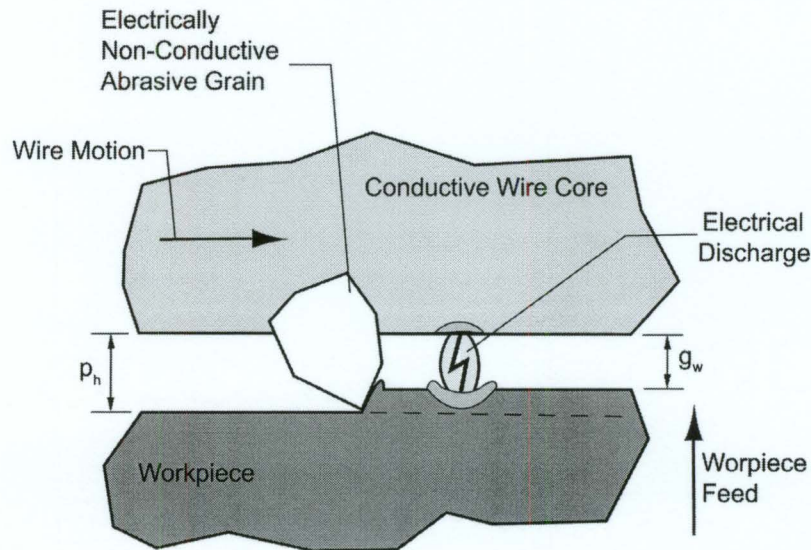


Figure 1.10: Schematic of abrasive protrusion and gap width relationship in AWEDM

During machining, the wire translates along its axis lateral to the workpiece, which is fed relative to the wire axis under servo control such that a gap is maintained between the workpiece and the wire core. As the gap width is sensed and controlled electrically, it is essential that the wire core and the workpiece are electrically conductive. For the same reason, in order for abrasion and EDM to be operative simultaneously, the abrasives must be

electrically non-conductive and be of a nominal protrusion height, p_h , greater than the nominal gap width, g_w , as shown in Figure 1.10. Hence, for a given average gap width, a wire with an appropriate abrasive grit size can be chosen, or alternatively for a given wire, the gap width can be altered by changing the machining parameters as is shown in Chapter 4.

Apart from the expected advantages in combining WEDM and abrasion, other advantages and limitations are to be expected. The presence of abrasives on the wire physically isolates the core from the workpiece reducing the possibility for electrical shorts. The same abrasives cause the build-up of grinding debris between the wire core and workpiece, which may increase the frequency of arcing. These effects are examined in the current work through analysis of the voltage and current signals acquired during machining. Another effect that results from the addition of abrasion is the manifestation of machining forces. Whilst the abrasives serve to minimize lateral vibration of the wire, the machining forces inherently cause its deflection in the cutting direction. All of these effects are to be considered in the development of the AWEDM process.

1.4 Scope and Organization of Present Work

The report presented herein outlines the idea of a novel hybrid machining process; an experimental apparatus is constructed, the process is tested and the results are analyzed.

In Chapter 2, relevant background information and research is presented in the areas of EDM with specific attention to WEDM. The development of the fixed abrasive wire sawing process is outlined with some description of the current research in the area. Examples of hybrid machining processes are presented while attention is focused on the research and development of Abrasive Electrical Discharge Machining processes. In Chapter 3, details on the experimental method are presented and discussed. The design and function of the experimental apparatus is outlined and the use of measuring equipment and sample preparation is detailed for each set of experiments. Chapter 4 presents the experimental results and discussion. The experiments discussed progress towards implementing AWEDM with

Chapter 2

Literature review

To provide a basis relating to the development of AWEDM, a review of some of the relevant literature is provided herein. Information here builds on the basics of EDM, Wire-Saw Machining and Hybrid processes presented in Chapter 1.

2.1 Electrical Discharge Machining

Electrical Discharge Machining is an area of intensive research. The focus is broad with work on the process fundamentals, as well as on practical issues and novel implementations. Some aspects of current research are presented here.

2.1.1 *Process Fundamentals*

To expand upon the basic operation of EDM, some background information on the process fundamentals is presented. Despite the efforts towards understanding the process fundamentals, many of the process intricacies are not yet fully understood. Over sixty years since the concept of EDM was proposed by Russian scientists B.R. and N.I. Lazarenko, the discharge mechanism remains still disputed [10]. At present, the most widely accepted process for discharge initiation is the idea that a thin particle bridge between the electrodes defines the discharge location. It is worthwhile to note that the discharge process in servo-controlled EDM differs greatly from single discharge tests with clean dielectric [10,11]. Substantial work has been done in determining the process by which discharges occur. As the discharge initiation process itself has little influence on the development of AWEDM, the reader is referred to review papers that evaluate and summarize much of the research completed with respect to the discharge phenomena and other process fundamentals [1,10].

2.1.2 *Process Control*

One of the requirements for EDM is a gap between the electrode surfaces, which is generally controlled by a servo-system. A set parameter, most commonly the average gap voltage, is used to provide the feedback to the control system, though other methods based on the discharge delay time may be used. This set-parameter, hereafter referred to as the servo-reference voltage, is a fraction of the open circuit voltage. For machining to begin, the servo system must advance the tool-electrode to a point where the gap is small enough for a discharge to initiate. Figure 2.1 illustrates the principle of the servo control used in EDM.

When the gap is large and no discharges occur, the average voltage is equal to the open circuit voltage. Since the measured average voltage is greater than the servo-reference voltage, the servo will attempt to decrease the gap. In the opposite situation, where the electrodes have made contact, the measured voltage will be zero, which is less than the servo-reference voltage, thus causing the servo to increase the gap. For the intermediate regions of operation, when discharges are occurring, the measured average voltage will vary with material removal. As material is removed and the gap size increases, longer discharge delay times occur, thereby increasing the average voltage and signaling the servo to advance the electrode. If the machining gap becomes too small, the discharge delay time will decrease and arcing may occur. Both of these will cause a decrease in the average voltage, signaling the servo to retract the electrode [1].

The machining gap is critical to the process stability and has thus seen significant research [10]. The potential use of in-process gap measurement and example devices for such are outlined in [10,12].

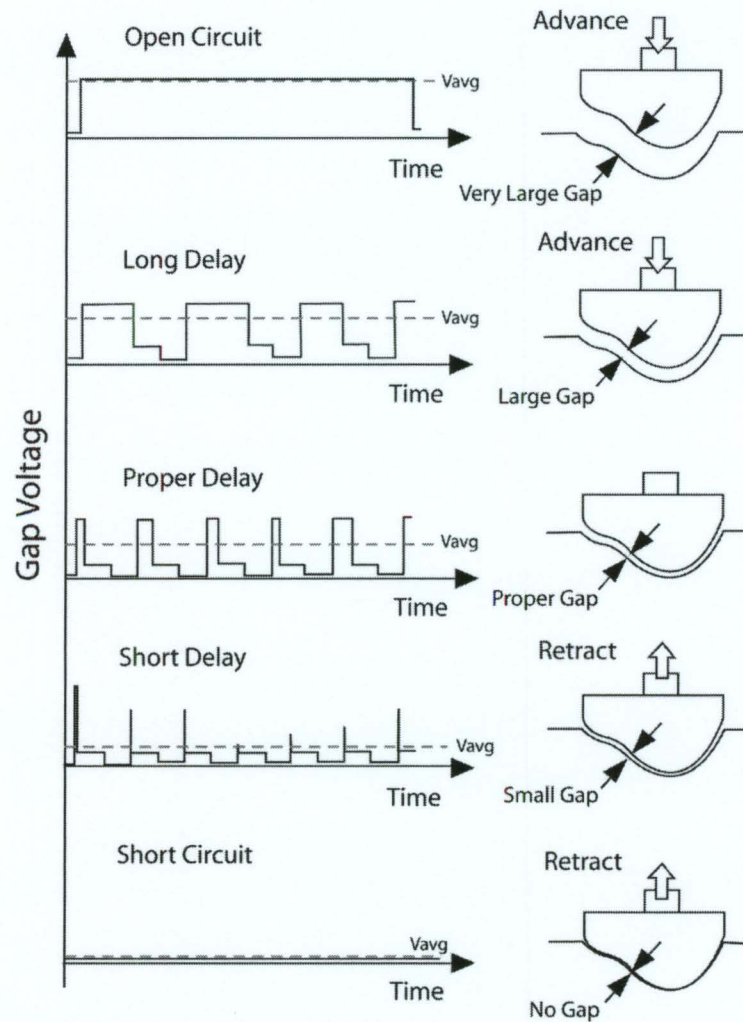


Figure 2.1: Schematic of the servo-controlled feed system in EDM (adapted from [1])

2.1.3 Recast Layer Formation

As discussed in Chapter 1, the formation of a recast or 'white layer' is a problem that is inherent to EDM. The white layer typically has undesirable characteristics that require its removal in certain applications. Defects in the recast layer, such as the micro-cracks shown in Figure 2.2 can create concentration points for crack initiation.

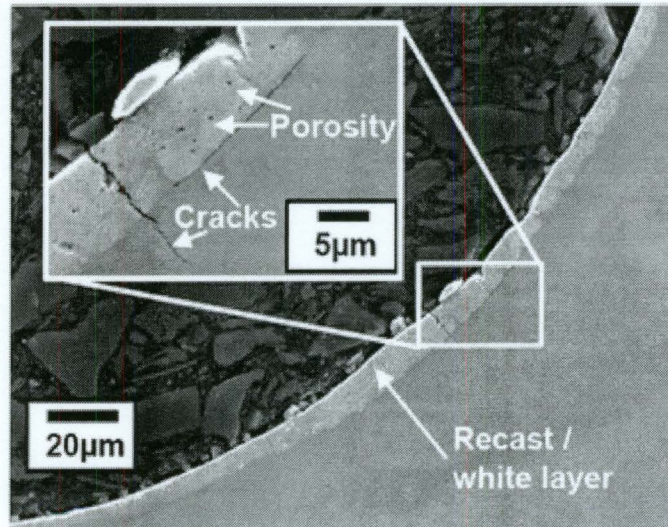


Figure 2.2: Defects in the recast layer of EDM machined AISI H13 steel [13]

Such defects are often not acceptable, as in the case of rotating components used in the aerospace industry. Various efforts to reduce the recast layer through process optimization have been employed. The use of empirical modeling techniques such as Response Surface Methodology (RSM) have enabled researchers to understand how the process parameters affect the recast layer formation and select appropriate parameters to reduce it [14]. In an effort to determine the recast layer thickness without having to section the workpiece and undertake metallurgical analysis, 3D surface parameters have been correlated to the recast thickness [15]. Parameters such as the arithmetic average surface height, core void volume and density of summits of the surface can be obtained using white light interferometry methods. Using regression, the use of such parameters was found to explain ~80% of the variation in the white layer thickness, an improvement to existing techniques [15]. Apart from efforts to determine and reduce recast layer thickness, the study of the properties of the white layer has also been undertaken. The recast layer is known to have different qualities than the bulk material. Kruth et al. [5], for example, have attempted to understand the influence of the workpiece material, electrode material and dielectric type on the recast layer. In machining of steel, the use of oil as a dielectric was found to increase the carbon content of the recast layer as carbon from the dielectric would diffuse into the metal. In contrast, the use of water as a dielectric has a

decarburizing effect on the recast layer. The microstructure of the recast layer has been found to include carbide dendrite structures in the Heat Affected Zone (HAZ) which are a result of the melting and re-solidification [5,16]. Closer to the surface, martensite and residual austenite are formed as is shown in Figure 2.3 and Figure 2.4 [16].

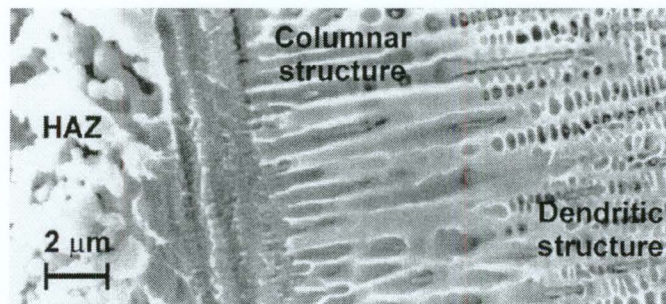


Figure 2.3: Micrograph showing columnar and dendrite structures in the HAZ of an EDM workpiece [16]

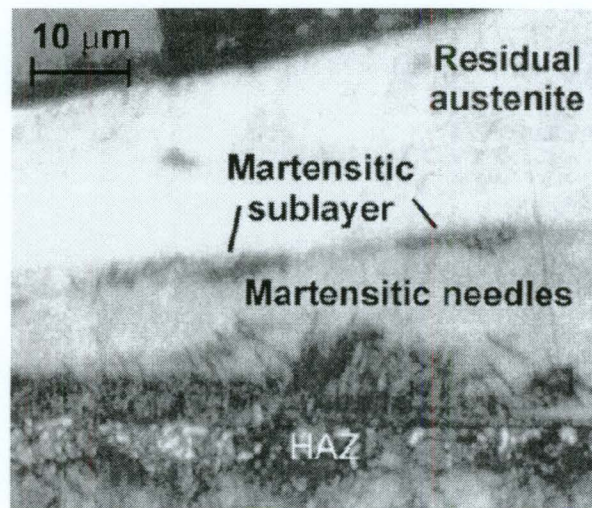


Figure 2.4: Micrograph of the recast layer showing different material structures [16]

The presence of the recast layer is typically undesirable with substantial efforts aimed at reducing it. In efforts to take advantage of the phenomena, work has been done to produce a controlled surface layer with specific properties as is discussed in [13,17].

2.1.4 Developments in WEDM

As the most employed variant of EDM, WEDM has seen significant developments, with many outlined in [3]. Developments such as the process termed Wire Electrical Discharge Grinding (WEDG) are discussed. The term WEDG however is actually a misnomer in the fact that no grinding or mechanical action occurs. The process uses a stationary wire guide in the machining area to confine the wire movement. This confinement minimizes wire vibration making it possible to manufacture a rod as small as $5\mu\text{m}$ in diameter [3]. The process is typically used for creating micro-pins or small diameter tools for micro-EDM applications [1]. Figure 2.5 illustrates the principle of operation for WEDG.

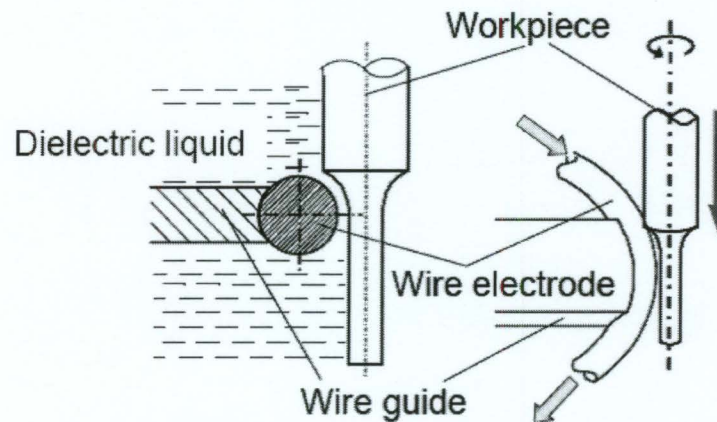


Figure 2.5: Schematic illustration of the WEDG process [1]

Apart from the work done towards process optimization, modeling and control, which are reviewed in [1,3] and [18], much of the progress in Wire-EDM is due to improvements in generator and wire technology. From initial use of plain brass electrodes to modern stratified wires and more advanced generators, removal rates in WEDM machining of steel have increased from $17\text{ mm}^2/\text{min}$ in 1970 to over $500\text{ mm}^2/\text{min}$ in 2003; a factor of thirty [19,20]. Advances in electronics have allowed for real time monitoring while transistor technology has enabled the use of very-high current and short pulse time parameters [1,3]. The evolution of the wire used tool has also been dramatic. In addition to providing an increase in the MRR, there has also been increase in the capabilities of the process due to improved wires. The

thickness of workpieces capable of being machined in the 1970's has increased from ~100 mm to over 400 mm today [19]. Modern composite wires use a copper alloy core with a zinc coating (20-30 μ m thick) that combines good electrical conductivity, thermal conductivity and sparkability [20]. Because of its relatively low melting temperature, the zinc coating serves to protect the wire core by evaporating around the discharge zone, and acting as a heat sink [19]. To achieve high accuracy cuts and sharp corners, high wire tension is required. Typically, wires made of high strength materials such as molybdenum are used at the expense of cutting rates. To combat this, the design of composite wires with high tensile strength cores, for high accuracy machining without loss in machining performance has been studied as detailed in [20].

The volume of research centered on EDM is enormous as there are numerous variations of the process, from Die-Sinking and Wire EDM to micro-EDM. Many of the process variation and the topics of current research are outlined in review papers [1-3,18]. Some of the more interesting applications of the process that may have some relevance to future uses of AWEDM are dry-electrical discharge machining [21-23] and multi-spark EDM [24] as it might apply to the simultaneous slicing of silicon wafers [25].

2.2 Abrasive Wire Saw Machining

In order to develop the AWEDM hybrid process, it is important to have an understanding of the constituent processes. In AWEDM, abrasion and electrical erosion mechanisms are to be combined using geometry similar to that of Wire Electrical Discharge Machining. This section presents an existing abrasive process with this same geometric configuration.

2.2.1 Wire Saw Technology

The concept of using a wire for sawing materials has been known for some time, originating from the carpenter wire saw for wood machining. The potential benefits for use in machining of silicon ingots into wafers for the electronics industry revitalized the development

of wire saw technology in the 1990's [26]. With a smaller kerf than obtained with ID saw cutting, more wafers are produced from each ingot [26]. Much of the work in the field is proprietary in nature with patents relating to the process beginning as early as the 1970's. Only two patents were filed in the 1980s while the numbers increased drastically in subsequent years. Table 2 lists the progression of filed U.S. patents relating to the process.

Table 2.1: Wire saw related US patents filed between 1970 - 2002 (adapted from [27])

<i>Decade</i>	<i>Filed U.S. Patents</i>	
1970	3,831,576 (1974)	4,016,856 (1977)
	3,841,297 (1974)	
1980	4,494,523 (1985)	4,655,191 (1987)
1990	4,903,682 (1990)	5,829,424 (1998)
	5,201,305 (1991)	5,878,737 (1998)
	5,269,285 (1993)	5,910,203 (1999)
	5,564,409 (1996)	5,944,007 (1999)
	5,758,633 (1998)	5,947,789 (1999)
	5,787,872 (1998)	5,964,210 (1999)
	5,810,643 (1998)	
2000-2002	6,065,462 (2000)	6,178,961 (2001)
	6,102,024 (2000)	6,178,962 (2001)
	6,098,610 (2000)	6,234,159 (2001)
	6,065,461 (2000)	6,237,585 (2001)
	6,109,253 (2000)	6,283,111 (2001)
	6,135,103 (2000)	6,352,071 (2002)
	6,070,570 (2000)	6,381,830 (2002)
	6,112,738 (2000)	6,408,839 (2002)
	6,105,568 (2000)	6,422,067 (2002)
	6,024,080 (2000)	6,311,684 (2002)
	6,279,564 (2001)	

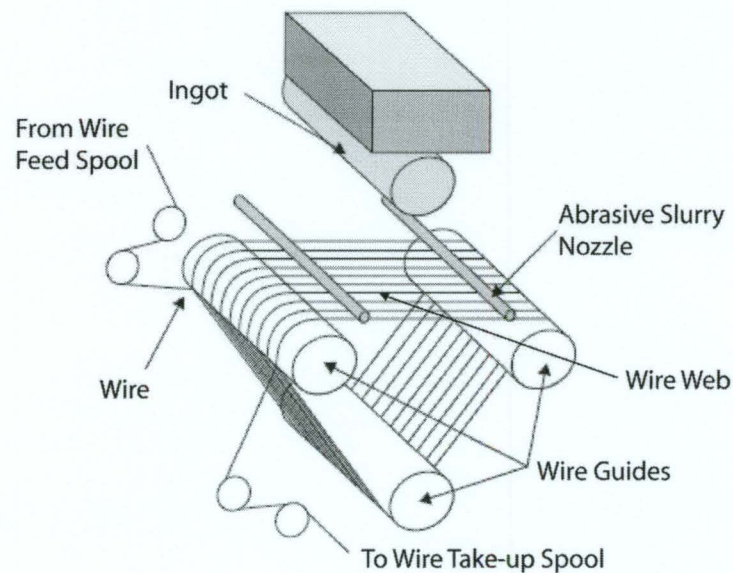


Figure 2.6: Schematic of multi-wire sawing
(adapted from [28])

2.2.2 *Free Abrasive Wire-Saw Machining*

Initial developments in wire saw technology utilized a plain steel wire with the application of an abrasive slurry solution in the cutting zone. The principle of operation for the process is depicted in Figure 2.6. A single plain steel wire is fed from a feed spool to the wire guides; each grooved with a constant pitch. Multiple strands of wire are wound around the rollers through 500-700 parallel grooves to form the web [29]. The wire is pulled by the torque exerted on the main drive roller, while the take-up spool collects the wire. Machining occurs as the ingot is forced against the wire and sliced into hundreds of wafers simultaneously. Cutting in the process is achieved by three-body abrasion as depicted in Figure 2.7.

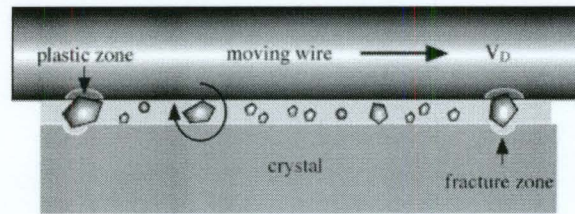


Figure 2.7: Schematic illustrating three-body abrasion [29]

The slurry is comprised of abrasive particles, typically SiC or diamond particles 5-30 μm size, at a volume fraction between 30-60% [29]. Table 2.2 lists some of the process parameters and indicates typical operating values. The wire speed and slurry viscosity are the two most important parameters in the process [29]. The three-body abrasion mechanism for material removal is complex, thus a significant portion of the literature on free-abrasive wire saw machining is focused on fluid mechanical effects, process dynamics and the material removal mechanics of the process. The fluid mechanics and tribology bear a significant influence on machining efficiency and precision. Extensive literature can be found with respect to the fluid mechanics; Bhagavat et al. [30] for example studied the elasto-hydrodynamic interaction in free abrasive slicing of wafers as is detailed in [29]. The topic of vibration and dynamics having a direct influence on the process precision has also seen significant research [31,32]. The mechanics involved in material removal for 3-body abrasion are complex and can vary depending on the material to be machined. Example studies on the process mechanics of free abrasive wire saw machining are detailed in [29,33].

Table 2.2: Typical free abrasive wire saw machining parameters [29,33]

<i>Process Variable</i>	<i>Typical Values</i>
Wire Speed	5-20 m/s
Wire Tension	20-35 N
Wire Diameter	175 μm
Abrasive Particle Size	5-30 μm
Abrasive Concentration	30-60%
Slurry Viscosity	1Ns/m ²
Sawing Rate	<0.7mm/min
Machining Load	1-5N

2.2.3 Fixed Abrasive Grain Wire-Sawing

Despite significant research efforts, the free-abrasive wire sawing processes suffers from technological drawbacks such as slow cutting speeds and wide variation of wafer thickness [6]. To overcome these limitations much of the recent progress in wire saw machining has been on the development of fixed abrasive wires. Similar to grinding wheels, both resin bonded and electroplated abrasive wires have been developed.

Resin Bonded Fixed Abrasive Wires

Striving towards the use of resin bonded abrasive wires; Sugawara et al. have reported the successful development of a fixed-diamond grain wire saw which is produced by continuous resin coating [34]. The design of the wire was studied from the basic wire structure to wire production. The designs are evaluated in terms of machining efficiency and grain retention. The basic design requires high strength wire of diameter no less than 130 μm to prevent breakage under tension [28]. Table 2.3 outlines the various wires developed in their research.

Table 2.3: Basic specification of resin bonded fixed abrasive wire saws developed by [28]

<i>Wire Generation</i>	<i>Wire Diameter (μm)</i>	<i>Abrasive Grain Diameter (μm)</i>	<i>Average Wire Saw Diameter (μm)</i>	<i>Kerf Width (μm)</i>
First	180	40-60	245	260
Second	155	10-20	175-180	190
	140	20-30		
	130	30-40		

From their results, the second-generation wire of 130- μm diameter provided the best results in terms of cutting speed. The improved cutting speed for small diameter wire and large abrasives is a result of the increased chip pocket volume available for the grinding debris to accumulate [28]. Additionally, the effect of abrasive treatment on the grain retention was studied. When the abrasives are treated with a Nickel plating or chemical reagent, a 60-70%

improvement in grain retention strength was found over untreated abrasives [28]. Other efforts to optimize the process using resin bonded abrasive wires are detailed by Tso et al. [35].

Apart from resin bonding, the manufacture of fixed abrasive wires can be achieved by the electroplating process as is discussed in the following section. The use of resin bonded abrasive wire has several advantages over the use of electroplated wire. The resin bonded wire has been found to have better flexibility and strength. Furthermore, resin bonded wire are capable of producing finer surfaces requiring less post processing, which can have significant bearing on the overall manufacturing costs [36].

Electroplated Fixed Abrasive Wire

Literature directly concerning the development of electroplated fixed abrasive wires is somewhat scarce with much of the research being proprietary. Their development is based upon the principle of composite electroplating using the brush technique [37]. Of the available literature, Chiba et al. presented a high-speed method for manufacturing electroplated diamond wire tools to increase the economic viability of the process [38]. Using brush composite electroplating, production rates as much as 30 times higher than conventional plating methods were achieved [38].

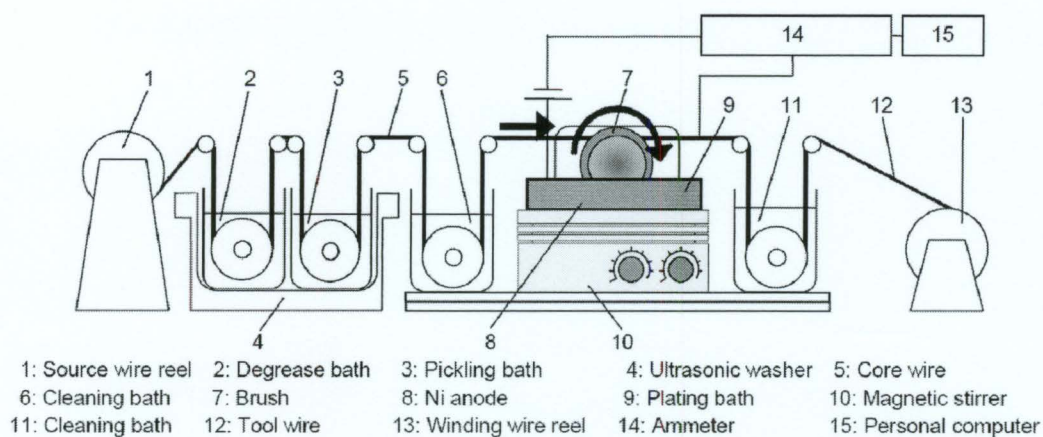


Figure 2.8: Schematic of the abrasive wire manufacturing process [38]

Using the process as shown schematically in Figure 2.8, production rates of 70 mm/min per brush were attained, while the overall rate was found to increase proportionally with the number of brushes used [38]. Using Nickel coated abrasives, the concentration of abrasives electrodeposited to the wire increased and provided improved grain retention over existing methods [38]. Other developments regarding the production of electroplated diamond wire include the possible use of new matrix materials. An increase in both hardness and toughness over traditional Nickel coatings is possible with a Nickel-Cobalt-Manganese (Ni-Co-Mn) coating without significant change to the manufacturing process [39].

The Fixed Abrasive Wire Sawing Process

The equipment and function thereof in fixed abrasive wire saw machining is much the same as is used in free abrasive wire saw machining; depicted in Figure 2.6. One difference is that no abrasive slurry is used in the fixed abrasive method. Instead, a water or water-based coolant is used. The elimination of the slurry from the process yields an immediate improvement in terms of environmental impact with only 1/50th of the waste produced [36]. Another difference is that the sawing rate is directly controlled instead of using load feeding. Lastly, depending on the workpiece geometry, the length of contact between the wire and the workpiece may change during machining. The addition of a rocking motion serves to produce a more consistent and reduced contact area [6,40]. Typical process parameters are listed in Table 2.4.

Table 2.4: Process parameters and typical values in fixed abrasive wire saw machining [6,28]

<i>Process Variable</i>	<i>Typical Values</i>
Wire Speed	5-15 m/s
Wire Tension	10-25 N
Down-feed	0.078-5.5 mm/min
Rocking Angle	2 degrees
Rocking Frequency	0-0.5 Hz
Coolant	Water/Water Based

Of the non-proprietary research in the field, Clark et al. [26] have presented process monitoring schemes. Due to the relatively low machining forces and long cutting times involved in the process, the use of piezoelectric force sensors is not feasible in measuring the normal machining force. The use of a capacitance sensor to measure the wire bowing due machining forces is detailed where the bow angle values are used to determine the normal cutting force component. Additional process instrumentation techniques such as a device for measuring the transverse motion of the wire have also been developed [41]. This technique utilizes a laser-photodiode combination to measure the movement of the wire.

The use of the process has been examined in machining of various materials including wood, foam ceramics and hard materials such as SiC. The feasibility of using the process in profiling of wood for furniture production is examined in [40]. Responses such as the roughness of the machined surface and the endurance of the wire are studied. Using SEM imaging of the debris and the worn wires, it was determined that the tool life in machining of wood with a diamond wire is low [40]. The performance of the process in machining of SiC is examined in [6]. The effect of wire down-feed on surface roughness and subsurface damage is presented while surface marking due to loose abrasives is discussed. In varying the wire down-feed rate between 0.0013 and 0.013 mm/s, the surface roughness did not vary significantly staying around $0.25 \mu\text{m } R_a$. Typical roughnesses achieved using the free abrasive method vary around $0.1 \mu\text{m } R_a$ [6]. The process was shown to be effective in machining hard materials such as SiC. Furthermore, abrasive particles smaller than $20 \mu\text{m}$ were recommended to achieve improved surface roughness and to reduce subsurface damage [27]. The literature concerning fixed abrasive wire machining is limited. Much more work is required in process modeling and optimization while the continuous improvement of the wires will help in establishing the process for wafer production.

Notable Developments and Uses of Abrasive Wire Saw Technology

Apart from the literature directly concerning fixed abrasive wire saw machining, developments in related areas are of interest with respect to the development of AWEDM.

The use of larger diamond wire saws to cut steel reinforced concrete with the specific aim of dismantling nuclear power plants has been studied by Tönshoff et al. [42]. The use of diamond wire sawing has seen much use in the field of quarrying and stone cutting. Relating to the possibility of using AWEDM for profiling of complex curves, the use of abrasive wire machining in profiling marble and granite is presented in [43] and [44].

The cost of the diamond abrasives can make up a significant portion of the cost in producing fixed abrasive wires. The possibility of recycling the abrasives is thus alluring and the focus of some research. Gebhard et al. [45] describe the development of environmentally friendly techniques for stripping nickel coatings from diamond tools.

2.3 Hybrid Machining Processes

There exist numerous HMPs today, each relying on different interactions. Hybrid processes have been developed based upon many of the possible combinations of interaction, energy carriers and work media; refer to the process condition scheme in Figure 1.7. For example, the use of lasers to locally heat areas to be machined by electrochemical operations can significantly increase removal rates and machining precision as is seen in Laser Assisted Jet Electrochemical Machining. Pajak et al [46] found increases in MRR up to 54% while reducing tapering by as much as 65%. Other processes such as Electrochemical Honing and Magnetic Abrasive Finishing have been developed. More information on cross process innovations can be found at [8].

Much of the work on HMP development is based around electro-discharge and electrochemical interactions. Some examples of processes that have been developed based upon electrochemical interactions are Abrasive Electrochemical Grinding (AECG) where the addition of abrasion serves to remove the passivation layer from the machined surface thereby enhancing electrochemical material removal [47]. Electrochemical Discharge Machining (ECDM) combines both electrochemical and electro-discharge interactions, increasing material removal rates and enabling the machining of non-conductive materials [48]. The combination

of Ultrasonic Machining (USM) and ECM (USECM) improves material removal rates as in AECG using a free-abrasives in the electrolyte [49]. Due to the similarities in the actual implementation of ECM and EDM, many of the processes based upon electrochemical interaction have been concurrently developed based on the electro-discharge interactions.

2.3.1 Hybrid EDM Processes

There exist several HMPs based on EDM; some involve the simple addition of ultrasonic vibration of the tool to enhance material removal rates [48]. Others are less obvious, utilizing electro-discharge and mechanical effects to improve the hardness and wear resistance of machined surfaces as in Brush Electro-Discharge Mechanical Machining (BEDMM) [50]. The majority of electro-discharge based HMPs are Abrasive Hybrid Machining processes, where the abrasion component generally provides increased material removal rates and improved surface roughness.

Electrical Discharge Machining with Ultrasonic Assistance

To fully understand this hybrid process some information on each individual processes is required. Ultrasonic Machining (USM) utilizes an ultrasonically vibrated tool, with frequencies greater than 20 kHz [51], to drive abrasive slurry against the workpiece. The abrasives in the slurry are typically Boron Carbide, Aluminum Oxide or Silicon Carbide and are accelerated by the rapidly vibrating tool causing micro-chipping of both the tool and workpiece [51,52]. Similar to EDM, the tool forms a reverse image in the workpiece as the abrasive loaded slurry removes material. USM is most frequently used in machining of non-conducting ceramics that cannot be EDM machined, however it can be employed with almost any work material and is most effective on materials with a hardness greater than 40 HR_c [51,52]. Because USM relies upon micro chipping for material removal, the machining rates are relatively low when compared to conventional processes. Furthermore, the abrasives act on both the tool and the workpiece causing tool wear. Tool to workpiece wear ratios between 1:1 and 100:1 are possible depending on the tool and workpiece material combination [52]. Due to the similar

physical implementation, researchers have investigated the effects of Ultrasonic Vibration (USV) of the tool or electrode in EDM.

Two different implementations of USM and EDM have been reported: One an abrasive hybrid process, the other not. In the non-abrasive HMP, EDM-USV, the tool or workpiece vibrates ultrasonically, as shown in Figure 2.9, generating pressure waves in the dielectric [53]. The pressure waves generate cavitations, which causes erosion or surface pitting on both the tool and workpiece. In EDM-USV, it is recognized that the acoustic waves and cavitations improve flushing thereby increasing material removal rates and generating improved surface quality [53].

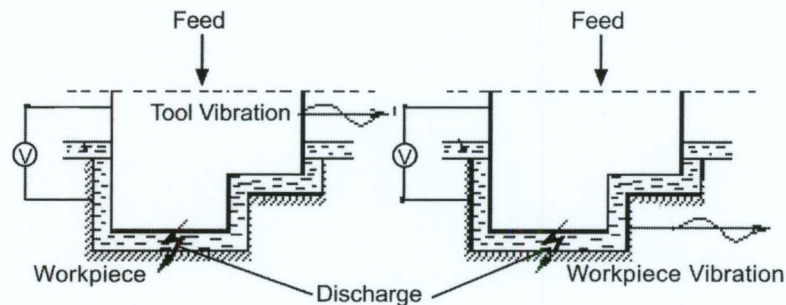


Figure 2.9: Schematic of EDM-USV (adapted from [8])

The improved surface quality or more specifically, the decreased recast layer is due to enhanced ejection of the molten metal from the craters due to the turbulence and cavitations in the dielectric caused by the ultrasonic vibration.

In a separate implementation, a more direct combination of USM and EDM is achieved. Ultrasonic Electrical Discharge Machining (USEDM) utilizes the abrasive nature of USM and the electro-erosive nature of EDM. The physical implementation is the same as in EDM with the addition of an ultrasonic actuator on the electrode or workpiece. Abrasive slurry is used where the abrasives must be non-conductive so as not to electrically short the EDM process. With non-conducting abrasives, such as diamond or aluminum oxide, the EDM process proceeds as it would normally. In USEDMD, the abrasive slurry acts as it does in USM where the abrasives impact against the workpiece removing material. The integration of EDM

and USM is intended to improve material removal rates and reduce/remove the recast layer. Improvements in MRR arise for various reasons; the addition of abrasion provides a clear mechanism for increased material removal. The vibration of the electrode also serves to increase discharge efficiency as discussed with respect EDM-USV. Less obvious is the benefit in reducing the occurrences of arcing and shortening the discharge delay time [54].

In a comparative study, Lin et al. confirmed the notion that the addition of ultrasonic vibrations increased material removal rates. Furthermore, it was found that an additional increase in material removal rates is obtained when abrasives are added to the process. Figure 2.10 summarizes these results illustrating not only the benefit in using USEDMM, but also the difference in using distilled water over kerosene. Despite finding that USEDMM produced larger surface roughnesses than both EDM-USV and EDM; Lin et al found that use of USEDMM yielded reduced recast layers when compared with EDM alone [55].

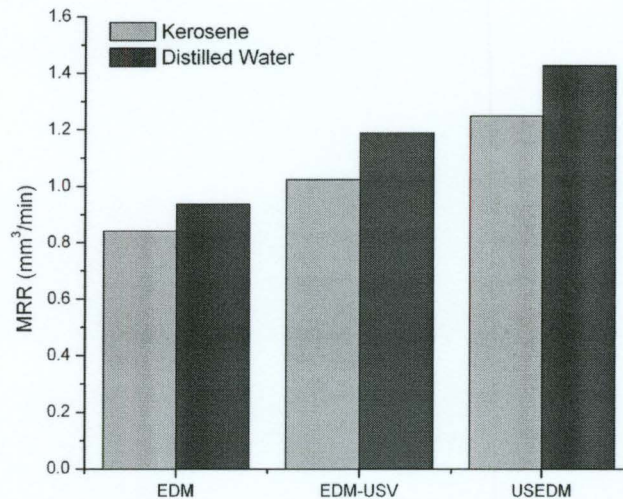


Figure 2.10: MRR comparison with EDM, EDMUS and EDM/USM (adapted from [55])

The combination of EDM and USM, either EDM-USV or USEDMM, has been shown to provide distinct advantages over the individual processes. Neither process has seen commercial development or significant academic interest with only a handful of related publications.

Abrasive Electrical Discharge Machining / Grinding

The integration of abrasion and EDM is presented here in two different, however similar forms. The material removal process in both Abrasive Electrical Discharge Machining (AEDM) and Abrasive Electrical Discharge Grinding (AEDG) is the same, only the physical implementation differs. Unlike USED, the abrasive hybrid process discussed here utilizes an electrode with fixed abrasives so that material removal occurs by two-body abrasion. The requirement for such a hybrid process is clearly apparent in machining of super hard material such as Polycrystalline Diamond (PCD), Polycrystalline Cubic Boron Nitride (PCBN), sintered carbides and other ceramics composites where diamond grinding is the most commonly used technique. The low G ratios (volume of work material removed to volume of the grinding wheel lost) and high cost of diamond abrasives are several problems associated with this processing technique [56]. Grinding of hard materials is, in general, problematic when the workpiece material hardness approaches that of diamond. High grinding forces reduce machining accuracy while wear flats form due to attritious wear further increasing the normal machining force. The grinding power in such cases has been shown to increase drastically with machining time [57,58]. To combat this effect, frequent wheel dressing is required to maintain suitable wheel topography. This results in significant loss of both wheel material and productive machining time [58].

Mechanical dressing methods are widely used, however they further the wear of the wheel by the nature of the process. In situ electro-discharge dressing is a process where an electrode is placed adjacent to the grinding wheel during machining [59]. Electrical discharges between the wheel and the electrode act to remove the bond material surrounding the abrasives; this results in a trued wheel with lower loss of wheel material [58-60]. It also allows for the creation of intricate profiles with negligible dressing forces, which helps to maintain form accuracy of the wheel [60]. Abrasive Electrical Discharge Grinding represents a step forward in this technique where discharges occur between the workpiece and the wheel bond.

To overcome the limitations in grinding and those associated with EDM; both processes are integrated into one hybrid process. Likely the earliest work on the concept in combining EDM and grinding is highlighted in publications [57,61,62] from the former Soviet Union. AEDG takes place in a form similar to Electrical Discharge Grinding (EDG), whose name is a misnomer in that no grinding actually occurs, except that the plain graphite/copper disk is replaced with a metallic bond grinding wheel. Figure 2.11 shows a schematic of the AEDG process.

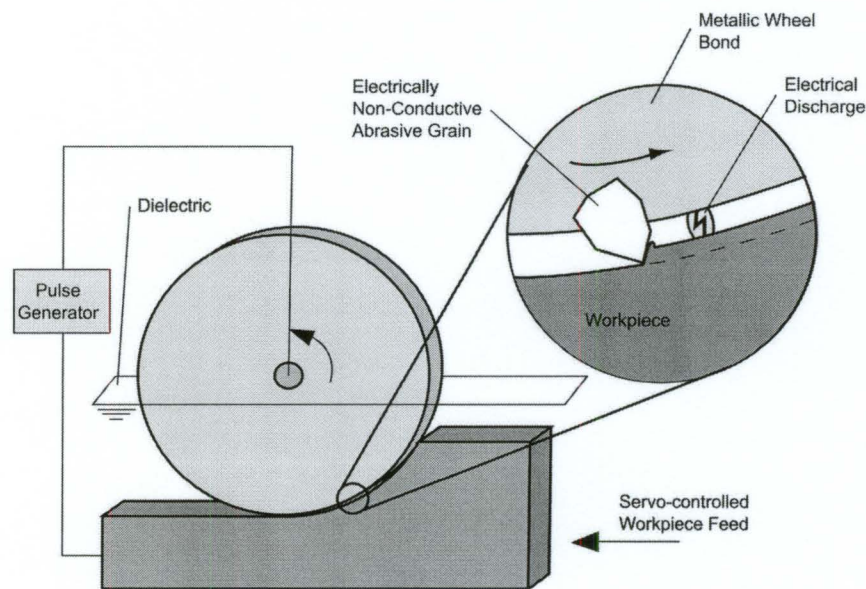


Figure 2.11: Schematic of the AEDG process

For both electrical discharges and abrasion to occur simultaneously, it is essential that the abrasive particles be electrically non-conductive. As such, the servo-control mechanism based upon the average voltage is essentially unaware that the abrasives are present. The ratio of EDM to grinding can be controlled by altering the machining gap and the relative speed between the electrodes. If the machining gap is larger than the protrusion height of the abrasives, the process is entirely EDM. If the machining gap is smaller than the abrasive protrusion height, the proportion of grinding to EDM increases as the gap size decreases.

With respect to improving upon the grinding process, experiments have shown that over time, the normal and tangential machining forces will actually decrease from the nominal grinding levels and approach a steady state. The reduction in force occurs when sufficient discharge currents are applied, and is a result of in-process dressing of the grinding wheel [63]. This effect is shown in Figure 2.12 where the percent change in the normal force, F_n , is shown over time in machining of cemented carbide.

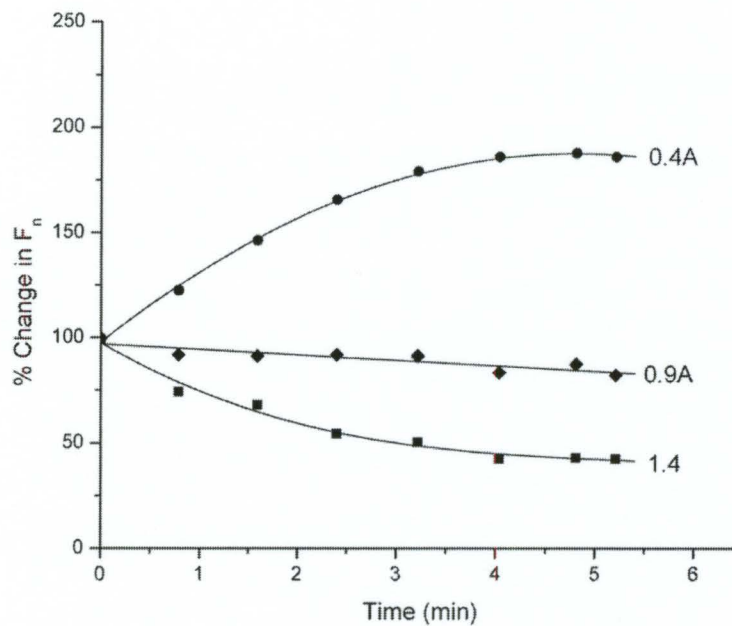


Figure 2.12: Time evolution of normal force in AEDG (adapted from [63])

The machining forces alone are not sufficient to establish the role of electrical discharges on improving grinding conditions. The MRR is a key factor in assessing the performance of any process. Figure 2.13 illustrates the effect of grinding wheel speed on the MRR at various discharge currents.

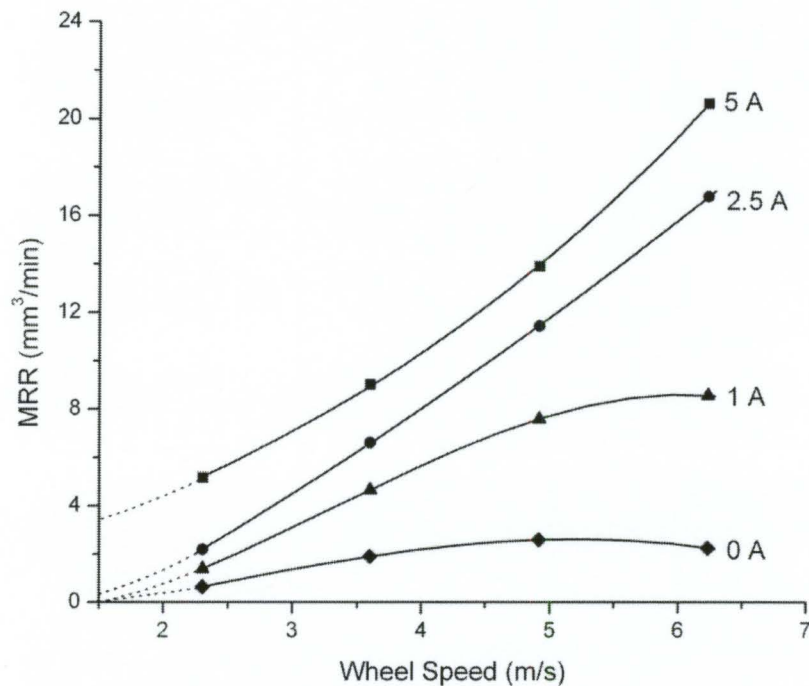


Figure 2.13: Effect of wheel speed on MRR at various discharge current (adapted from [58])

The case of zero amperes discharge current represents the case of pure grinding while the case of pure EDM can be extrapolated by extending the curves toward a zero wheel speed. This data represents experiments carried out by Koshy et al [58] where machining was performed on hardened high-speed steel. In this case, the presence of electrical discharges clearly produces an increase in MRR.

The increase in MRR with the presence of electrical discharges is also confirmed in the machining of Aluminum composites reinforced with Silicon Carbide (Al-SiC) where a 500% increase over EDG alone is obtained [47,56]. Material removal rates have also been shown to improve with electrical discharges in machining of $\text{Si}_3\text{N}_4+\text{TiN}$, PCBN and PCD [56]. Figure 2.14 shows the effect of machining time on MRR in machining of PCD under different conditions.

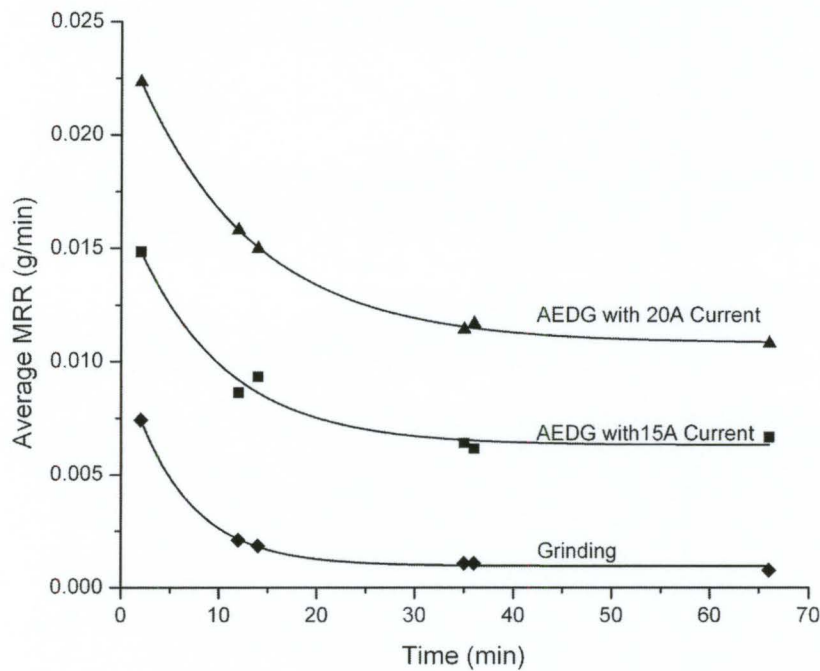


Figure 2.14: Effect of machining time on MRR in machining of PCD (adapted from [56])

From the figure, it is clear that the electrical discharges contribute significantly to material removal. Furthermore, in machining of PCD, G ratios of 0.3-0.8 were achieved, which represents a 5-10 times increase when compared to diamond grinding [56]. In machining of cemented carbides however, the combination of hardness and toughness of the material make an increase in MRR achievable at the cost of high wheel wear [63]. Abrasive Electrical Discharge Grinding has been shown to be an effective method for increasing the performance of grinding hard materials such as PCD.

In addition to the MRR and grinding forces, other responses have been researched to aid in understanding the work – tool interaction during the use of AEDG. In collecting the machining debris, Koshy et al. were able to observe the effect of discharge current on the proportion of EDM to grinding in the process [58].

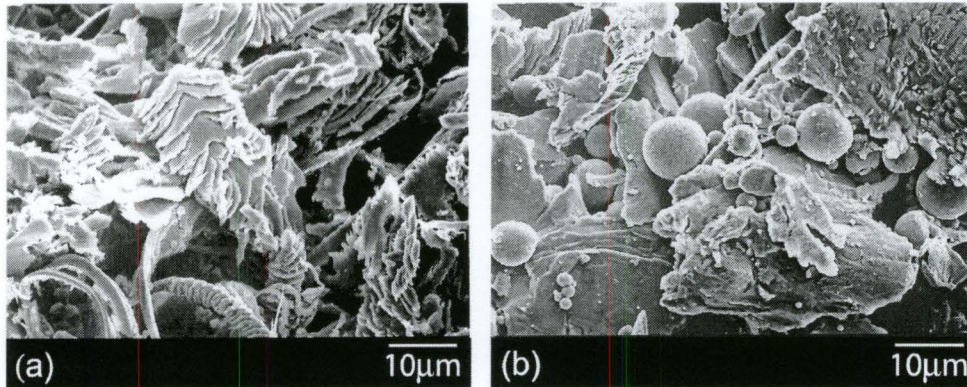


Figure 2.15: Micrographs of chips collected at discharge currents of: (a) 1A; (b) 5A [58]

SEM micrographs of the debris obtained from AEDG of HSS at different discharge currents are shown in Figure 2.15. At low discharge currents, the chip formation has a lamellar structure typical of grinding. At higher discharge current, the lamellar structure of the chips disappears and spherical particles typical of EDM debris are found [58].

The quality of a machined surface is of great importance in many applications especially when brittle materials are used. EDM, as was previously discussed inherently leaves a recast layer, which is prone to micro-cracks. Grinding too can damage the machined surface due to high machining forces and heat build-up. In applying AEDG, a machined surface that is indicative of both EDM and Grinding is obtained. Depending on the ratio of abrasion to EDM, the appearance of the surface will differ greatly as is shown in Figure 2.16.

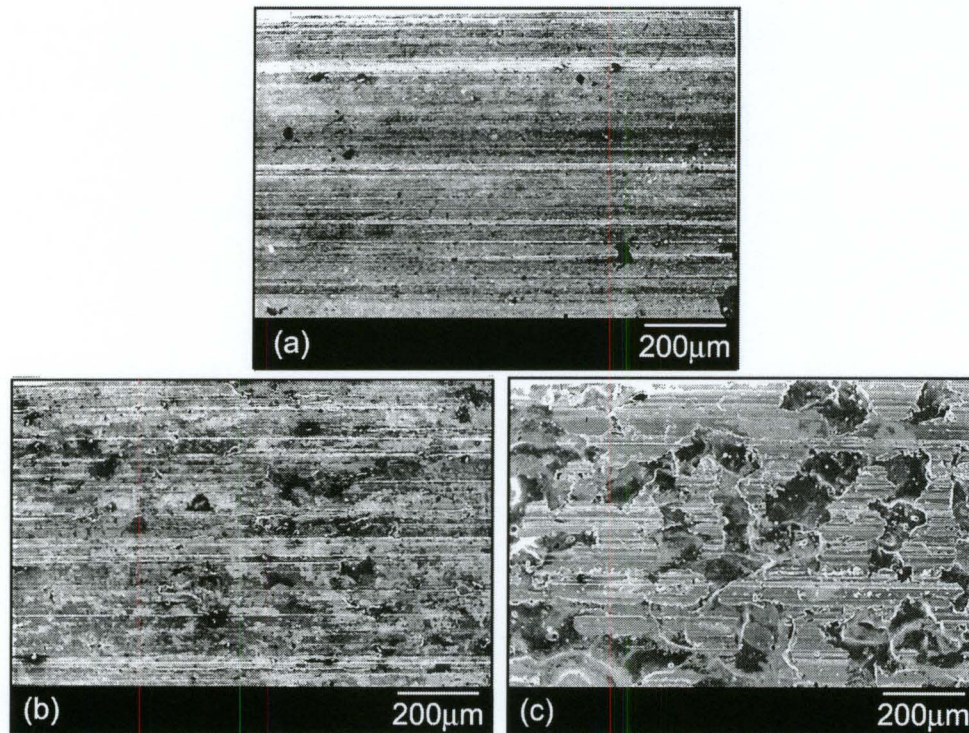


Figure 2.16: Micrographs of surfaces machined at discharge currents of: (a) 0A; (b) 1A, (c) 5A [58]

The effect of discharge current is again clearly indicated where the addition of electrical discharges causes melting of the machined surface. The extent of the melting is seen to increase with current [58]. Similarly, the surface roughness tends to increase with discharge current [56]. The problem however can be easily resolved by turning off the current during the final pass to perform pure grinding, as the melted layer is typically only several micrometers in thickness.

The machining forces in AEDG decrease with an increase in discharge current [58,63,64]. This result is in part attributed to the thermally softening of the workpiece. Due to the thermal softening, it has been suggested that less hard abrasives such as Aluminum Oxide (Corundum) might be used in place of diamond to help render the process more economical [58].

In a slightly different implementation of the technique, Abrasive Electrical Discharge Machining (AEDM) was achieved using a metal matrix composite electrode comprised of a copper binder material with Silicon Carbide (SiC) abrasives. Using a cylindrical electrode with an orientation more familiar to EDM Milling than AEDG, experiments were performed on a Die-Sinker EDM outfitted with a rotational head capable of 0-2500 rpm. Shu et al. observed successful implementation of the hybrid process in machining of mould steels with machined surfaces similar to those in Figure 2.16 [65]. When the abrasive size and process conditions are matched correctly, a 3-7 times increase in MRR over EDM was observed [65]. Figure 2.17 illustrates how the abrasive size and machining gap must be considered to properly implement the process.

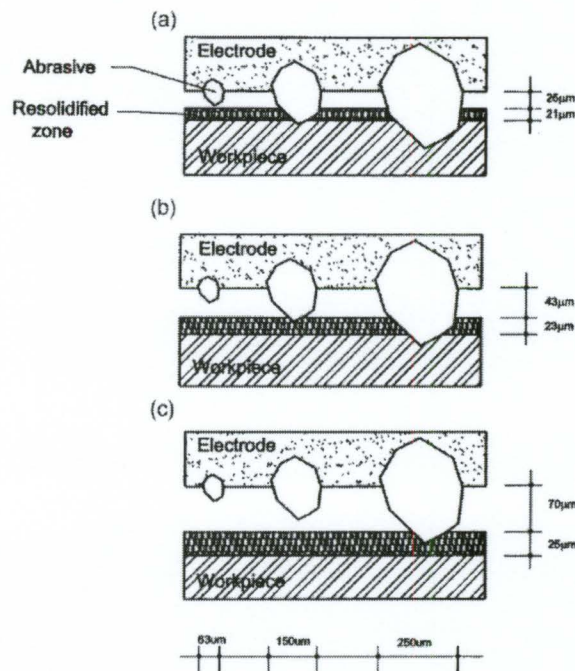


Figure 2.17: Schematic illustration of the relationship between abrasive particle size and gap width [65]

A significant portion of the available literature with respect to AEDG is focused on experimental work. Attempts to model the process have been made, though the complexity of the process requires significant simplification of the model. For example, Koshy et al.

developed a model to evaluate the reduction in normal force due to thermal softening of the workpiece. The model simulation results were found to agree well with experimental values [58]. In a more complex analysis of the process, Yadava et al. modeled the temperature distribution during AEDG [66]. In this work, finite element based mathematical models were created to simulate the AEDG process. The predictions of the temperature distribution in the workpiece due to electrical discharges are intended for use in calculating the thermal stresses in the machined component [66]. Again, the results of the simulation agree favorably well with experimentally obtained values. The FEM simulations may therefore serve to reduce the need for expensive experimental measurements to determine the workpiece temperature [66]. In an attempt to predict the machining performance in AEDG, Kozak et al. presented a comparison study between the use of Artificial Neural Networks (ANN) and Multiple Regression analysis [56]. In predicting both the surface roughness and material removal rates, the use of ANN provided better estimates than multiple regression analysis. Further, the improved estimates were obtained with less training data; hence, fewer experiments need be performed for accurate prediction using ANN [56].

Hybrid Wire Machining Processes

To date, no literature was found on the specific topic of Abrasive Wire Electrical Discharge Machining. The previous topic of AEDG is similar in principle; the geometrical implementation however, differs significantly. Two hybrid processes based on a wire orientation are acknowledged here. Due to fundamental differences in the processes, the applicability of this information in the development of AWEDM is limited.

In an extension of Electrical Discharge Grinding similar to the extension of AEDG to AWEDM, Guo et al. presented the use of an abrasive coated wire tool for use in ECM. The abrasive on the tool in this case serve the same purpose as in ECG, to remove the passivation layer. A steel wire of 2mm diameter with abrasives coated in a helical pattern was developed for use as the tool. As with AECG, higher removal rates were obtained with surface roughnesses on the order of 0.4 μm [67]

An interesting combination of processes in a wire configuration is detailed by Stelter in U.S. Patent 6,737,602 entitled “EDM apparatus and method incorporating combined electro-erosion and mechanical saw features” [68]. Intended for machining of composite workpieces comprised of a conductive metal jacket and non-conductive core, the process involves features familiar to a band saw and WEDM as shown in Figure 2.18. Example uses include sectioning of explosive ordinances with hard metal outer shells and granular or epoxy based explosive cores. The patent describes a process for cold forming of a wire to exhibit teeth, which would cut the non-conductive material, while electrical discharges machine the conductive jacket. Though the mechanical sawing action does not act in true synergy with the electrical discharges, the process illustrates how the combination of two distinct processes can overcome some of the limitations of the part processes where EDM would fail to machine the core, and sawing would fail to machine the hard outer shell.

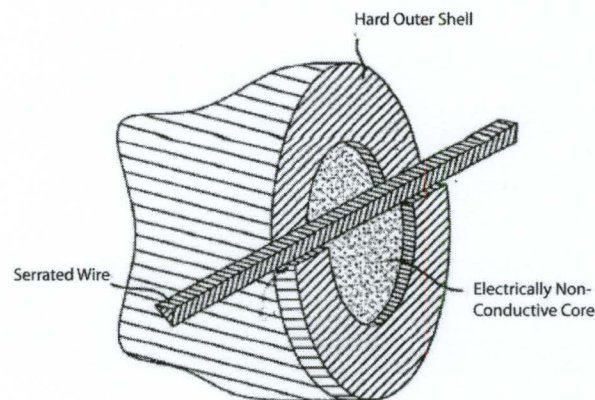


Figure 2.18: Schematic of combined Sawing - WEDM process (adapted from [68])

A review of the literature related to AWEDM has been presented. To begin to establish a body of work with respect to AWEDM, the following Chapters outline the experimental methods used throughout this work, experimental results from AWEDM testing, economics analysis and discussion.

Chapter 3

Experimental Details

Much of the work presented as part of this thesis is experimental in nature. Specific details on the equipment and parameters used in testing as well as various techniques used throughout the work are presented in this Chapter.

3.1 Experimental Apparatus

Machining experiments were performed on an Agietron Impact 2 Ram EDM system. To realize the combined Wire-EDM and abrasion process, a wire feed device was designed and built so that the process could be performed on a Die Sinker EDM. Figure 3.1 shows the machine tool while Table 3.1 outlines the machine specifications.

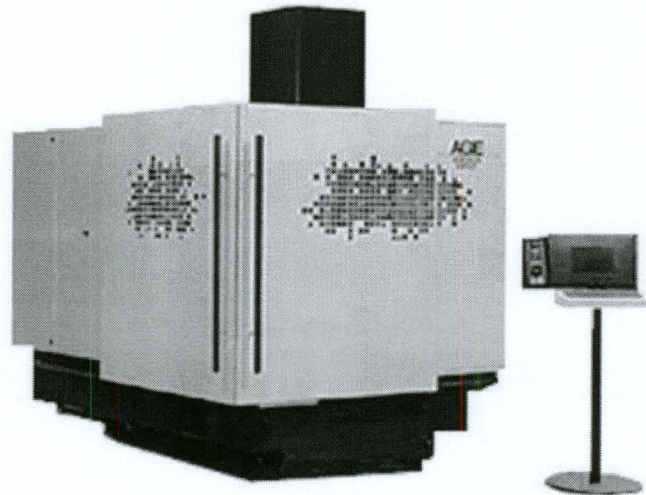


Figure 3.1: Agietron Impact 2 EDM system

Table 3.1: Agietron Impact 2 specifications

Machine Features	Machine Features 4 Axis CNC, (X/Y/Z/C) Max Working Current, 72A Max Flushing Pressure, 1.5 Bar
Dielectric	Common Wealth Oil - EDM Super Supreme Synthetic Dielectric Oil Low Viscosity (3.0 mm ² /s @ 40°C) High Flashpoint (>115°C)

A wire feed attachment, Figure 3.2, was designed to mount directly to the ram of the machine. The wire is fed from a spool through several alignment pulleys to the guiding pulleys where the wire traverses a horizontal span where the machining takes place. The guiding pulleys are adjustable so that the span can be set appropriately for the machining to be performed. From the guidance pulleys, the wire is fed around a drive roller while spring loaded pinch rollers provide the necessary traction. From there, the wire is fed through a polyethylene tube to a plastic receptacle for disposal.

Once designed and built, the apparatus was tested and calibrated. First, the maximum wire tension was tested, and then the possible wire speeds were determined. Since the motor is of limited power, the maximum permissible wire tension was first determined by running the wire feed and increasing the drag on the wire spools until the motor could no longer overcome the friction. Once this point was reached, the wire tension was determined by suspending weights from the wire until the drag on the spool could no longer hold the applied weight. The wire tension is then simply calculated by multiplying the applied weight and the acceleration due to gravity ($g = 9.81 \text{ m/s}^2$). To measure the minimum and maximum wire speeds, a regulated DC power supply and a digital tachometer were used. The specification for the apparatus as determined are listed in Table 3.2.

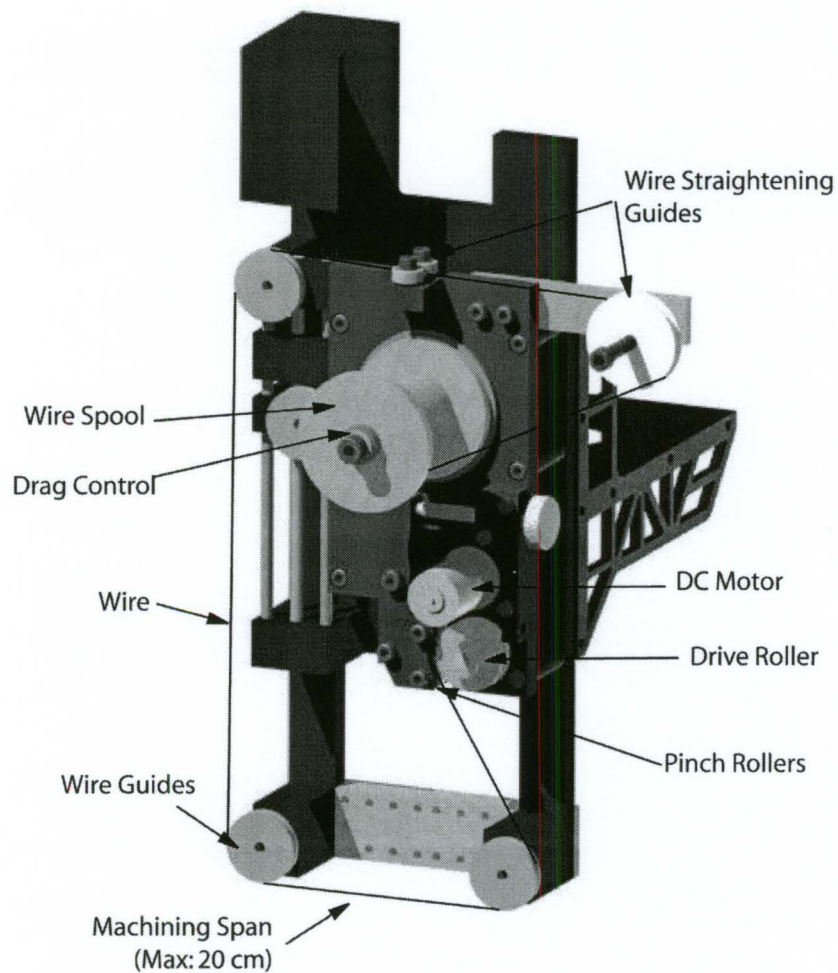


Figure 3.2: 3-D rendering of the wire-feed apparatus

Table 3.2: Wire feed apparatus specifications

Wire Tensioning	Adjustable Drag System Maximum Tension, 8 N
Wire Drive	DC Motor Driven Pinch Roller System Min, Max Wire Speed; 3, 8 m/min
Spool Sizing	Holds Standard DIN 100 Spool or Smaller

3.2 Experimental Procedure

Throughout the experimental work conducted, various sets of test conditions, apparatus and specimens were used. These test parameters were chosen for the specific experimental applications are listed in their respective section.

3.2.1 Machine Characterization and Process Modeling

The purpose of the testing as part of the Design of Experiments (DOE) was to characterize the conventional WEDM process and model several process responses with respect to various inputs. The responses of interest were the material removal rate, recast layer thickness and the machining gap.

Experimental Setup and Measurement Techniques

In order to capture these responses, an experimental setup was designed to allow for simple calculation of the material removal rate, accurate measurement of the machining gap and recast layer. The specimens used in the testing were of AISI M2 tool steel. To have standardized samples, 2mm diameter hardened and ground drill blanks were used. The material removal rate was determined by the geometry of the cut performed and the length of time it takes to complete the cut. The use of the standard drill blanks ensured that the cut geometry remained constant while the time was measured using a digital timer. To avoid confusion between volumetric and areal removal rates, as is conventionally used for WEDM, the term Areal Material Removal Rate (AMRR) in mm^2/min , is used in discussing WEDM and AWEDM operations. The AMRR is calculated as follows:

$$AMRR = \frac{A_m}{t} \quad (3.1)$$

$$A_m = \frac{\pi}{4} D^2 \quad (3.2)$$

where t is the machining time and A_m is the machined area given by Equation (3.2) and D is the diameter of the drill blank.

A fixture was used that allowed the samples to be cut in half while holding each half in place so that the kerf could be measured. Based upon the measured kerf width and known wire diameter, the machining gap was determined. Since the machining gap is on the order 5-50 μm , a digital microscope, computer and calibrated software were used to measure the gap to a resolution of 0.1 μm .

Apart from the benefit of standardized samples in using the drill blanks, the hardened M2 tool steel provides a clear distinction between the base material and the recast for inspection. The details for the metallurgical sample preparation and recast layer measurement are outlined in Chapter 3.

Test Parameters and Design of Experiments

In an effort to characterize the operation of the machine tool, a series of design of experiments were carried out as is detailed in Chapter 4. The progression of the DOE was to conduct a two-level design with repeated centre points to check for curvature in the responses while obtaining an estimate of the error involved. Once the presence of curvature was confirmed, the original test design was expanded to a Face-Centered Composite Design (CCF) to capture the non-linear effects.

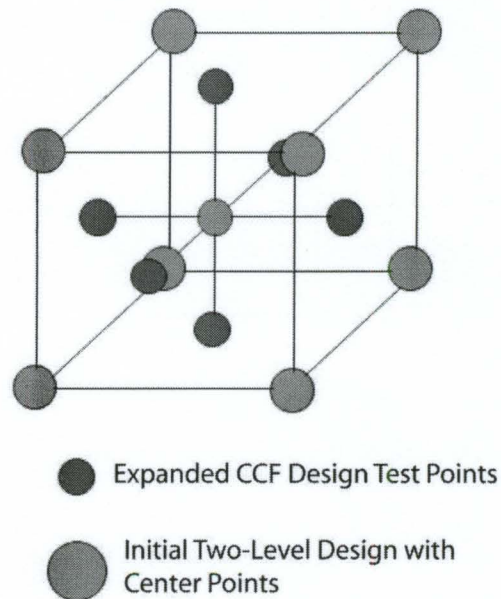


Figure 3.3: Illustration of DOE with three parameters

The parameters used in the CCF testing and their levels are listed in Table 3.3 while Figure 3.3 graphically illustrates the principle of the initial design and the expanded CCF design for three variables.

Table 3.3: Parameters and their levels as used in the DOE

<i>Parameter</i>	<i>Low</i>	<i>Centre</i>	<i>High</i>
Peak Discharge Current, I (A)	10	17	29
Open Circuit Voltage, OCV (V)	120	150	180
Pulse ON Time, T (μ s)	1.64	2.7	4.9
Duty Factor, DF (%)	10	30	50

It is interesting to note that variation in both the peak discharge current and the pulse-on time are not linear. This is because the selectable parameters on the machine increase logarithmically. When these parameters are used in the analysis and further discussion, they are referred to by the logarithm of their value in order to linearize them. There are several other machine parameters not varied in the tests, as are listed in Table 3.4.

Table 3.4: Constant parameters used in DOE testing

<i>Parameter</i>	<i>Setting</i>
Compression	20 %
Servo - Gain	20
Flushing	1 Bar
Wire Speed	5.5 m/min
Wire Type	Intech Superbrass 500

3.2.2 *Abrasion Assisted WEDM Testing*

The experiments performed in this section were used to establish the functionality of the AWEDM process. The effect of changing the EDM parameters, wire types and workpieces are examined. Numerous responses were observed including the material removal rate, recast layer, generated surfaces and machining debris.

Experimental Setup and Measuring Techniques

Upon determining suitable machining parameters to be used in the combined process, it was realized that a new experimental setup was required. Due to the low material removal rates that were obtainable to maintain stable machining, and the excessive wire costs that would be associated in conducting tests using the setup outlined in Section 3.2.1 a new setup was devised. In the new setup, a simple SAE 1018 steel plate, 1.2 mm thick was used as the test specimen. To conserve wire, machining time was limited to 5 minutes.

Calculation of Material Removal Rates

The AMRR is as before, Equation (3.1), except the machined area is that of a rectangle and is calculated as:

$$A_m = d_c * t_w \quad (3.3)$$

where d_c is the machined depth and t_w is the thickness of the steel plate. In this setup, the length of the cut is measured using a toolmaker's microscope with digital micrometers of 0.001 mm resolution.

Current and Voltage Waveform Analysis

To assess the stability of the EDM component of the process, both voltage and current waveforms were acquired using a digital acquisition system. A DC voltage probe was used with a 50:1 voltage step-down in order to reduce the voltage signal to a level that could be acquired by the acquisition system. To obtain the current signal, an inductive coil type sensor was installed. The specifications for the current sensor are given in Table 3.5.

Table 3.5: Current sensor specifications

<i>Sensor Specification</i>	
Sensitivity	0.1 V/Ampere +1/-0%
Maximum Peak Current	5000 Amperes
Maximum RMS Current	50 Amperes
Drop Rate	0.9% / millisecond
Useable Rise Time	20 nanoseconds
Low Frequency 3dB point	1 Hz
High Frequency 2dB point	20 MHz

The signals from the voltage probe and current sensor were acquired using a National Instruments data acquisition system coupled with LabView software. The data acquisition specifications are given in Table 3.6.

Table 3.6: Data acquisition system specifications

<i>Component</i>	<i>Details</i>
PC Specifications	AMD X2 Processor 2 GB Ram 4 x 250 GB WD Hard drive in RAID-0
Data Acquisition Card	National Instruments PCI-6115, 64MS onboard memory 4 Channel Simultaneous Sampling 10 MS/s Max Sampling Rate
Software	LabView 8.2 DAQMx 8.2 Hardware Drivers

In order to perform statistical analysis on the waveform data, a large number of samples were taken. To accomplish this, one second (10 million data points) of waveform data was acquired once per minute during testing. Based upon the machining pulse-on and pulse-off times used, this corresponds to a possible 30 thousand discharges captured during testing.

Analysis of the waveform data was accomplished using Matlab. A script based upon the criterion as detailed by Snoeys et al. was used to analyze the signals for proper discharges, arcing and electrical shorting [69].

Measurement of the Normal Machining Force

The presence of cutting forces in the AWEDM process provides a clear indication that mechanical abrasion is occurring. Initially, a piezoelectric dynamometer was designed and built to measure these cutting forces. Unfortunately, the low forces and long cutting durations associated with the process made reliable force measurement difficult. Further, the presence of a flowing dielectric proved to deteriorate the reliability of the measurements.

In the work by Clark et al. [26], a capacitive sensor was used to measure the angle of wire bow during a wire saw operation. From the angle and a known wire tension, they were able to determine the Normal Cutting Force Component. Unfortunately, due to the electrical

nature of the EDM process, a capacitive sensor could not be used. To overcome this, the wire bow was measured after each test noting the indicated depth on the Z-axis display of the machine tool. Figure 3.4 illustrates this technique.

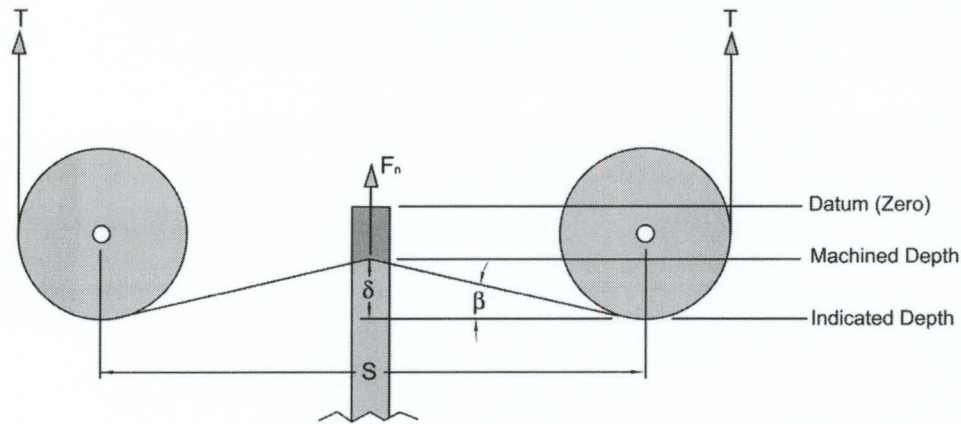


Figure 3.4: Geometric interpretation of the cutting force calculation

Once the machined depth was measured using a microscope, the wire bow, δ , is readily determined by subtracting the machined depth from the indicated depth. Once the wire bow is determined, the normal machining force, F_N , can be calculated based on the geometry and known wire tension as is shown in Equations (3.4) through (3.7). Because the workpiece is very thin compared to the span of the pulleys, S , the force, F_N , is assumed to be a point load.

$$\delta = \text{Indicated Depth} - \text{Machined Depth} \quad (3.4)$$

$$\beta = \tan^{-1}\left(\frac{S}{2\delta}\right) \quad (3.5)$$

$$\Sigma F_y = 0 = F_n - 2T \sin(\beta) \quad (3.6)$$

$$F_n = 2T \sin(\beta) \quad (3.7)$$

Test Parameters

Upon establishing a suitable set of test parameters through trial and error, testing to evaluate the performance of the process began. To accomplish this, a simple two parameter, four level test matrix was employed. The use of a design of experiments allows for minimal

testing, as well as improved understanding of the relationship between each of the parameters and responses. The parameters used in these experiments and the reasoning for their selection is detailed further in Chapter 4, while the levels used are detailed in Table 3.7. Furthermore, Table 3.8 lists the machining parameters that were held constant during these tests.

Table 3.7: Parameters and levels used in 4-level AWEDM testing

<i>Parameter</i>	<i>Values</i>			
Peak Discharge Current (A)	1.2	2.4	4.4	8
Average Voltage (V)	108	126	144	162

Table 3.8: Constant machine settings used in 4-level AWEDM testing

<i>Parameter</i>	<i>Setting</i>
Pulse-ON time (μs)	4.9
Pulse-OFF time (μs)	100
Open Circuit Voltage (V)	180
Servo - Gain	20
Flushing Pressure (bar)	1.0
Wire Speed (m/min)	5.5
Wire Tension (N)	6.8

3.3 Other Procedural Techniques

Apart from setting up and performing the experiments as detailed previously, several other techniques were employed in this research. Imaging, metallurgical sample preparation and recast measurement techniques are presented here.

3.3.1 Diamond Wire Characterization

In order to characterize the diamond abrasive wire, various techniques were employed. Initially, it was attempted to measure the protrusion height of the abrasives using a Scanning Electron Microscope (SEM). This method proved to be very time consuming and impractical for characterizing the distribution.

The use of an optical microscope does not allow for easy depth measurement. The use of sophisticated software, however, allows users to stitch images taken in a series of focal depths to create a 3-D image as shown in Figure 3.5. From these images, 3-D measurements can be made, however the focal depth stepping size, of approximately $10\ \mu\text{m}$, does not provide sufficient resolution to measure abrasives protrusion heights that are approximately $10\text{-}50\ \mu\text{m}$.

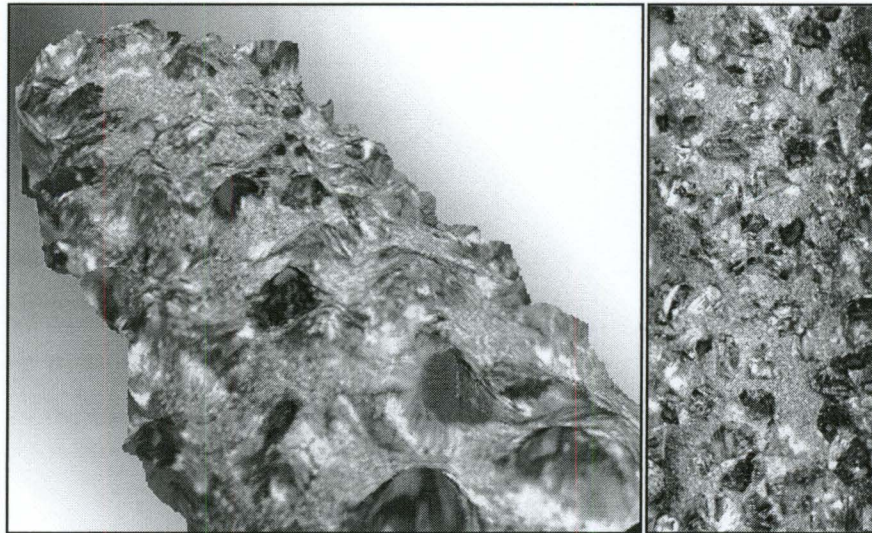


Figure 3.5: 3-D optical images of fixed abrasive wire after gold sputtering

To obtain a large number of accurate measurements of the grain protrusion heights, white light interferometry techniques were ultimately used and to prevent the diamond grains from refracting the light, the wires were sputtered with a thin layer of gold. Taking four 25mm sections of each type of wire, white light interferometry was used to measure the 3-D surface map as shown in Figure 3.6. From the 3-D surface map, section profiles at the location of an abrasive were taken to measure and record the abrasive protrusion height.

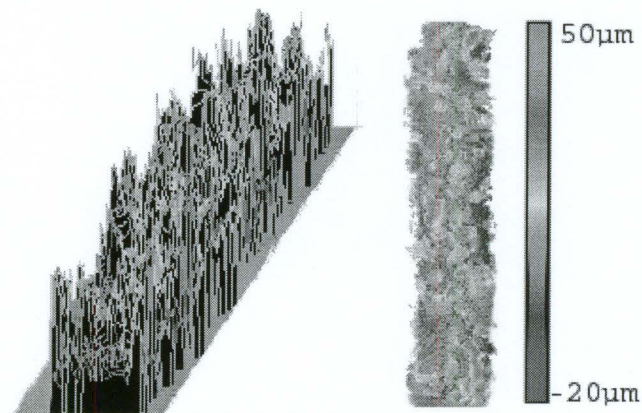


Figure 3.6: 3-D surface map of abrasive wire obtained using white light interferometry: isometric view (Left), contour view (Right)

3.3.2 Sample Preparation

Before the recast layer was measured, the machined samples were prepared. To do this, a schedule of mounting, grinding, polishing and etching was followed for each sample. Three different preparation schedules were used for the three materials examined as part of this work. The first step in the sample preparation was to mount the samples in a Bakelite mould. Graphite reinforced Bakelite was used to achieve good edge retention during the grinding and polishing operations. Table 3.9 outlines the specific schedules for each sample type.

Table 3.9: Details on the sample preparation procedure

	<i>AISI M2</i>	<i>AISI 1010</i>	<i>INCONEL 600</i>
Grinding	500 SiC 1200 SiC 4000 SiC	320 SiC	500 SiC 1200 SiC
Polishing	1 μ m/DP-NAP	9 μ m/MD-Largo 3 μ m/DP-DAQ 1 μ m/DP-NAP	3 μ m/DP-DAQ 1 μ m/DP-NAP 0.5 μ m/OPS-CHEM
Etching	2% Nital	2% Nital	10 ml HCL 30 ml HNO ₃ 20 ml Glycerol

Polishing specifications are given according to the automatic polisher used. A specification of 1 μ m/DP-NAP, for example, corresponds to 1 μ m polishing compound and DP-NAP polishing cloth.

3.3.3 Measurement of the Recast Layer

Once the samples were prepared, the recast layer was measured using a digital microscope. Due to the irregular nature of the recast layer, the thickness was calculated as an average where the area of the recast layer was measured using imaging techniques. This area was then divided by the width of the area under inspection, which is mathematically equivalent to the Arithmetic Mean Surface Roughness, R_a .

3.3.4 Debris Collection and Surface Examination

Other information that was collected for the AWEDM tests were sample machined surfaces and process debris, for examination in a SEM. For the desired parameters, an extended cut was performed in the thin steel plate. The machining was ceased once the cut reached a length of at least 3mm so that there would be a sufficient amount of surface to be examined.

To collect and observe the machining debris in the SEM, a special technique was developed. The machining debris was collected during the extended tests described previously for generating the surfaces for examination. During these tests, a magnet was placed directly under the machining location. A thin stainless steel sheet was used to cover the magnet and collect the debris. Once the machining was completed, the stainless steel cover was removed and placed in a vial. To prepare the sample for observation in the SEM, the sample was cleaned to remove the dielectric. To do this, Ethyl Alcohol was used to rinse all the debris off the stainless steel cover into the vial. The vials were then placed in an ultrasonic bath to help separate the debris from the oil. Letting the debris settle to the bottom, the top 80% of the oil-alcohol mixture was removed from the vial using a syringe. The debris was cleaned once more

with Ethyl Alcohol after which as much liquid as possible was removed without disturbing the debris. The vials were heated with the lid off to evaporate any of the remaining alcohol. Once the debris was dried, it was collected and placed on a SEM sample stub. Since the debris was loose on the surface and contained some non-conductive particles, the samples were sputter coated with a ~25 nm layer of gold. This gold layer helps prevent the non-conductive particles from charging inside the vacuum chamber. SEM images were taken of each sample as required.

Chapter 4

Results and Discussion

As the concept of AWEDM is a novel one, this work is the first in the area. The experiments performed therefore cover a wide basis in order to lay the foundation for future work. The experimental work presented here is introduced in consecutive order, describing the methodology used in the development of this process. Figure 4.1 provides a graphical illustration of this methodology where each section corresponds to a process in the flow chart.

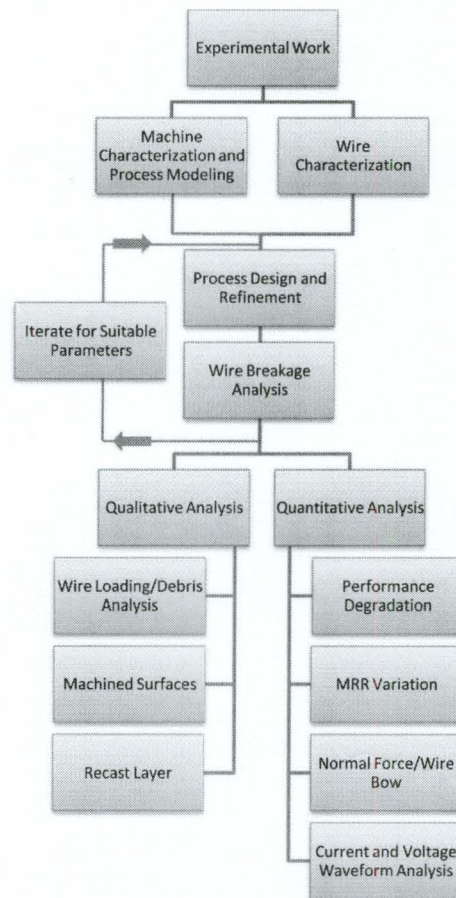


Figure 4.1: Flow chart outlining the experimental work presented in Chapter 4

4.1 Experimental Assessment of the Conventional WEDM Process

Traditionally the specific operating conditions in EDM for a given machine are specific to the machine manufacturer and are determined through their own experience. Further, most machine tool manufacturers use proprietary control systems with specific parameters often unique to each machine. When operating outside the standard operating regime of the machine, it is often necessary to perform in-house experimentation [70]. These experiments can provide the operator with improved knowledge on how changing the EDM parameters alter the process. In the following sections, two designs of experiments and corresponding analyses were employed to understand the effects of certain EDM parameters on various responses. The experimental details on the nature of the design of experiments, the analysis type and the various techniques used in measuring the responses are outlined in Chapter 3.

4.1.1 Linear Modeling

Using a four factor, two-level full factorial DOE with centre points, regression models were created to understand machining characteristics in the conventional wire EDM process. The measured responses are the material removal rate (MRR), machining gap width and the recast layer thickness. The Four EDM parameters considered to have the most significant impact on these responses are Peak Discharge Current (I), Open Circuit Voltage (OCV), Pulse-ON time (T) and Duty Factor (DF). To obtain the desired duty factor for a given on time, the pulse-off time was varied according to the relationship:

$$DF = \frac{T_{ON}}{T_{ON}+T_{OFF}} \quad (4.1)$$

Preliminary models were built for all three responses to assess their validity. For the material removal rate, a linear model provided a good fit to the data with an adjusted R² of 99.32%. The inclusion of repeated centre points in the DOE allowed for better assessment of the models, where they provide an indication of both curvature and repeatability. Using Analysis of Variance (ANOVA) to assess the model results for the MRR indicated the significant sources in the model as shown in Table 4.1. In general, high values of the 'F'

statistic and low values of the ‘P’ statistic indicate that the corresponding source has a significant influence on the model. For the remaining analysis a significance level of $\alpha=5\%$ is used. To determine if an effect is significant, the ‘P’ statistic should be less than the significance level.

$$\text{if } P > \alpha, \text{ accept the null hypothesis} \quad (4.2)$$

$$\text{if } P < \alpha, \text{ the effect is significant} \quad (4.3)$$

From this model, the main effects are the most significant source, while two and three way interactions have some influence. Four way interactions, however, do not have a statistically significant influence.

Table 4.1: F and P statistics from ANOVA results for MRR

<i>Source</i>	<i>F Statistic</i>	<i>P Statistic</i>
Main Effects	480.24	0
2-Way Interactions	91.78	0
3-Way Interactions	42.45	0.002
4-Way Interactions	6.72	0.061
Curvature	293.59	0
Adjusted $R^2 = 99.32\%$		

Furthermore, based on the ‘F’ and ‘P’ statistic, it is apparent that there exists significant curvature in the model. Similarly, in modeling machining gap the ANOVA results, Table 4.2, indicated that curvature was as significant as the main effects.

Table 4.2: F and P statistics from ANOVA results for Gap

<i>Source</i>	<i>F Statistic</i>	<i>P Statistic</i>
Main Effects	43.01	0.002
2-Way Interactions	14.57	0.011
3-Way Interactions	12.55	0.016
4-Way Interactions	36.13	0.004
Curvature	46.65	0.002
Adjusted $R^2 = 94.96\%$		

For the recast layer thickness, the ANOVA results, as shown in Table 4.3, indicate that a linear model was sufficient, though it only explained 67% of the variation in the recast thickness.

Table 4.3: F and P statistics from ANOVA results for Recast

<i>Source</i>	<i>F Statistic</i>	<i>P Statistic</i>
Main Effects	11.31	0.019
2-Way Interactions	1.57	0.344
3-Way Interactions	0.57	0.702
4-Way Interactions	0.27	0.632
Curvature	0.28	0.624
Adjusted $R^2 = 67.48\%$		

From these preliminary analyses, it was found that a two-level design of experiments was insufficient to characterize the curvature associated with the MRR and Gap responses in relation to the input parameters. Though the linear model was deemed sufficient for the recast layer thickness, its response was included in the expanded analysis to verify that the linearity held true. The following section contains the details and results from an expanded DOE analysis.

4.1.2 Expanded Analysis

As the preliminary results indicated significant curvature within the response space of the DOE, a more expanded analysis was required. To account for the curvature, a CCF design of experiments is used. One of the benefits of using a designed set of experiments is the ability to expand the model to a higher level without having to redo a large set of experiments. In this case, the original two-level factorial design with centre points was expanded to a face centered central composite design as discussed in Chapter 3.

In developing the models for each of the responses presented, a process of model refinement was used. In refining the model, an improved fit was obtained by eliminating predictors that do not contribute in a significant manner to the response or that worsen the

model fit to the data. A predictor is an input to the model and is based on the DOE inputs as well as their squares and combination thereof. The significance of a predictor is based on the student's 't' statistic. The critical value of this statistic for the models created herein is 2.040 for a problem with 31 degrees of freedom and a 5% significance level¹. Aside from the significance level of the predictors, the ANOVA provides a measure of the lack of fit. For this parameter, the 'P' statistic is used to determined significance, where if $P > \alpha$, the lack of fit is not significant.

4.1.3 Modeling of the Material Removal Rates

In characterizing the machine tool and assessing the WEDM process, it is important to understand how the parameters of interest affect the material removal rate, one of the most important process responses. In terms of developing the AWEDM process, understanding how the material removal rate is affected by the input machining parameters is important in determining the source of improvement when the abrasion-assisted process is tested.

From the experiments performed, a model with a very good fit was achieved with an adjusted R^2 value of 80.6%. The parameters used in the model as well as the calculated regression coefficients and 't' statistics are shown in Table 4.4

Table 4.4: Model terms, regression coefficient and 't' statistics for MRR

<i>Term</i>	<i>Regression Coefficients</i>	<i>t Statistic</i>
Constant	-1.97832	-2.057
log(T)	3.26287	4.767
DF	-0.11476	-3.247
log(I)	1.90146	2.702
DF*DF	0.00153	3.899
log(T)*DF	-0.06868	-3.556
DF*log(I)	0.05005	2.520
Adjusted $R^2 = 80.6\%$		

¹ The 't' distribution is double sided, thus a value of $\alpha = 0.025$ is used in determining the critical value.

The regression coefficients obtained from the model show the effect and influence of the input parameters. As theory would predict, the material removal rate increases with an increase in pulse-on time and peak discharge current. The effect of duty factor and the parameter interactions are more complicated and are best visualized using the contour plot, as is shown in Figure 4.2 to Figure 4.4

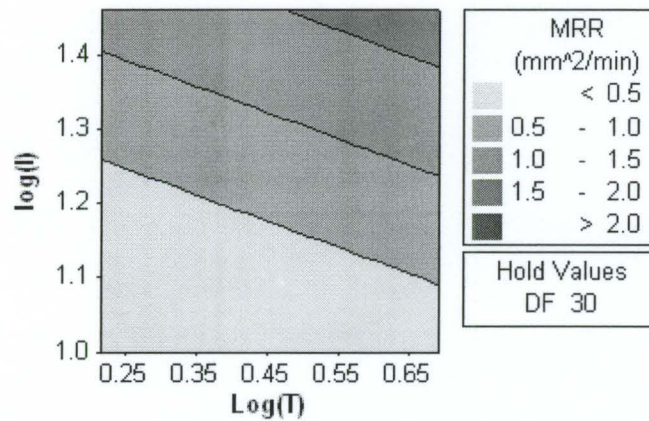


Figure 4.2: Contour plot for MRR response, $\log(I)$ - $\log(T)$

The trends in Figure 4.2 behave consistently with no curvature. There is a direct relationship between the peak discharge current, the pulse-on time and the MRR. It is clear that an increase in either of these parameters results in an increase in the MRR within the operating domain.

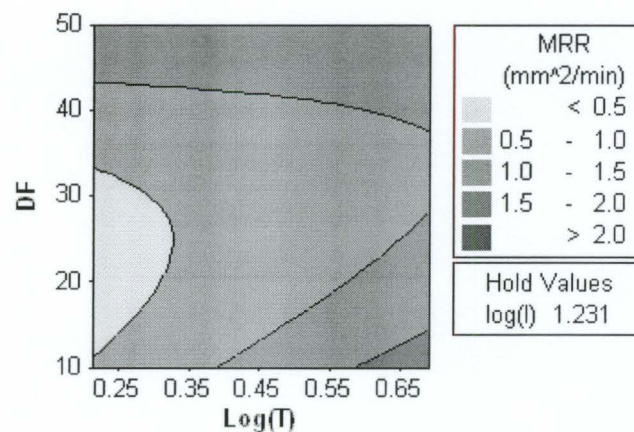


Figure 4.3: Contour plot for MRR response, DF - $\log(T)$

The effect of duty factor and its interaction with the discharge time shows an optimum. For very short discharge periods, a high duty factor can be used to increase machining rates. As the discharge duration increases, two high MRR regions exist. When T is high and duty factor is high, discharges will be more frequent; but the process will tend to be less stable. With a low duty factor, the gap has more time to regenerate, and discharging is more stable.

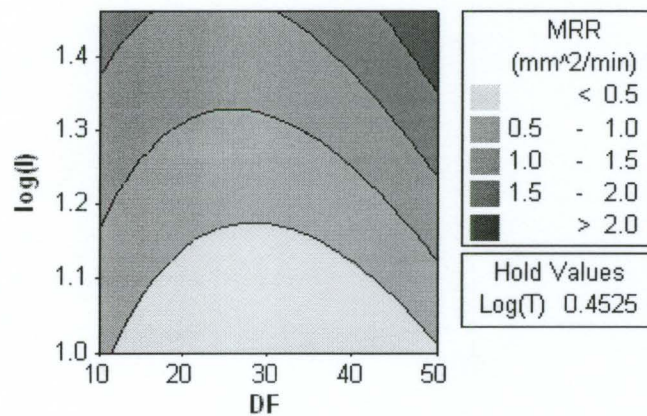


Figure 4.4: Contour plot for MRR response, $\log(I)$ -DF

Similar to the interaction between the pulse-on time and the duty factor, Figure 4.4 shows optimal regions for operation for peak discharge current and duty factor. This result is again likely attributable to machining stability and the frequency of discharges.

From the preceding model, it is important to note the increasing MRR with discharge energy. The duty factor is an important parameter with respect to the material removal rate in that the MRR is strongly dependent on the stability of the process, which is strongly influenced by the duty factor. Furthermore, for a given pulse-on time, a change in the duty factor directly relates to a change in the pulse-off time and thus the productive machining time. The open circuit voltage was found to not have a significant effect on the MRR over the operating region studied. This result is further discussed in Section 4.1.7.

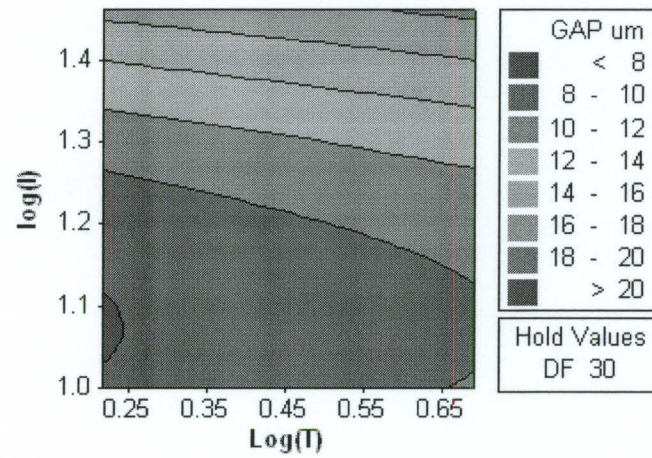
4.1.4 Modeling of the Machining Gap

With respect to AWEDM, the gap width is perhaps the most important in terms of process control. It is therefore necessary to obtain an understanding of how the machining gap varies with different input parameters. From the experimental data, a refined model was created that explained most of the variation in the data with an R^2 of 88.6%. The input parameters, their corresponding coefficients and 't' Statistics are indicated in Table 4.5.

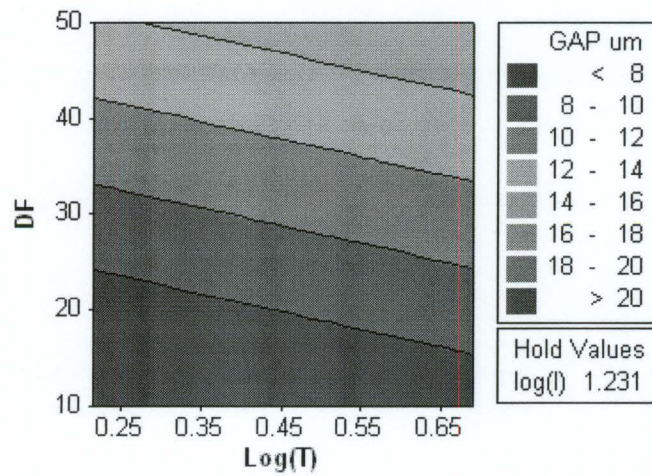
Table 4.5: Model terms, regression coefficient and 't' statistics for Gap

<i>Term</i>	<i>Regression Coefficients</i>	<i>t Statistic</i>
Constant	83.164	3.774
log(I)	4.098	2.289
DF	-0.343	-2.813
log(l)	36.438	-3.807
log(I)*log(l)	57.105	3.941
DF*log(I)	0.46	4.707
Adjusted $R^2 = 88.6\%$		

The regression coefficients indicate the relationship between the input parameters and the machining gap. Further, these coefficients could be used to predict the machining gap for a given set of input parameters. The following contour plots provide a visual interpretation to the effect of the input parameters.

Figure 4.5: Contour plot for Gap response, $\log(I)$ - $\log(T)$

From Figure 4.5 and Figure 4.7 it is clear that the machining gap tends to increase with an increase in peak discharge current. This increase is expected as higher currents produce more debris in the gap and an increase in gap debris is known to increase the machining gap [10].

Figure 4.6: Contour plot for Gap response, DF - $\log(T)$

In Figure 4.5 and Figure 4.6, it is clear that the pulse-on time has a slight increasing effect on the machining gap. This can also be attributed to an increase in machining debris as in the case of the peak discharge current.

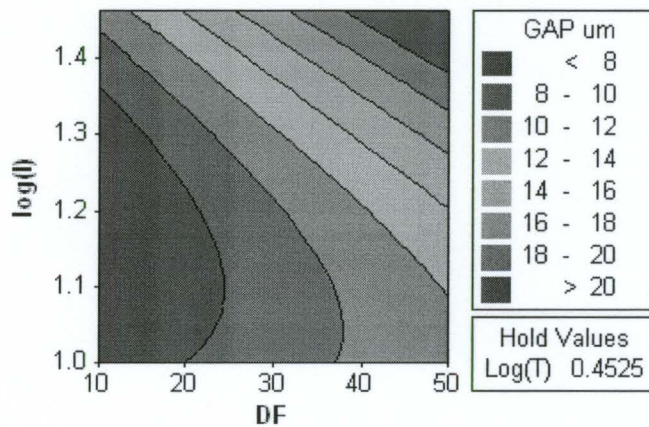


Figure 4.7: Contour plot for Gap response, $\log(I)$ - DF

Figure 4.7 shows the most significant changes and indicates that duty factor and peak discharge current are the most important factors that affect the gap size, where an increase in either factor causes an increased gap. The increase in gap size with duty factor is due to both an increase in gap contamination, where for constant flushing conditions the gap will become more contaminated, and an increase in the average gap voltage as a result of shortened pulse-off times.

What is perhaps most interesting to note is that the open circuit voltage has no significant effect on changing the machining gap. This finding is contrary to expectations, as the machining gap is servo-controlled with feedback from the average gap voltage. This result is discussed further in the Section 4.1.7.

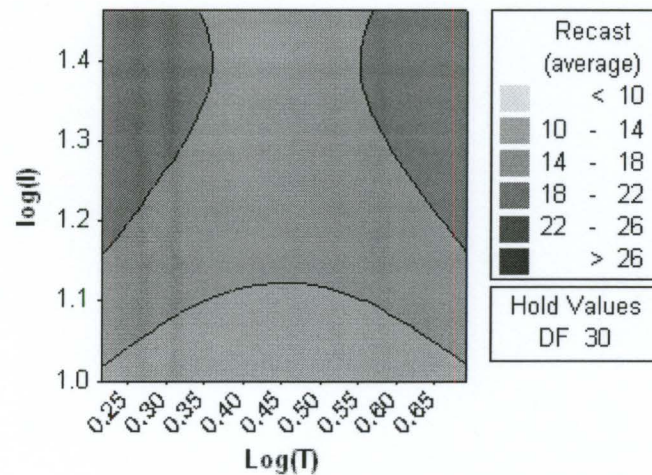
4.1.5 Modeling of the Recast Layer Thickness

The formation of recast layer is inherent to the EDM process. The depth of this recast layer provides an indication as to the depth at which the material is melted from a discharge. In implementing AWEDM, knowledge of this depth can help to select parameters in order to minimize or eliminate the recast layer. Though the linear model discussed in Section 4.1.1 for the recast layer was deemed sufficient, analysis of the expanded experimental results explained roughly 82% of the data, a significant improvement over the linear model. In the refined model, the parameters are as listed in Table 4.6. Note that the open circuit voltage has here too been found to have little effect on the response.

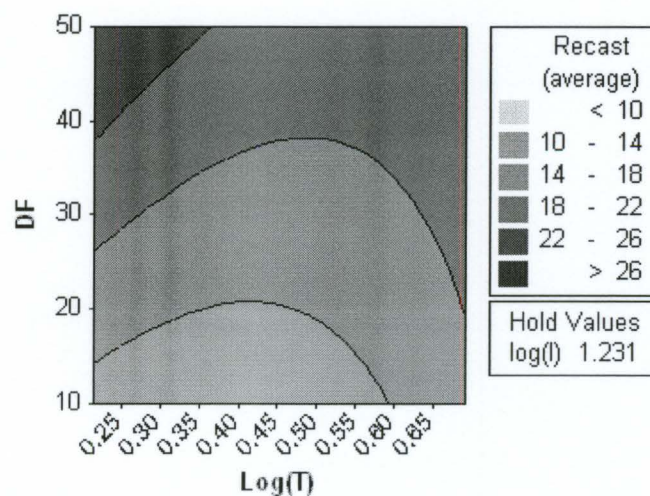
Table 4.6: Model terms, regression coefficient and 't' statistics for Recast

<i>Term</i>	<i>Regression Coefficients</i>	<i>t Statistic</i>
Constant	-62.297	-2.040
log(I)	-36.708	-1.874
DF	0.083	0.519
log(I)	118.316	2.143
log(I)*log(I)	55.49	2.624
log(I)*log(I)	-45.351	-2.049
log(I)*DF	-0.457	-3.892
DF*log(I)	0.285	2.367
Adjusted R ² = 81.9%		

The inclusion of the linear parameters for duty factor and pulse-on time, despite their lower than critical 't' statistics, was required by MINITAB to include their interactions and squares. The following contour plots illustrate the effect of the input parameters on the thickness of the recast layer.

Figure 4.8: Contour plot for Recast response, $\log(l) - \log(I)$

From Figure 4.8 and Figure 4.9, the pulse-on time is seen to have a slight increasing effect on the thickness of the recast layer. This follows well with literature as the pulse-on time has the most significant effect on the diameter of the discharge crater, but also allows more time for heat to penetrate into the surface [71]. In terms of the depth of the crater, the discharge current has the most significant effect and this effect is shown in both Figure 4.8 and Figure 4.10 where an increase in peak discharge current results in a thicker recast layer [72].

Figure 4.9: Contour plot for Recast response, $DF - \log(I)$

The influence of the duty factor on the recast layer depth also agrees with one's expectations. As was previously mentioned, an increase in duty factor tends to increase the gap contamination. This increased gap contamination increases the probability that debris will re-attach to the workpiece. Furthermore, the ejection efficiency is likely to be reduced when the gap is not sufficiently regenerated.

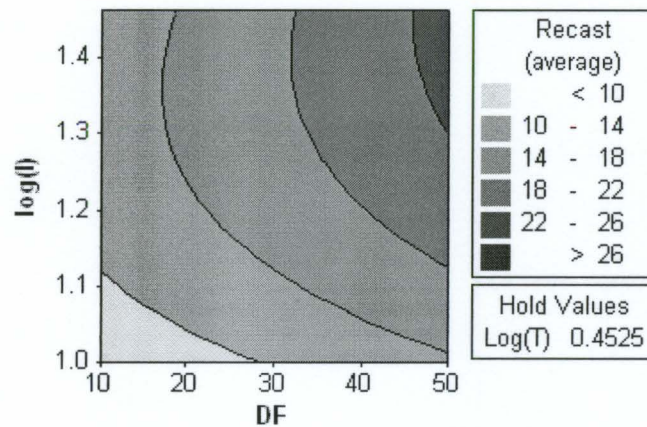


Figure 4.10: Contour plot for Recast response, $\log(I)$ - DF

4.1.6 Discussion of Model Results

A significant amount of information can be obtained from each of the models generated in the previous section. Using a process of model refinement, the initial design of experiments was expanded to account for curvature in the data. The subsequent models were refined by including only the predictors that were deemed to have statistical significance.

From the refined models, it was found that the peak discharge current was perhaps the single most important parameter controlling the MRR, the machining gap and the recast layer. The effect of the peak discharge current, duty factor and pulse-on time all correspond with expectations. This analysis however, still provided information on the magnitude of the machining gap and the recast layer, information that is invaluable in implementing AWEDM. Contrary to expectations, the open circuit voltage was found to have no significant effect on any of the responses. This result is confirmed and studied in the following section.

4.1.7 The Effect of the Open Circuit Voltage

In general, the MRR can be related to the discharge energy defined as

$$E = \int_0^T I(t)V(t)dt \quad (4.4)$$

where $I(t)$ is the discharge current, $V(t)$ is the discharge voltage and T is the Pulse-ON time². This relationship indicates that an increase in V will increase the MRR. The voltage over the discharge duration, $V(t)$, is usually a fraction of open circuit voltage and is typically a function of the gap width and the tool/workpiece materials. The independence of $V(t)$ with respect to the OCV was confirmed by analyzing the voltage waveforms acquired at various open circuit voltages. As the recast layer is largely dependent on the discharge energy, it too was not affected by open circuit voltage.

In terms of the Gap response, it was assumed that an increase in the open circuit voltage would tend to increase the machining gap since the average voltage is the feedback used to control the gap width. In measuring the average voltage over a range of open circuit voltages, it was found that the servo-reference voltage scales with the open circuit voltage in order to maintain the gap. Results from these tests are presented in Table 4.7. All tests were performed without varying the other process parameters.

Table 4.7: Change in the average voltage with open circuit voltage

<i>Open Circuit Voltage</i>	<i>Measure Average Voltage</i>	<i>Calculated Compression</i>
60	50	16.7
120	95	20.8
180	140	22.2
250	195	22.0

In addition to verifying that the servo-reference voltage scales with the open circuit voltage, the effect of the 'Comp' parameter was studied. Described in the manual as

² Refer to Figure 1.2

‘Compression of the discharge delay time’, the ‘Comp’ parameter controls the servo-reference voltage³, the parameter used for controlling the gap size. The relationship between this compression parameter and the servo-reference voltage is shown in Table 4.7 and Table 4.8. In varying the OCV, the compression was kept constant at 20%. Similarly, the OCV was kept constant at 120 V when the set compression was varied.

Table 4.8: Variation in the average voltage with the compression setting

<i>Set Compression</i>	<i>Measured Average Voltage</i>	<i>Calculated Compression</i>
10	105	12.5
20	95	20.8
30	80	33.3
40	70	41.7

From these tables it is apparent that the COMP setting is directly related to the servo-reference voltage as:

$$\text{Servo-Reference Voltage} = OCV \left(1 - \frac{\text{Comp}}{100} \right) \quad (4.5)$$

This relationship was used to calculate the ‘Calculated Compression’ values in Table 4.7 and Table 4.8, where the correlation is clear. Because the compression setting is one that is specific to this machine tool and manufacturer, compression will be from this point onward converted to servo-reference voltage as per Equation (4.5). This conversion will allow for discussion that is more consistent with the literature and commonly accepted process parameters. The open circuit voltage was originally chosen, as it was understood to have an effect on gap size and the discharge voltage. From the preceding analysis, the open circuit voltage was found to have no effect on either of these parameters and is no longer considered a parameter of interest.

³ When the Servo-Control system is set to be controlled by the average voltage feedback.

4.2 Characterization of Fixed Abrasive Wire

To understand the interaction that occurs in the hybrid machining process it is necessary to properly characterize the abrasive wire to be used. As with any abrasive product, an abrasive wire is produced using grits that fall within certain size limits. There is inherently a distribution to the size of the grits themselves. Further, in the electroplating process, the orientation and location of the grits with respect to the wire core cannot be precisely controlled, and thus the protrusion height of the abrasives beyond the metallic bond will be of a certain distribution. As the engagement of the abrasives depends on the protrusion height relative to the gap width, this section focuses on determining the distribution of the protrusion height.

4.2.1 SEM Inspection of the Diamond Wire

There are currently only a few manufacturers of fixed abrasive diamond wire for use in wafer production. The details on the wire from two such companies, which will be examined as part of this work, are listed in Table 4.9.

Table 4.9: Manufacturers and details on fixed abrasive diamond wires

	<i>Wire Specification</i>	<i>Construction Details</i>
Manufacturer A	250 μm total diameter Unspecified core size Unspecified Abrasive	High tensile strength steel core Electrolytic copper sheath with impregnated abrasives Nickel overstrike
Manufacturer B		
<i>Wire 1</i>	180 μm core 50 μm abrasives	High Tensile Strength Steel Core Composite Brush Electrolytic Nickel- plated; no sheath.
<i>Wire 2</i>	250 μm core 70 μm abrasives	Diamond abrasives

The wires were examined in a scanning electron microscope to study their topography. The difference in the wires, between the two manufacturers, is evident as shown in Figure 4.11.

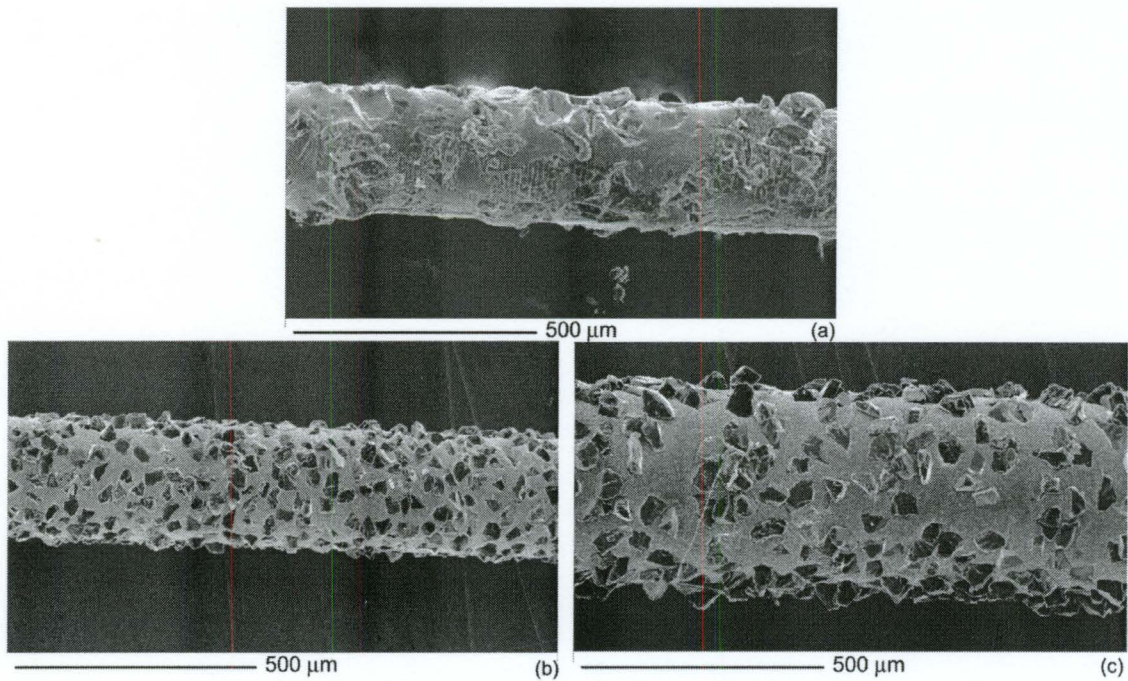


Figure 4.11: SEM micrographs of abrasive wire: (a) Manufacturer A; (b) Manufacturer B - Wire 1; (c) Manufacturer B – Wire 2

As can be seen from Figure 4.11, the wire from Manufacturer A is made with a nickel overstrike to provide improved grain retention during wire sawing operations. This layer limits the protrusion height of some abrasives while covering others entirely. In contrast, the wire from Manufacturer B does not have this nickel overstrike and the abrasive protrusion is prominent as is shown in Figure 4.12. Furthermore, the grain distribution in the wire from Manufacturer B is denser and more consistent.

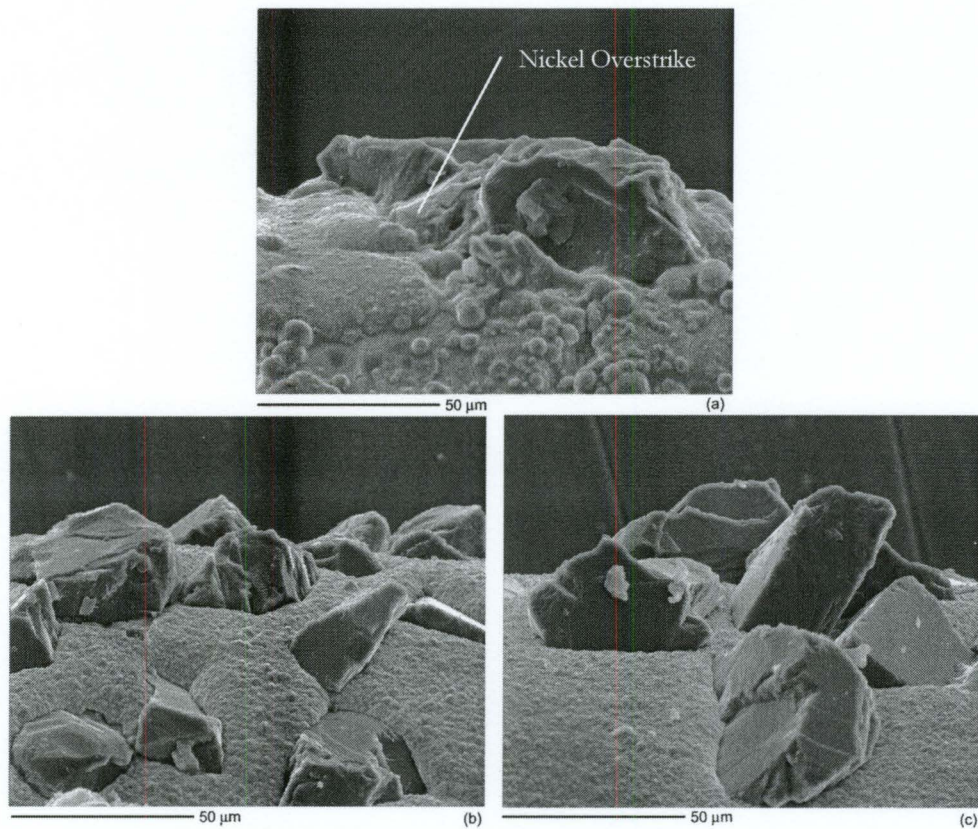


Figure 4.12: Close-up SEM micrographs of abrasive wire: (a) Manufacturer A; (b) Manufacturer B - Wire 1; (c) Manufacturer B – Wire 2

In addition to the longitudinal views, cross sections of each wire were also examined with a SEM to visualize the distribution of the abrasives both radially and circumferentially in the wire. Figure 4.13 shows the cross sections for each of the wires studied.

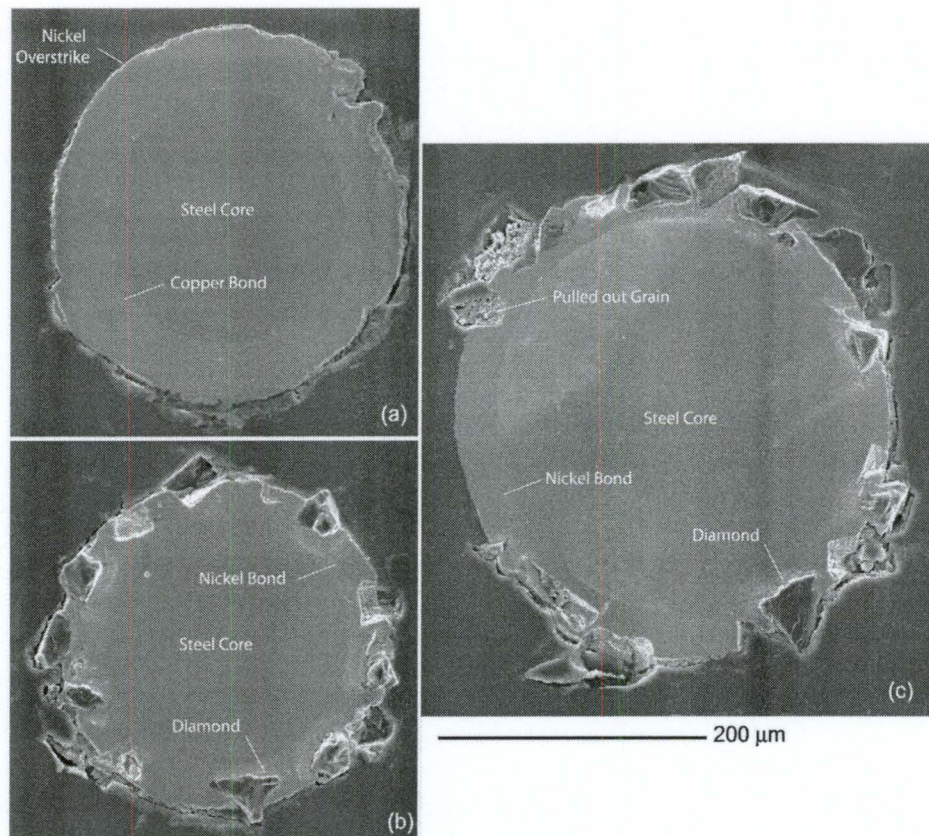


Figure 4.13: SEM micrographs of wire cross-sections: (a) Manufacturer A; (b) Manufacturer B - Wire 1; (c) Manufacturer B - Wire 2⁴

In looking at the wire from Manufacturer A, no abrasives are present at this wire cross section⁵. The thin nickel overstrike is however seen intermittently around the wire circumference. Further, from the cross section, the conductive wire core is observed to be irregular both axially and circumferentially.

The wires from Manufacturer B show a uniform circumferential distribution of the abrasives, while the bond material is seen to have consistent thickness around the circumference of the wire core. In contrast to the wire from Manufacturer A, the thickness/uniformity of bond material is not affected by the presence of the abrasives.

⁴ Pulled-out abrasive is due to the cross-sectioning and polishing process.

⁵ No abrasives were found in any of the four cross sections that were examined.

4.2.2 *White Light Interferometry of the Wire Surface*

There exist several methods to characterize abrasive surfaces in terms of grain protrusion including the use of 2-D and 3-D contact surface profiling and pneumatic gauging [73 - 75]. Most of the work however, is focused on stylus measurement techniques for grinding wheels. Due to the small size and cylindrical shape of the wire, contact measurement is not ideal. To this end, a non-contact technique was developed that enables the surface topography to be measured and the protrusion height distribution to be determined. This technique is detailed in Chapter 3. Using white light interferometry, height maps of surfaces can be generated as shown in Figure 4.14.

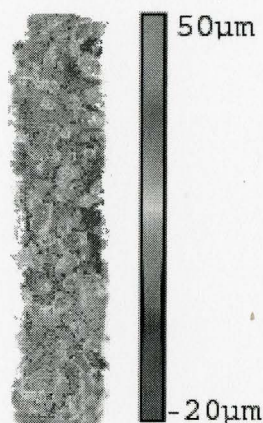


Figure 4.14: Surface map of Manufacturer B -Wire 2, obtained by white light interferometry

These maps are used to measure the peak height of the abrasives from the core of the wire. As discussed previously, the protrusion of the abrasives from the bond is irregular in the wire from Manufacturer A. This made it difficult to measure the protrusion heights for this wire reliably, and thus the wire from Manufacturer A was not included in the following analysis.

Using the measured protrusion heights for both wires from Manufacturer B, a distribution can be determined. For a sample size of $n=230$ measurements, for each wire, the

following histograms were created using Scott's Choice for bin size, Equation (4.6); which works well with small sample sizes and little knowledge of the underlying function. [76]

$$k = 3.5 \frac{\sigma}{n^{1/3}} \quad (4.6)$$

Where σ is the estimated standard deviation of the data, and n is the number of samples.

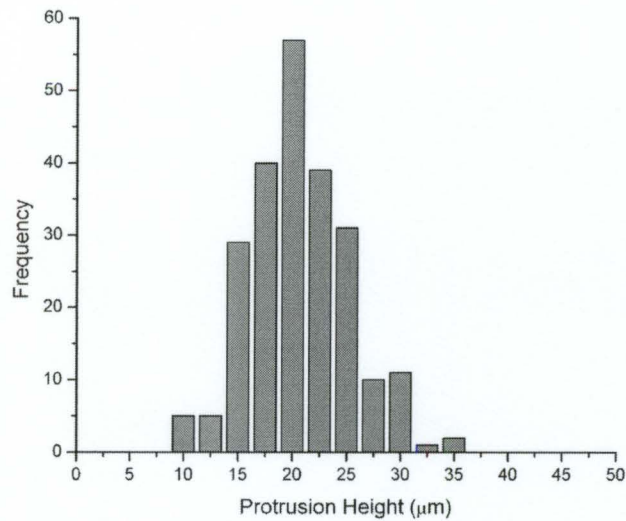


Figure 4.15: Protrusion height distribution for Manufacturer B - Wire 1

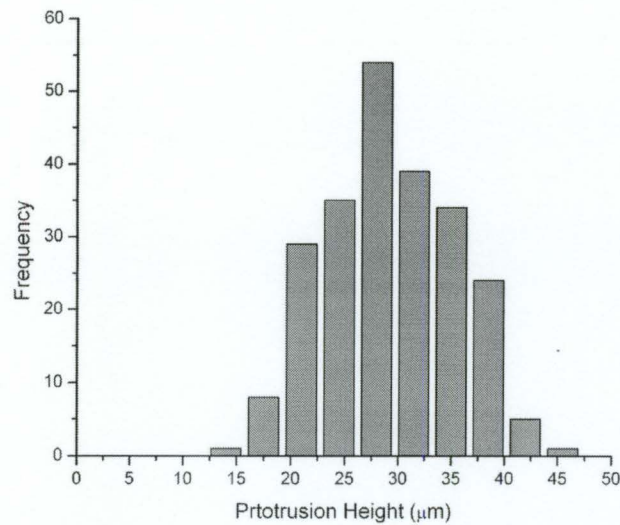


Figure 4.16: Protrusion height distribution for Manufacturer B - Wire 2

Based on the histograms shown, the distribution appears to be normal. In the case of the wire with 70 μm abrasives, Figure 4.16, the peak of the distribution occurs at a protrusion height of 28 μm . In the case of the wire with the smaller 50 μm abrasives, Figure 4.15, the peak occurs at a protrusion height of 20 μm . The mean percentage of the abrasive held in the bond for both wires is 60%. This value is typical of the maximum protrusion of abrasives on a grinding wheel as any grains protruding beyond this value are generally removed during the dressing process. In the case of abrasive wire, where no dressing is performed, these abrasives would be pulled out quickly after machining is initiated. For AWEDM, wire dressing prior to machining may be suitable to avoid possible damage of the workpiece as a result of grain pullout.

From the preceding analysis using both SEM imaging and white light interferometry, it is possible to identify the wire design that is most suited to the hybrid application. The wire by Manufacturer A is made with a Nickel overstrike that reduces and almost eliminates grit protrusion. This makes it impossible to engage the abrasives as the Nickel covered diamonds would electrically short out the process. Furthermore, the irregular wire core diameter would affect the stability of the EDM process, as the machining gap would be constantly changing. These findings and the fact that the wire has a low abrasive density and irregular distribution make this wire not ideal for use in an AWEDM process.

The wires from Manufacturer B feature a denser and uniform distribution of abrasives along the surface of the wire. This means that the gap condition will be more consistent and that each abrasive will be more likely to abrade an area that has been thermally softened by a discharge. The protrusion height was shown to be normally distributed with the most frequent heights similar in size to the machining gaps measured in Section 4.1.2. This allows for both abrasion and EDM to operate simultaneously. The regular diameter of the conductive wire core, which is not affected by the presence of abrasives, also provides a more constant gap width, yielding a more stable process.

In order to vary the process from mostly EDM to mostly abrasion, the wire with the proper protrusion height must be used for testing the AWEDM process. As the machining gap widths observed in Section 4.1.2 ranged between 8 and 20 μm , and the mean protrusion height of Wire 1 from Manufacturer B was 20 μm , this wire will therefore be used in all subsequent testing of the process. The Wire 2 from Manufacturer B could be used in AWEDM where conditions permit, however, the wire from Manufacturer A is deemed unsuitable for the process.

4.3 Preliminary Testing and Process Refinement

Prior to extensive testing of the AWEDM process, some preliminary testing and refinement was done to establish suitable test methods and operating regimes.

4.3.1 *Wire Effectiveness after Repeated Usage*

Before the wire feed apparatus as discussed in Chapter 3 was designed and built, an apparatus was available that fed a short, 25 metre length of wire between spools. As it was unsure how repeated usage of the wire would affect performance, some preliminary testing was conducted. Testing was performed on a 10 mm thick aluminum workpiece. The test was paused every five passes of the wire to measure progress. The results from the tests show a decrease in performance as depicted in Figure 4.17. Initially a nearly 300% increase in removal rate over WEDM alone is achieved. The effectiveness of the abrasive wire drops significantly after the first few passes, with the material removal rates approaching those of WEDM alone. This indicates that after the wire has been used, material removal occurs mainly by electrical erosion. This degradation in wire performance can be attributed to the loss of abrasive action resulting from the possible graphitization of the diamond abrasives and by the adherence of machining debris to the wire. Reduction in abrasion due to graphitization is due to both the soft, non-abrasive nature and electrically conductive nature of graphite. The presence of debris adhered to the wire reduces the effective gap width, thereby reducing abrasion.

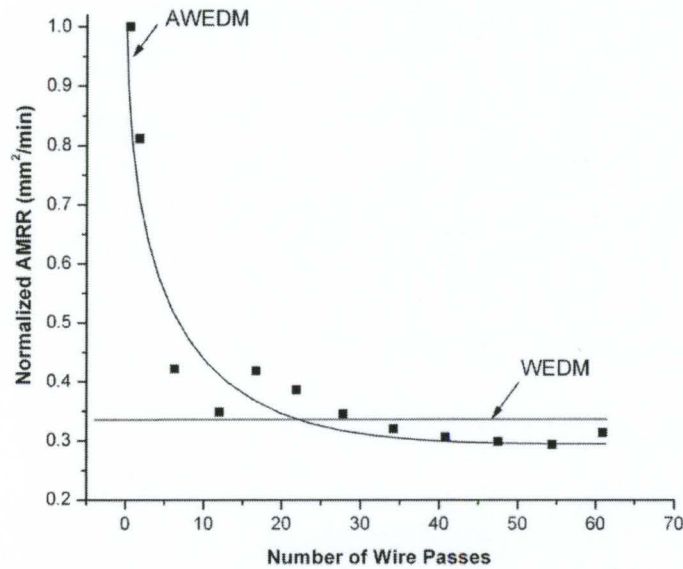


Figure 4.17: Effect of repeated use of abrasive wire on MRR
 ($T=1.0 \mu\text{s}$, $I=3.2 \text{ A}$, $U=250 \text{ V}$, $DF=10 \%$)

The presence of machining debris on the wire is shown in Figure 4.18. The occurrence of discharges near an abrasive may cause graphitization of diamond, which is a documented phenomenon [77]. Though it is not clear whether graphitization has occurred, Figure 4.19 shows the location of a discharge in close proximity to the abrasives.

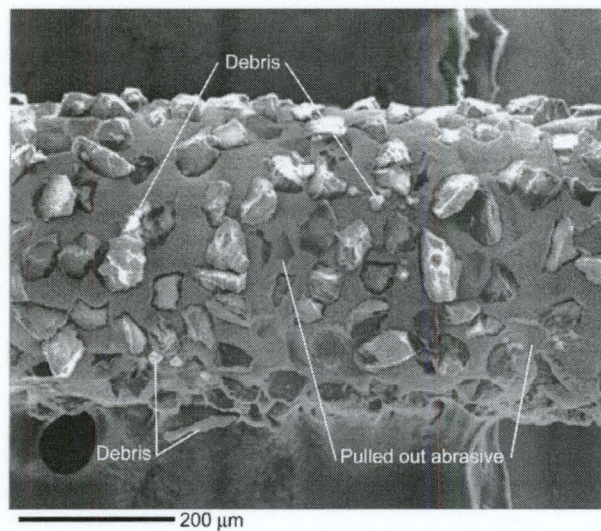


Figure 4.18: SEM micrograph showing condition of used diamond abrasive wire

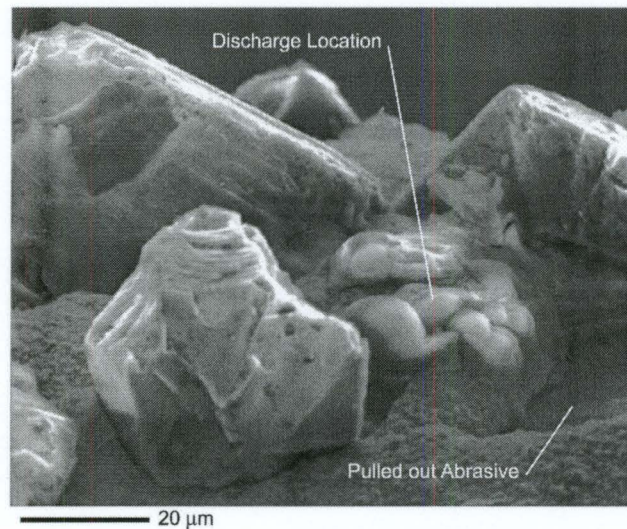


Figure 4.19: SEM micrograph showing the location of a discharge on used abrasive wire

Because of the wire degradation, a new, one use wire feed apparatus was designed and built. Details on the apparatus are listed in Chapter 3. The new apparatus was used in all subsequent testing. It is worthwhile to note that the graphitization of diamond would not be an issue if aluminum oxide abrasive were used in place of diamond.

4.3.2 Preliminary Testing

Using parameters based upon the DOE and process design, preliminary experiments were completed to characterize the process. In order to minimize the abrasive engagement at first, a peak discharge current of 29A with 50% duty factor was used as this combination provides the largest gap width. These tests were however unsuccessful as the wire broke almost immediately upon machining. The machining parameters were then varied within the range used for the design of experiments to establish a stable operating regime. Unfortunately, none of those parameters could be used, as the process was unstable and frequent wire breakage occurred. This phenomenon is looked into further in the following section, as the wire would break at even the most conservative settings used in the DOE.

4.3.3 Wire Breakage Analysis

During preliminary testing of the process, the breaking of the wire limited the machining parameters that could be used in the process. It was observed that the wire did not break as it passed through the discharge region, but as it passed through the pinch and drive rollers. Upon inspection, it was noticed that the wire was brittle and broke easily when bent. To determine the cause for the apparent embrittlement of the wire, several samples were collected. These samples were initially viewed under a microscope to observe if the process had simply eroded some of the wire weakening it. As seen in Figure 4.18, the core of the wire after being used appears to remain intact. Next, the samples were sectioned to examine the wire core and measure the hardness of the wire core before and after machining using a micro-hardness tester. Figure 4.20 shows the measured Vickers hardness of the wire, where a clear change in hardness is found between the new and used wire.

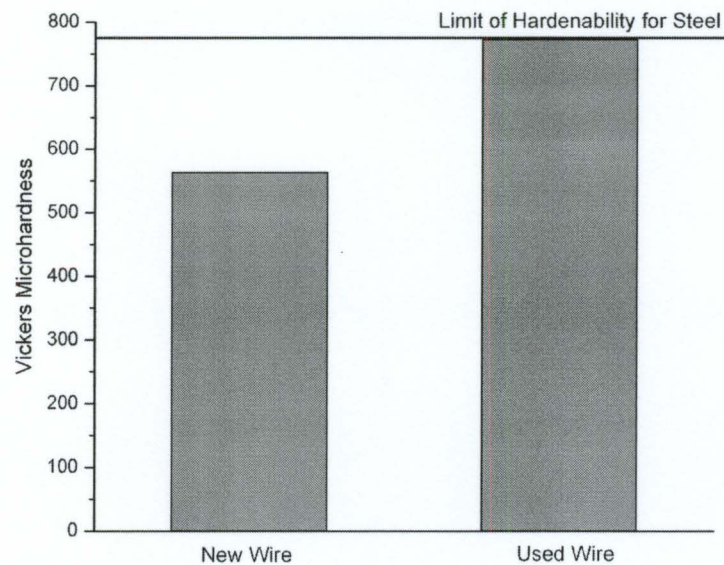


Figure 4.20: Comparison of wire core hardness between new and used wires

When the steel core is exposed to very high temperatures and rapid cooling rates such as those the wire would experience in WEDM, martensite formation is likely. Martensite is the

strongest and hardest microstructure for steel with negligible ductility. As indicated, the hardness of the wire core increases from ~ 560 HV in the new wire to ~ 776 HV, approximately 64 HRC, the maximum achievable hardness for steels. Such a high hardness would indicate close to 100% Martensite formation in the used wire providing reason for the brittleness of the wire and cause for the wire breakage.

Due to the embrittlement of the wire under even modest machining parameters, the use of a wire with a low carbon steel or non-steel core is recommended. Apart from the heat from the discharges, the relatively high electrical resistivity of steel is likely to heat the wire, adding to the problem. Regardless of the cause of heating, rapid cooling and embrittlement is unavoidable as the process occurs submerged in dielectric.

4.3.4 Process Refinement

In order to find a suitable operating regime, a trial and error approach was used. Preliminary testing indicated that wire fracture was mainly due to embrittlement of the wire. In the trial and error testing, the servo-reference voltage was varied in order to control the gap while varying the other machining parameters. Initially, conservative machining parameters, as in Table 4.10, were selected to ensure that wire breakage would not occur. These parameters were then varied to increase the material removal rate due to EDM until the point of instability was reached. The order in which the parameters were varied was selected based upon their effect on the material removal rate. Table 4.10 also indicates the point of instability for each parameter.

Table 4.10: Machining parameter limitations of AWEDM

<i>Parameter</i>	<i>Start</i>	<i>Limit</i>	<i>Notes</i>
Current	1.2 A	8.0 A	Above 8A wire breaks
Pulse OFF Time	100 μ s	100 μ s	Below 100 μ s arcing is prevalent
Pulse ON Time	0.64 μ s	4.9 μ s	Above 4.9 μ s wire breaks

The stability of the process was assessed by observing the appearance of the cut, the average voltage on an analogue voltmeter and the current and voltage waveforms on a digital acquisition system. An unstable process was identified by wire breakage, localized arcing, large variation in the average voltage and repetitive arcing on the waveform display. It is interesting to note that a decrease of even 10 μs in the pulse-off time resulted in an unstable process. Apart from the parameters listed in Table 4.10, the effect of open circuit voltage was also examined. From the voltage waveform display, low voltages produced longer and hence more inefficient discharge delay times, while voltages above 180 resulted in arcing.

Based on these findings, a new operating regime is identified and shown in Table 4.11. The range for the servo-reference voltage was obtained by varying from the points where no bowing of the wire occurred, thus minimal abrasion, at one extreme to the point where the wire bowing was high and the desired gap voltage could not be achieved. This provided the full useable range of servo-reference voltage under the specified conditions.

Table 4.11: Final AWEDM testing conditions

<i>Parameter</i>	<i>Setting</i>
Peak Current	1.2 - 8 A
Pulse Off Time	100 μs
Pulse ON Time	0.64 - 4.9 μs
Servo-Reference Voltage	108 - 162 V
Open Circuit Voltage	180 V

Having established a stable range of machining parameters, further testing of the process is possible. Testing was conducted to determine the performance of the process under the newly defined operating conditions. To limit the number of tests to be performed, only the peak discharge current and servo-reference voltage are varied as these parameters have the most significant effect on the machining gap width and the material removal rate due to EDM.

To establish a basis for comparison, preliminary tests were conducted for conventional WEDM. For a more accurate comparison, a non-abrasive wire from Manufacturer B was used that is identical in construction and size to the abrasive wire used, less the abrasives. Figure 4.21 shows the relationship between AMRR and peak discharge current at various servo-reference voltages (V_{Ref}) for the conventional WEDM process.

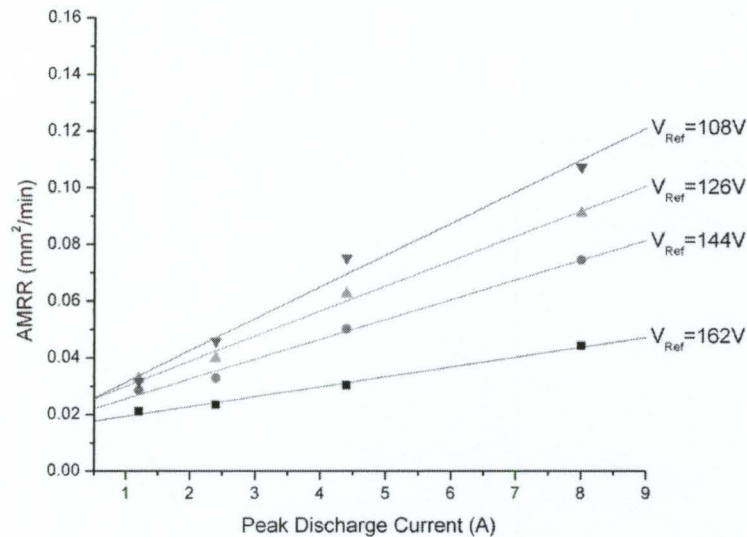


Figure 4.21: WEDM material removal rates within stable operating regime

As expected, the AMRR increases with peak discharge current while an increase in the servo-reference voltage produces lower removal rates. The increase in removal rate with decreasing servo-reference voltage is likely a result of the decrease in the average discharge delay time due to a smaller gap width. Shorter discharge delays provide more discharges in a given period. This result is further explored in Section 4.4.4.

4.4 Results from Abrasive Wire EDM Testing

To understand the characteristics of the AWEDM process, the effect of varying the machining parameters is considered. In all of the following tests, EDM parameters are chosen within the operating regime specified in Table 4.11.

4.4.1 Effect of Varying the Abrasive Engagement

One of the most important characteristics to understand is how the proportion of material removal by EDM to abrasion changes with varying parameters. One way to vary this proportion is to vary the engagement depth of the abrasive particles. This engagement directly affects both the thickness of the recast layer and the material removal rate. An increasing abrasive engagement, at least to a point, should result in improved removal rates and a reduced recast layer. The experiments conducted in this section aim to show this relationship.

Of the parameters that can be readily changed without affecting the process stability, the peak discharge current and the servo-reference voltage have the most significant effect on the material removal rate due to EDM and the machining gap width. The following study thus focuses on the process behaviour while varying these parameters. A matrix of experiments is performed varying the parameters of interest at four levels. The same levels as shown in Figure 4.21 are used here to allow for direct comparison between conventional WEDM with brass wire and the hybrid process. From these tests the AMRR, normal machining force, F_N , and the recast layer thickness are measured. Figure 4.22 below shows the variation in the AMRR with increasing servo-reference voltage at different peak discharge currents.

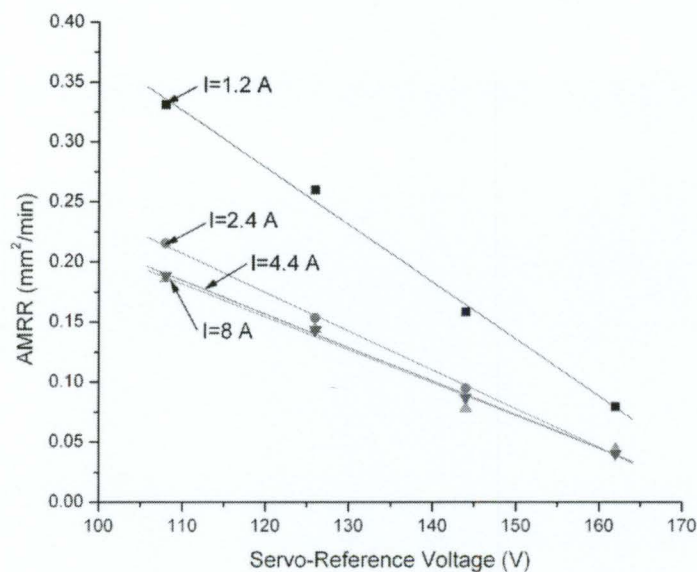


Figure 4.22: Variation in removal rate with servo-reference voltage for AWEDM

As shown, there is a linearly decreasing relationship between the removal rate and the servo-reference voltage. This phenomenon is also true with WEDM alone as shown in Figure 4.21. The change in removal rate for WEDM alone however is not nearly as significant as the change seen in Figure 4.22. To understand the benefit that abrasion incorporates into the WEDM process, the percent increase in removal rate is shown in Figure 4.23.

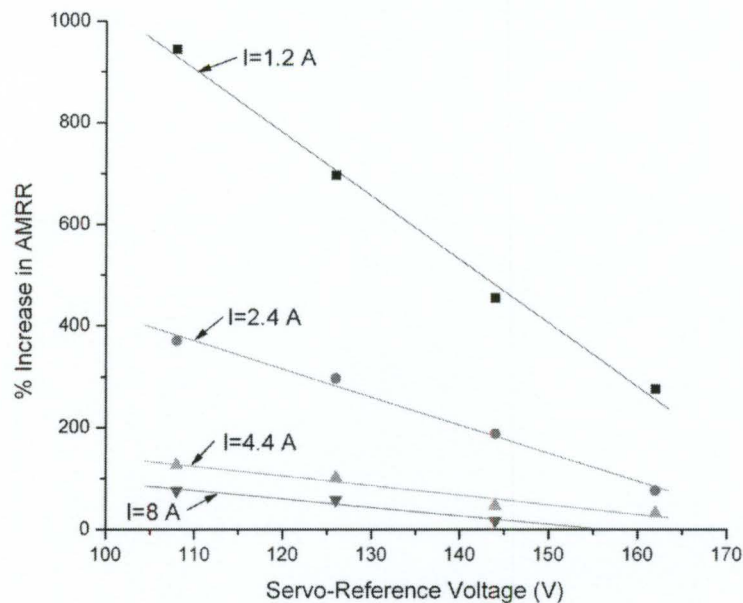


Figure 4.23: Percent increase in removal rate with AWEDM over WEDM

From this figure, it is clear that the abrasion component contributes significantly to the overall removal rates increasing the removal rate by as much as 1000%. The linear relationship, as in Figure 4.22, holds here, which indicates that the servo-reference voltage has a direct linear effect on the amount of abrasion occurring in the process. This is conceivable as the servo-reference voltage is a measure of the gap width, and hence the abrasive engagement. This aspect is further confirmed in analyzing the machining forces discussed later.

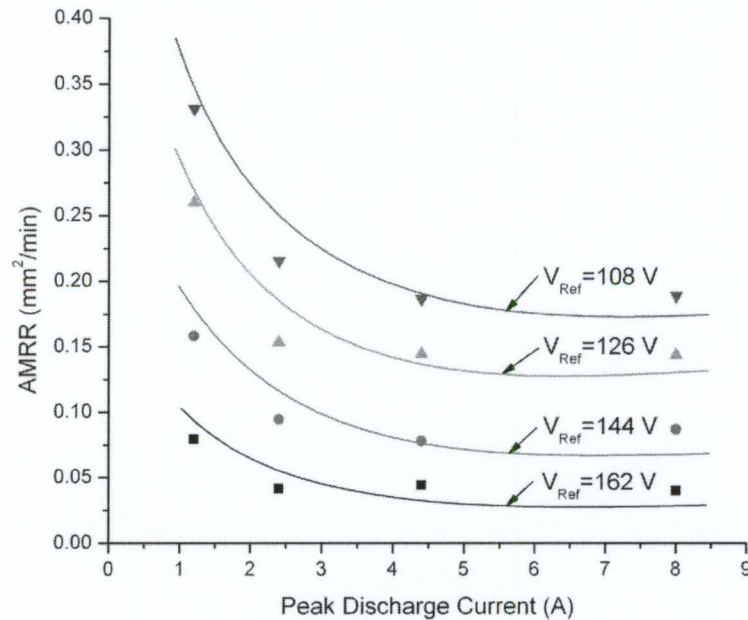


Figure 4.24: Variation in removal rate with peak discharge current for AWEDM

Presenting the same results with the peak discharge current plotted on the X-axis, as shown in Figure 4.24, more clearly illustrates the non-linear decreasing effect on the removal rate. The rapid initial decrease in removal rate with increasing current is a result of a drastic reduction in the abrasion component. The removal rate is seen to approach a constant at larger discharge currents, which is due to the increase in material removal by the EDM component. As was found previously, the material removal rate tends to increase linearly with the peak discharge current. Figure 4.25 shows the percent increase in the AMRR of AWEDM over WEDM for increasing peak discharge current, where the percentage increase in AMRR decreases rapidly at first and then approaches constant value.

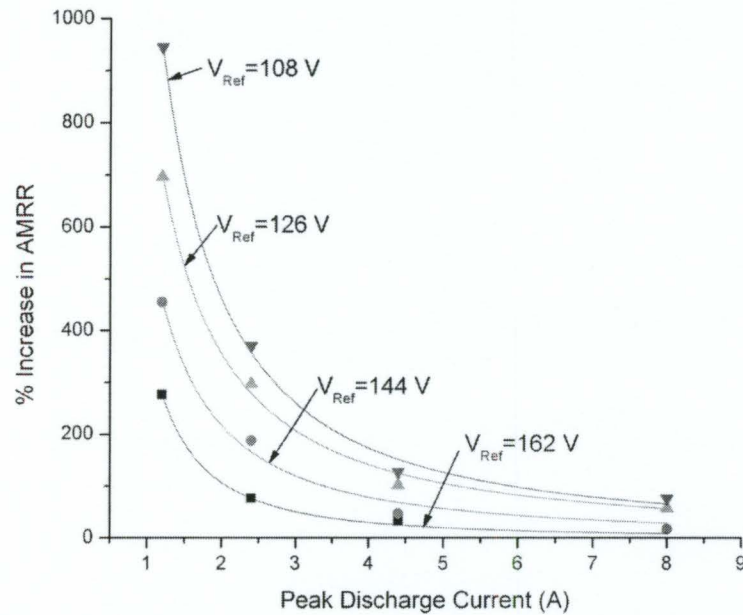


Figure 4.25: Percent increase in removal rate with AWEDM over WEDM

Figure 4.22 through Figure 4.25 show the parametric effect of the peak discharge current and servo-reference voltage on the AMRR in application of AWEDM. There exists a strong interdependency between the peak current and the servo-reference voltage as they both affect the proportion of material removal by the two mechanisms: EDM and abrasion. Figure 4.26 shows a contour plot based on the experimental data showing the combined effects of both parameters on the material removal rate.

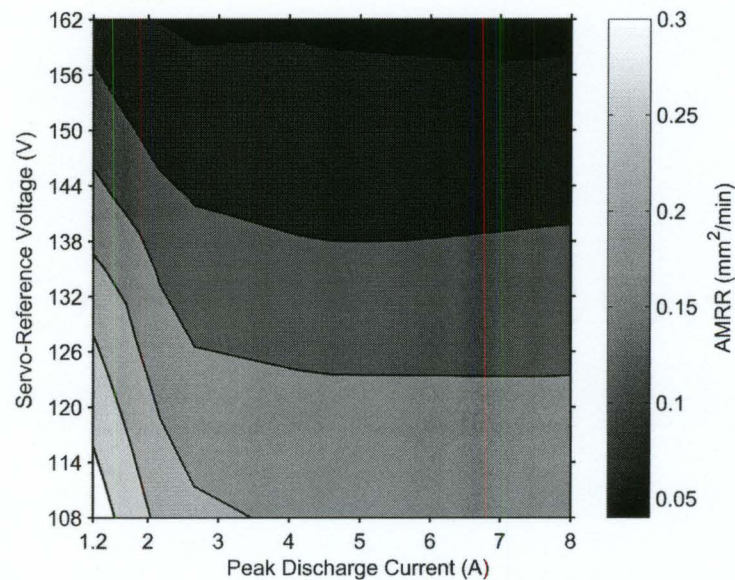


Figure 4.26: Contour plot showing the variation in AMRR with Servo-Reference Voltage and peak discharge current for AWEDM

The combined effects of peak current and servo-reference voltage can be clearly seen in the contour plot where the highest removal rates occur at the lowest peak currents and servo-reference voltages. Both parameters have direct effects on the gap size and thus lower values of these parameters provide a smaller gap. Physically, it is clear that a smaller gap imposes more abrasion. The examination of both the machining debris and machined surfaces testify to this finding. Under SEM examination of the machining debris, as is shown in Figure 4.27 to Figure 4.29, there is a clear transition from EDM debris to that of grinding with decreasing servo-reference voltage.

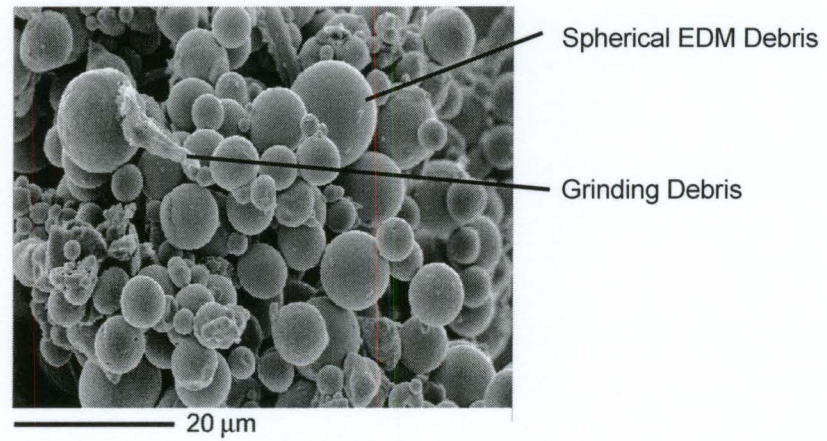


Figure 4.27: Micrograph of AWEDM debris ($I=8A$, $V_{Ref}=162V$)

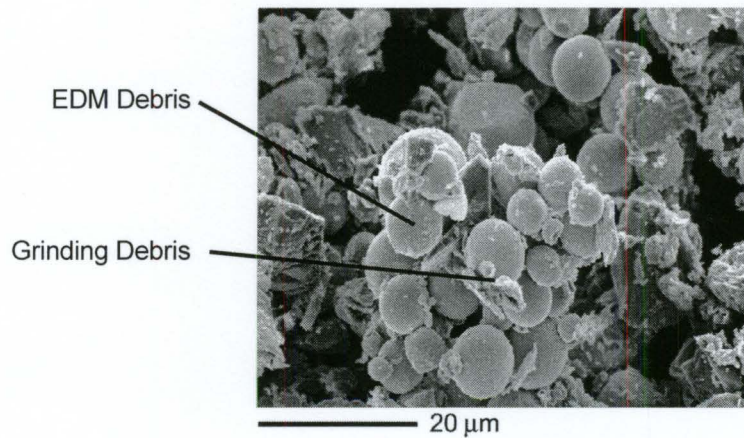


Figure 4.28: Micrograph of AWEDM debris ($I=8A$, $V_{Ref}=144V$)

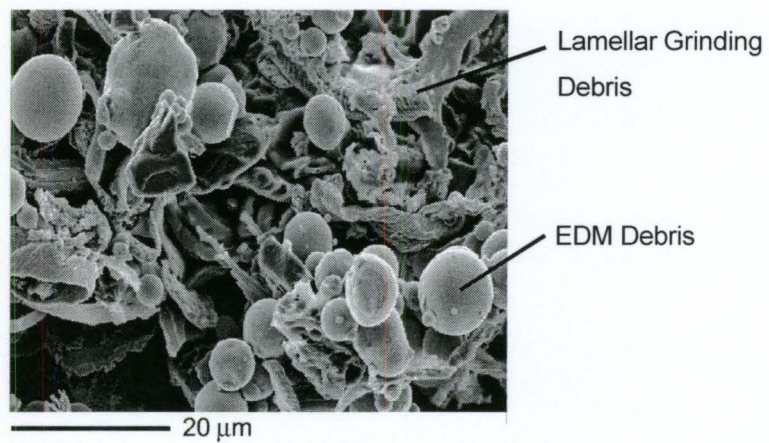


Figure 4.29: Micrograph of AWEDM debris ($I=8A$, $V_{Ref}=108V$)

At high settings of the servo-reference voltage, the debris is mostly of spherical form that is characteristic of EDM [58]. When the servo-reference voltage is reduced, an increase in the amount of grinding debris is shown. When the servo-reference voltage is 144V, the grinding debris appears as small metallic fragments, indicating that abrasion was occurring somewhat intermittently. In the case of the lowest servo-reference voltage, meaning the smallest gap, the majority of the debris appears to be that of grinding, indicating that material removal occurs mostly by abrasion. Some small, metallic particles are present, however the presence of long chips with lamellar structure indicate a condition of more continuous grinding.

Just as the debris indicates the extent of abrasion occurring, the machined surfaces too show this result. Figure 4.31 through Figure 4.33 show SEM images of the produced surfaces machined under the same conditions as was used in the collection of the debris, respectively. A micrograph of a machined surface obtained by WEDM alone is also presented in Figure 4.30 for comparison.

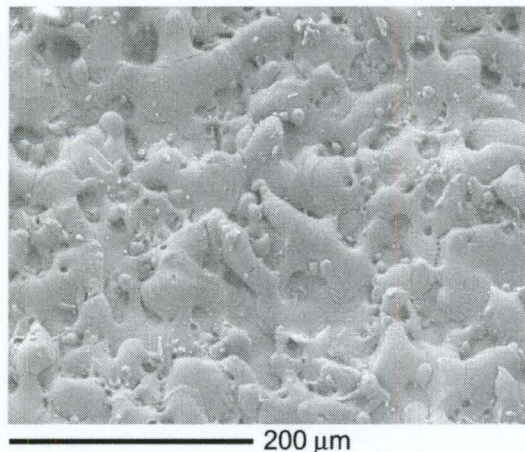


Figure 4.30: Micrographs of WEDM machined surface ($I=8A$, $V_{Ref}=126V$)

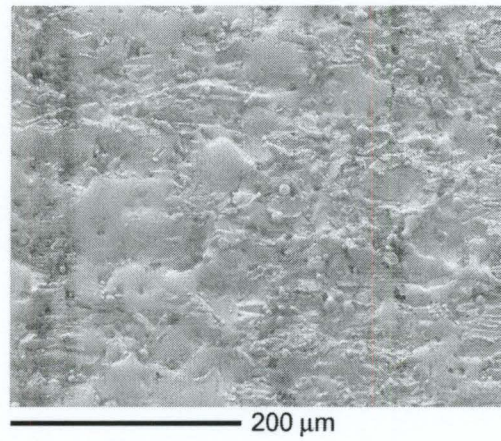


Figure 4.31: Micrograph of AWEDM machined surface ($I=8A$, $V_{Ref}=162V$)

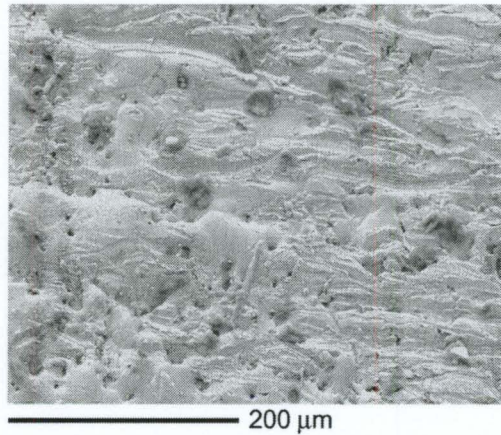


Figure 4.32: Micrograph of AWEDM machined surface ($I=8A$, $V_{Ref}=144V$)

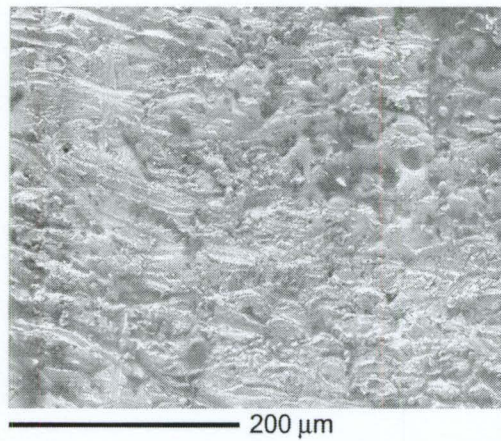


Figure 4.33: Micrograph of AWEDM machined surface ($I=8A$, $V_{Ref}=108V$)

In comparing the surfaces obtained by AWEDM to that obtained by WEDM, there is a clear difference in the directionality of the surface. WEDM alone tends to generate isotropic surfaces, where grinding produces surfaces with anisotropic surfaces with directionality in the direction of machining. In lowering the Servo-Reference voltage creating a smaller gap, the directionality of the surfaces increases. This again indicates that the process tends more towards abrasion with decreasing gap size.

Since the EDM component is very small under the parameters used, the effect of abrasion is more pronounced. If the same level of abrasion were maintained under more aggressive EDM parameters, the percent increase in removal rate due to abrasion would be less significant. This concept is explained further in Section 4.4.4.

The effect of the input parameters on the removal rate alone does not provide sufficient information on the process. Because the proportion of the material removal due to abrasion is extremely high under certain conditions, it is necessary to further examine what effects the abrasion has on the process.

4.4.2 *Forces in the AWEDM Process*

Once abrasion is incorporated into the process, the benefit of minimal machining forces in WEDM is lost. To understand the limitations and applicability of this process, it is thus necessary to understand what forces are induced by the addition of abrasion. In varying the peak discharge current and servo-reference voltage, the level of material removal due to abrasion was shown to vary widely. It is therefore expected that the forces too will vary drastically, and hence the effects of these parameters on the normal component of the machining force are shown here. Figure 4.34 shows the reduction in the Normal Machining Force with increasing servo-reference voltage over various peak discharge currents. Figure 4.35 shows the variation of the Normal Force with increasing peak discharge current. In both figures, it is interesting to note the similarity in the trends when compared to trends in AMRR shown in Figure 4.22 through Figure 4.25. This similarity confirms that the changing removal

rates are mainly due to change in the proportion of abrasion to EDM. The normal force is directly related to the abrasive engagement and thus the amount of material removed by the abrasives.

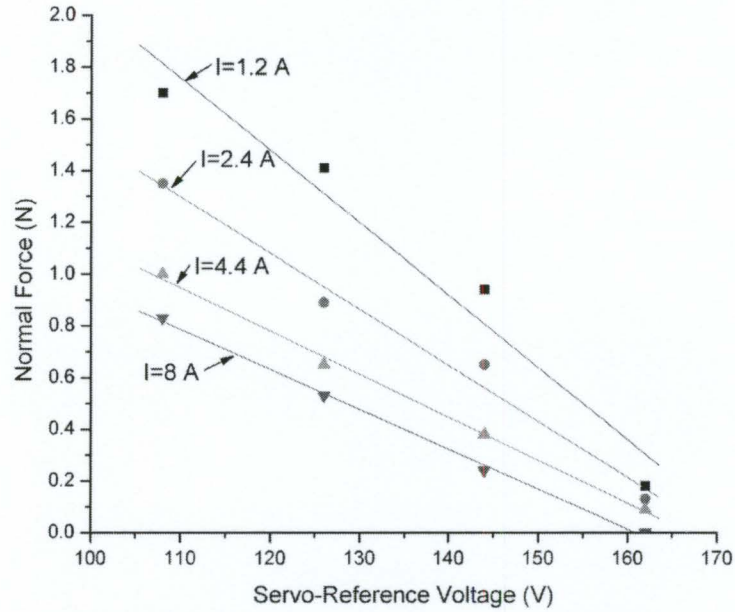


Figure 4.34: Normal force variation with servo-reference voltage

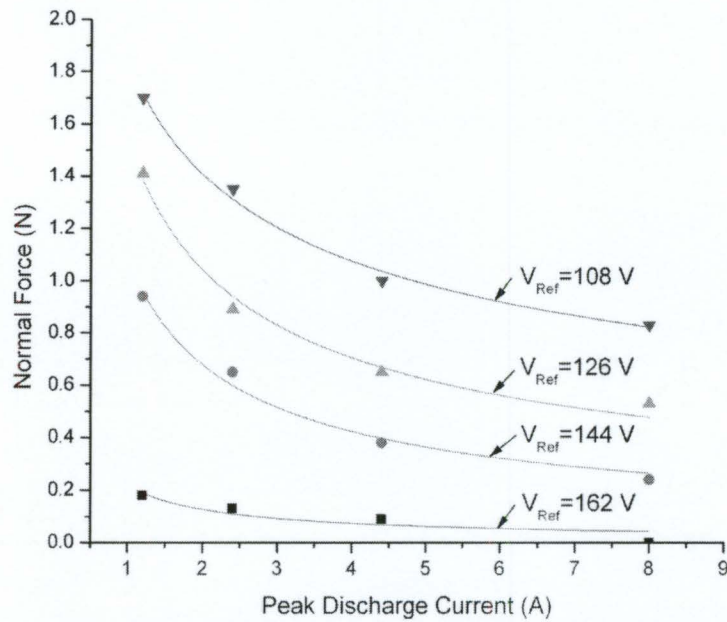


Figure 4.35: Normal force variation with peak discharge current

Again, the effects of both parameters on the normal machining force can be visualized in the contour plot of Figure 4.36. From this and comparing with Figure 4.26, it is noted that the regions of high material removal rate and highest normal force are coincident, occurring at low values of both servo-reference voltage and peak discharge current.

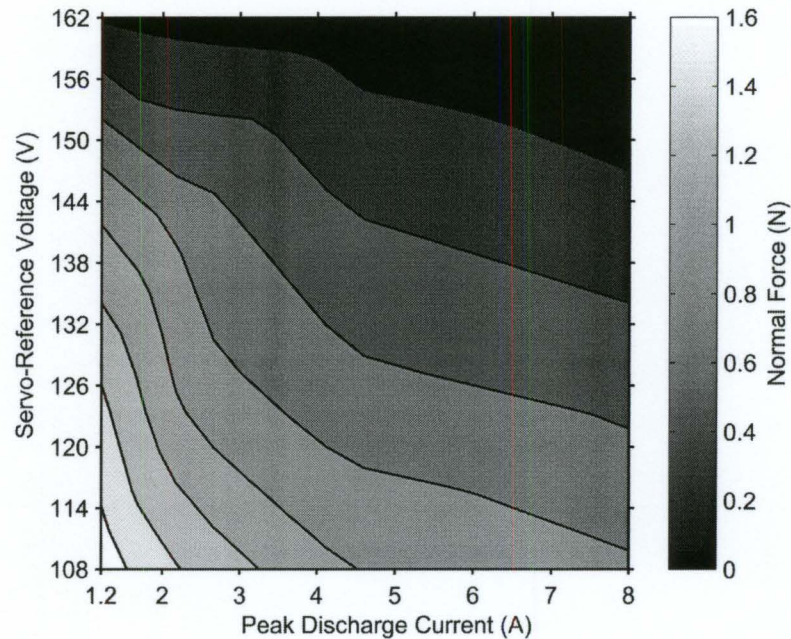


Figure 4.36: Contour plot showing the variation in the normal force with servo-reference voltage and peak discharge current for AWEDM

In comparing these figures, it can be seen that the material removal rates tends to level off at higher levels of discharge current due to the increasing EDM action, while the normal force continues to decrease with increase current. To understand the effect of machining force on the process, both the force and the removal rates must be considered. To accomplish this, the machining force is modeled using linear regression as the contours in Figure 4.36 are reasonably linear over the range of parameters studied. From the regression analysis, a model of the form:

$$F_N = 3.809 - 0.089 * I - 0.02 * V_{Ref} \quad (4.7)$$

is obtained, which explains 88.5% of the variation in the data based upon the adjusted R^2 statistic. It is possible to calculate the required machining parameters to achieve a desired machining force using Equation (4.7). This result is shown in Figure 4.37 where lines of constant machining force are superimposed on the contour plot from Figure 4.26.

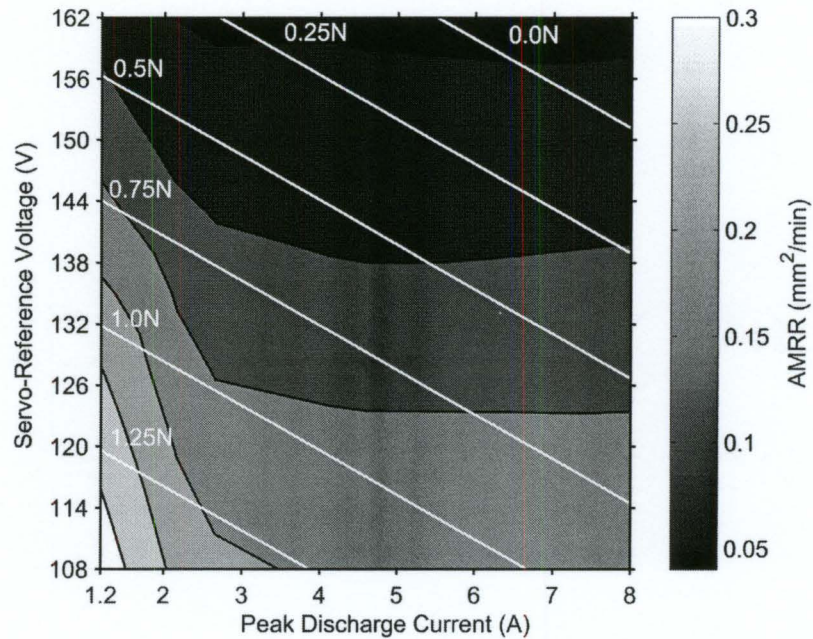


Figure 4.37: Contour plot showing the AMRR and operating regimes with constant normal force for AWEDM

The magnitude of the machining force is an important factor in practical application of the process. Because a force applied to the wire implies a slight bowing of the wire, the accuracy of the part being machined begins to suffer. Furthermore, the amount of wire bowing will limit the minimum corner radius achievable by the process. From Figure 4.37 it is clear that to achieve a specified removal rate, the servo-reference voltage and peak discharge current can be varied to minimize the machining force and thus improve the machining accuracy. This is especially true in the plateau region of the graph where increasing the discharge current reduces the machining force without affecting the overall material removal rate.

The maximum magnitude of the normal force in the tests conducted is approximately 1.7 N. Comparing to the typical values for abrasive wire sawing, the magnitude is on the same order, but slightly lower than those found by Clark et al. [40]. Because the maximum wire tension was limited by the wire feed apparatus to approximately 6.8 N, the amount of actual wire bowing was quite significant; as high as 2.9 mm. Practically, higher wire tension, more in line with those used in the wire saw process, would provide improved accuracy.

From these tests, it has been shown that a drastic increase in material removal rate is achievable by incorporating abrasion into the WEDM process. Furthermore, the proportion to which abrasion contributes to the material removal rate can be controlled by varying the servo-reference voltage and the peak discharge current. The servo-reference voltage has a direct effect on the machining gap width and thus the abrasive engagement. The discharge current acts to control the proportion in two ways. One, an increase in the discharge current tends to increase the machining gap and two, increasing the discharge current directly increases the material removal rate due to EDM. The recast layer is another process response that bears great significance on the performance of the process. The following section discusses how the addition of abrasion affects the recast layer formation on the machined surface.

4.4.3 Recast Layer Formation

The recast layer in electrical discharge machining is a result of the thermal material removal mechanism the process relies upon. Regardless of machining parameters, it is not possible to entirely prevent material from being recast on the machined surface. By incorporating mechanical abrasion into WEDM, the reduction of the recast layer is possible.

From the testing where the peak discharge current and Servo-Reference were varied, the recast layer was also measured. Samples from these tests, both the abrasive and conventional WEDM, were prepared and the recast layer measured as detailed in Chapter 3.

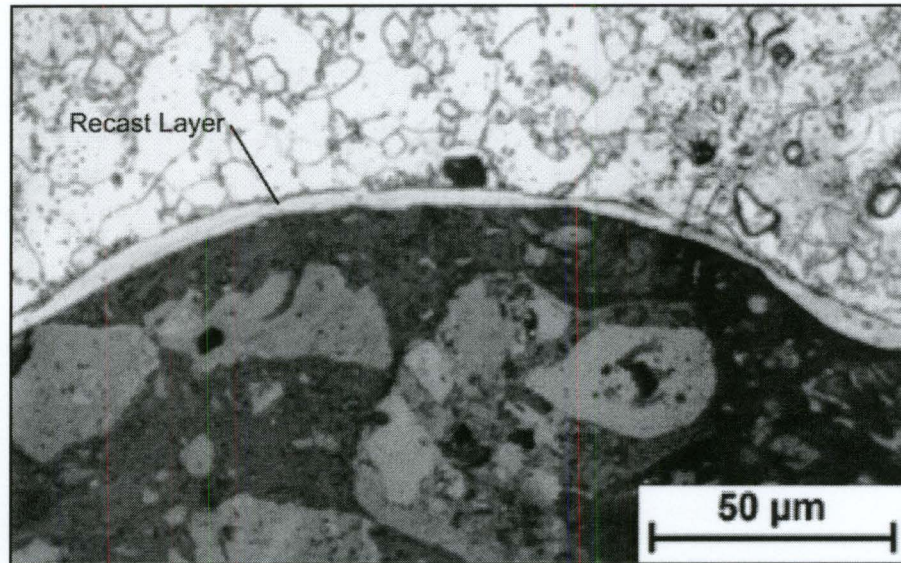


Figure 4.38: Micrograph of the cross section of a WEDM machined steel sample showing the recast layer ($I=2.4\text{A}$, $V_{\text{Ref}}=126\text{V}$)

Figure 4.38 shows a typical micrograph of a conventional WEDM machining cross section. The recast layer can be clearly distinguished from the base workpiece material. In this figure, the average recast layer thickness is $5.4\ \mu\text{m}$. Due to the smaller range of discharge parameters, the recast layer thickness of the WEDM machined samples did not vary as significantly as in Section 4.1.5. The layer thickness for all the tests here varied only between $3\text{--}6\ \mu\text{m}$ in average thickness.

From these results, it is clear that even under the modest machining conditions used in these experiments, a recast layer is present. In stark contrast to the results from conventional WEDM, Figure 4.39 shows a typical cross section from an AWEDM machined sample.

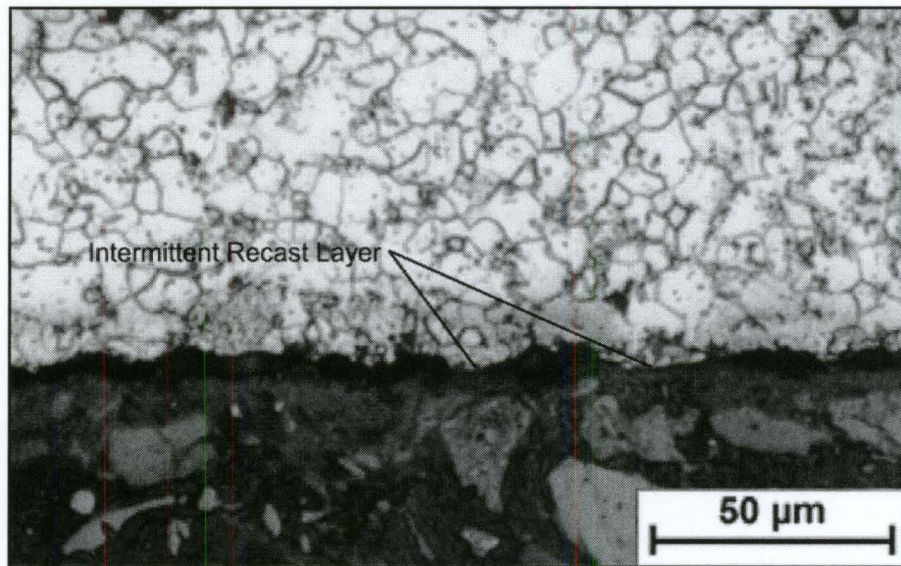


Figure 4.39: Micrograph of the cross section of an AWEDM machined steel sample showing the intermittent recast layer ($I=2.4\text{A}$, $V_{\text{Ref}}=126\text{V}$)

The presence of only intermittent recast material on the surface of an AWEDM machined sample further indicates the effect of abrasion. Regardless of the machining parameters used, in all the AWEDM test specimens examined, the recast layer was intermittent and of minimal thickness, less than $2\mu\text{m}$.

As the presence and thickness of the recast layer is of great importance in the aerospace industry, the effectiveness of AWEDM to reduce the recast layer in Nickel alloys is also presented. Figure 4.40 and Figure 4.41 shows the cross sections of WEDM and AWEDM machined samples respectively. From these figures, it is clear that the use of AWEDM provides a significant benefit towards reducing the recast layer thickness in aerospace components made of Nickel Super-Alloys.

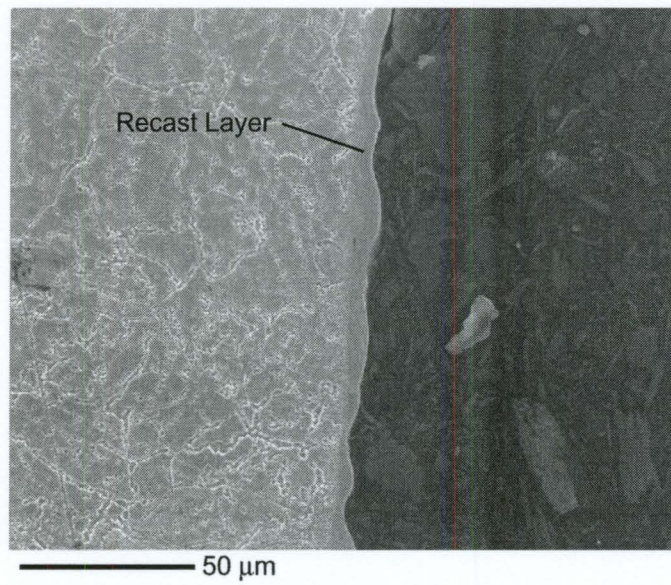


Figure 4.40: SEM micrograph of the cross section of a WEDM machined Inconel 600 alloy showing the recast layer

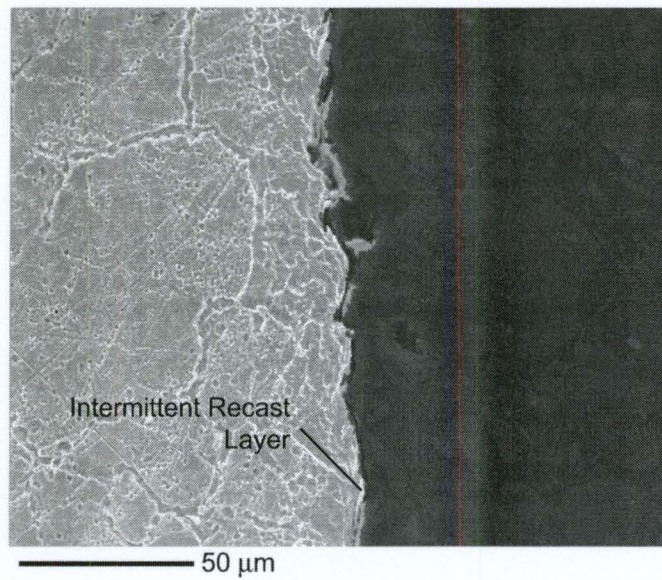


Figure 4.41: SEM micrograph of the cross section of an AWEDM machined Inconel 600 alloy showing the intermittent recast layer

4.4.4 Current and Voltage Waveform Analysis

In all the tests conducted for both conventional WEDM and AWEDM, the voltage and current waveform of the process were sampled and analyzed. The sampling and signal analysis details are outlined in Chapter 3. The signals were analyzed for the number of successful discharges, arcs and shorts. Figure 4.42 and Figure 4.43 show the results from this analysis for conventional WEDM and AWEDM respectively.

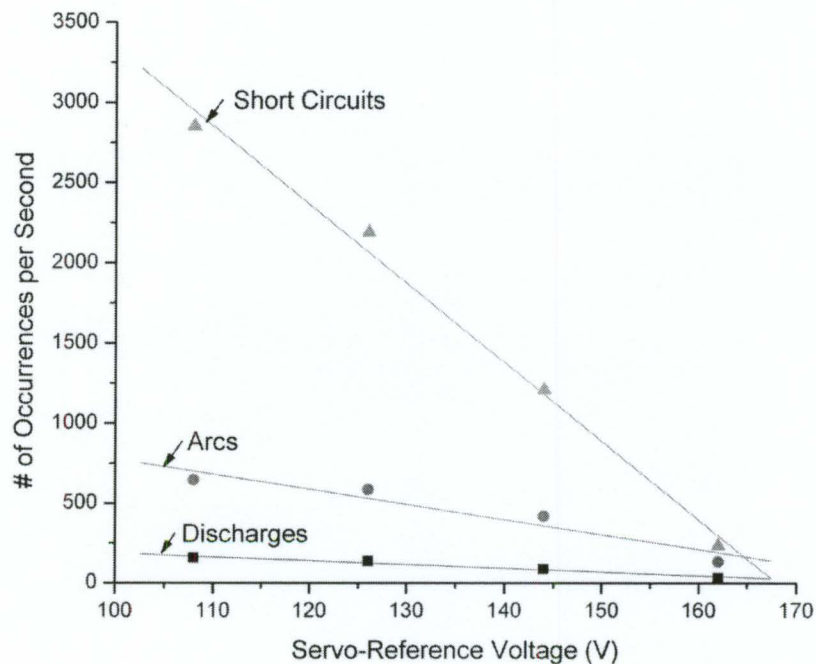


Figure 4.42: Waveforms analysis for WEDM ($I=2.4A$)

In WEDM alone, the frequency of each discharge classification increases with decreasing servo-reference voltage. Despite the drastic increase in the number of shorts, the removal rates tend to increase with decreasing servo-reference voltage as is shown in Figure 4.21. These trends are similar in AWEDM except that the frequency of arcing increases drastically with decreasing servo-reference voltage and there are generally more successful discharges with far fewer shorts. This is likely because the abrasives serve to isolate the wire core from the workpiece. The large increase in arcing seen in AWEDM is believed to be due to accumulation of grinding debris at lower servo-reference voltages. At larger servo-reference

voltages, when grinding is lessened, the debris serves to increase the number of successful discharges by aiding discharge initiation [10].

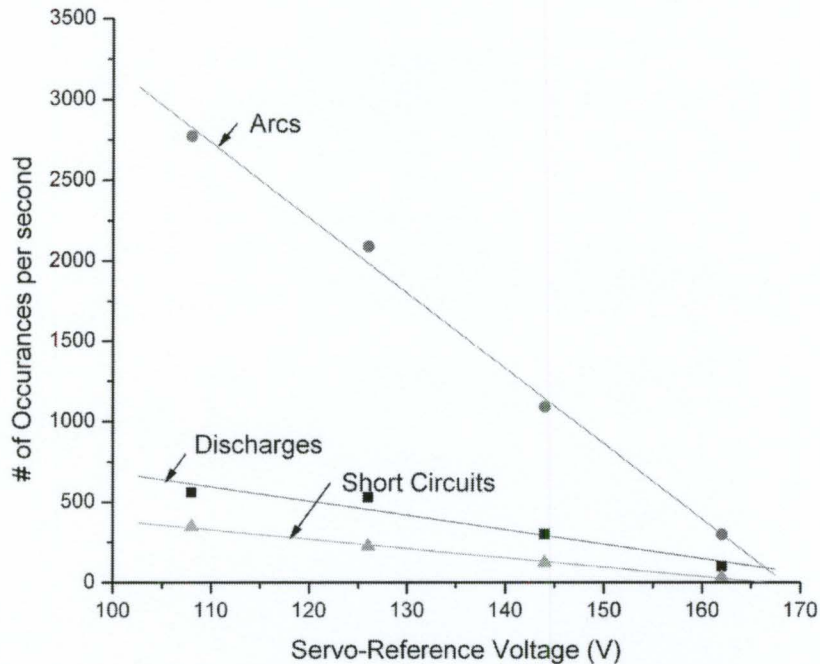


Figure 4.43: Waveform analysis for AWEDM ($I=2.4$)

The variation in the frequency of each type of discharge class is significant with respect to the servo-reference voltage, as is shown. The effect of the peak discharge current however is not as dramatic. In conventional WEDM, the discharge current does not greatly affect the discharge classification. In comparing AWEDM with WEDM, there is not much difference in the number of successful discharges or shorts, the frequency of arcing however, increases quite significantly as is shown in Figure 4.44. This is likely due an increase in EDM debris under limited flushing conditions.

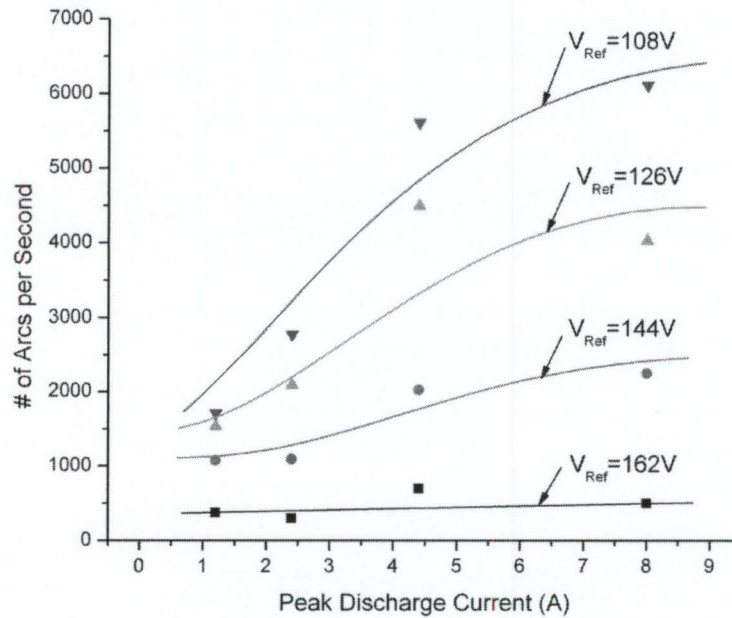


Figure 4.44: Arcing frequency in AWEDM with increasing discharge current

Clearly, the addition of abrasion to the WEDM process influences the EDM component of the hybrid process. The increased frequency of arcing is likely the most significant factor that will limit the amount of abrasion that can be applied in the process. Only a limited analysis of this sort has been presented for the work herein, though the effects shown here should be considered in future process development.

4.5 Related Discussion

Thus far, experimental results pertaining to the AWEDM process have been presented. In this section, a discussion of the mechanism for material removal in AWEDM is presented with an economic analysis to substantiate the feasibility for practical use of the process.

4.5.1 Mechanism for the Increase of Material Removal Rates in AWEDM

In developing AWEDM, it is important to understand how the dramatic improvements in MRR have been achieved. From the preceding analysis and discussion, it is

clear that the benefit is a result of abrasion; however, the mechanism for and limits to this assistance have not yet been studied.

In AECG for example, material is removed due to abrasion and electrochemical dissolution. This combination provides true synergy, as the abrasion process actually improves conditions for electrochemical dissolution to occur by removing the passivation layer. In AWEDM, apart from the thermal softening of the workpiece aiding the abrasion, no such synergy exists. This implies that both mechanisms remove material independently. If the material removal mechanisms are independent, it follows that the overall material removal rate should be the sum of those of constituent processes, assuming they do not negatively affect each other.

The absolute value of the material removal rates obtained during testing, regardless of the percent increase over WEDM, are much lower than those that are achievable on a dedicated WEDM machine. This fact puts the potential benefit into question. For the process to be economical, the addition of the abrasion component must be capable of substantially increasing the material removal rates obtainable in WEDM today. The following analysis estimates the maximum achievable material removal due to abrasion, and compares with typical removal rates achievable in WEDM.

To estimate the maximum material removal rates for an abrasive process, one can consider the amount of material that corresponds to the chip space in the wire. Figure 4.45 shows a simplified schematic of an abrasive surface. To analyze the case of an abrasive wire, the width of this surface is specified as the half of the perimeter of the wire; as only half of the wire is engaged in cutting. The length is left as unit length to calculate the removal rate per length of wire.

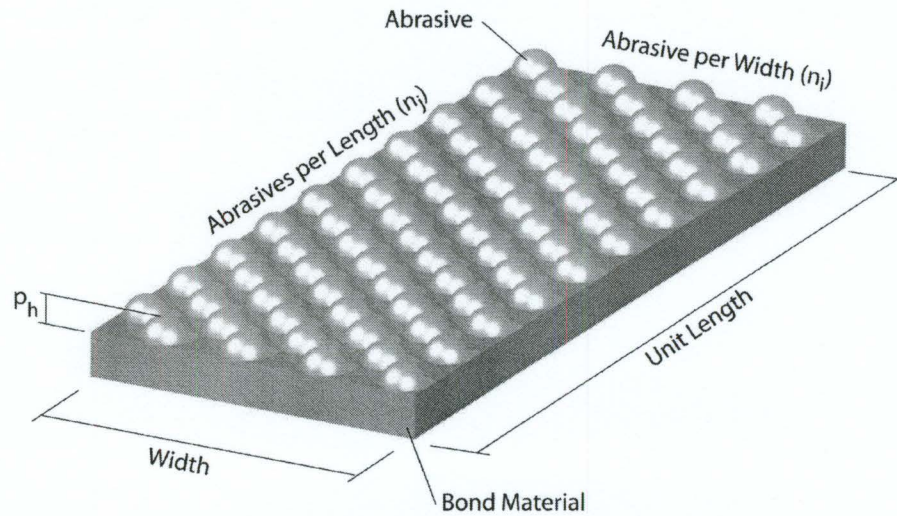


Figure 4.45: Schematic of a simplified abrasive surface

To further simplify the geometry, the abrasives are modeled as spheres protruding from the bond by 40% of their diameter, which was the mean protrusion height, P_h , as determined in Section 4.2. Knowing the geometry, the volume for machined material to accumulate can be calculated as:

$$V_{Debris} = k(V_P - V_A) \quad (4.8)$$

Where k , is the packing density of the debris and V_P is the potential volume given by:

$$V_P = Width * Length * P_h \quad (4.9)$$

and the V_A is the volume of abrasives:

$$V_A = \sum_1^n V_{A_i} \quad (4.10)$$

where n is the number of abrasives on the surface and V_{A_i} is the volume of a single abrasive.

Since the abrasives are modeled as spheres, the protruding volume is that of a dome which is given by:

$$V_{A_i} = \pi \frac{p_h}{6} (3R'^2 + p_h^2) \quad (4.11)$$

$$R' = \sqrt{2p_h r_a - p_h^2} \quad (4.12)$$

where r_a is the nominal radius of the abrasive grain.

The number of abrasive on the surface is calculated simply by dividing each the length and the width by the diameter of the abrasives. This gives the number of rows, n_j , and columns, n_i , of abrasives. Since the abrasives do not generally cover the entire surface, they are assumed here to be staggered. The number of abrasives, n , is thus:

$$n = \frac{n_i * n_j}{2} \quad (4.13)$$

Using the value for the wire used in testing, an abrasive size of $50\mu\text{m}$ is used with a wire diameter of $250\mu\text{m}$. Under this configuration, the wire has approximately 80 abrasives per millimeter of wire length.

The potential volume is:

$$V_p = 7.840 \frac{\text{mm}^3}{\text{m}} \quad (4.14)$$

The abrasive volume is:

$$V_A = 4.356 \frac{\text{mm}^3}{\text{m}} \quad (4.15)$$

and the volume available for accommodating debris is:

$$V_{Debris} = 3.484 * k \frac{\text{mm}^3}{\text{m}} \quad (4.16)$$

The material removal rate due to abrasion is thus:

$$MRR_{abr} = 3.484 * k * v_w \frac{\text{mm}^3}{\text{min}} \quad (4.17)$$

where v_w is the wire speed in metres/minute.

To compare this with typical WEDM removal rates, it is converted to an areal material removal rate by dividing by the kerf thickness of 0.29 mm:

$$AMRR_{abr} = 12.014 * k * v_w \frac{\text{mm}^2}{\text{min}} \quad (4.18)$$

Typical maximum material removal rates reported for WEDM range between 300 mm^2/min in D2 Steel to 750 mm^2/min in Aluminum [3]. Though these speeds are rarely reached in practice, 300 mm^2/min will be used here for comparison purposes. The benefit that is to be obtained by abrasion is directly related to the wire speed as shown in Equation (4.18). If wire speeds on the high end of those typically used in WEDM today were used in AWEDM, 10m/min for example, and a packing density of 50%, $k=0.5$, were used, the material removal rate due to abrasion would at most be 60 mm^2/min . This corresponds to a cutting speed that is 120% of that for WEDM alone. Though these are not nearly the improvements obtained during testing, this is still a significant increase in terms in productivity. If the addition of abrasion is applied to a process where such high material removal rates are not possible, the benefit of the process increases dramatically. Applying the same level of abrasion WEDM rates of 40 mm^2/min that might be typical in machining of PCD, an increase to 250% of the speed for WEDM alone is achievable [78].

4.5.2 Economic Feasibility

For any new process to be viable it must not only offer distinct advantages over existing processes such as increases in productivity, it must also be economically viable. For the process in question, the benefits in material removal rates and reduced recast layer are remarkable. This section serves to establish the economic feasibility of the process through a cost/savings analysis.

The typical mindset for determining whether a change in a process is economical is based upon the rule “double the cost – double the productivity.” This rule however rarely holds true, and many people miss potentially profitable changes as such. To fully determine whether a process should or should not be implemented would require a specialized analysis by the company in question. A more generalized analysis is performed here with the cost factors as described in Table 4.12.

Table 4.12: Description of the factors included in the analysis

<i>Variable</i>	<i>Description</i>
Machine Center Cost	Hourly cost to run the machine center not including wire costs. This ranges due to equipment type, age, labour and accounting practices
Base Cost	The base cost used for comparison and includes machine center cost and standard wire cost
Speed Ratio	The ratio of cutting speed for AWEDM to conventional WEDM (MRR_{AWEDM}/MRR_{WEDM})
Time Cost	Machine center cost divided by the speed ratio. (For example; if a one-hour job is cut 3 times faster, only 1/3 of the machine time is required.)
Wire Cost	Cost of the new wire per hour divided by the speed ratio. (For example; if a job is done in 1/3 the time, only 1/3 the wire is used.)
Savings	Potential job savings for using the new wire and is calculated as: $Base\ Cost - (Time\ Cost + Wire\ Cost)$

By varying machine center costs, speed ratios and cost per metre of the abrasive wire, a wide range of results are obtained. In this analysis, a base wire cost, for a conventional stratified wire, of \$19.00/kg or \$0.012/m is used. Based upon experimental results and the discussion in the previous section, a wire speed of 6 m/min is used and the speed ratio is varied from 2-6. Figure 4.46 shows the potential job savings in using the abrasive wire at its current cost of approximately \$0.80 /metre.

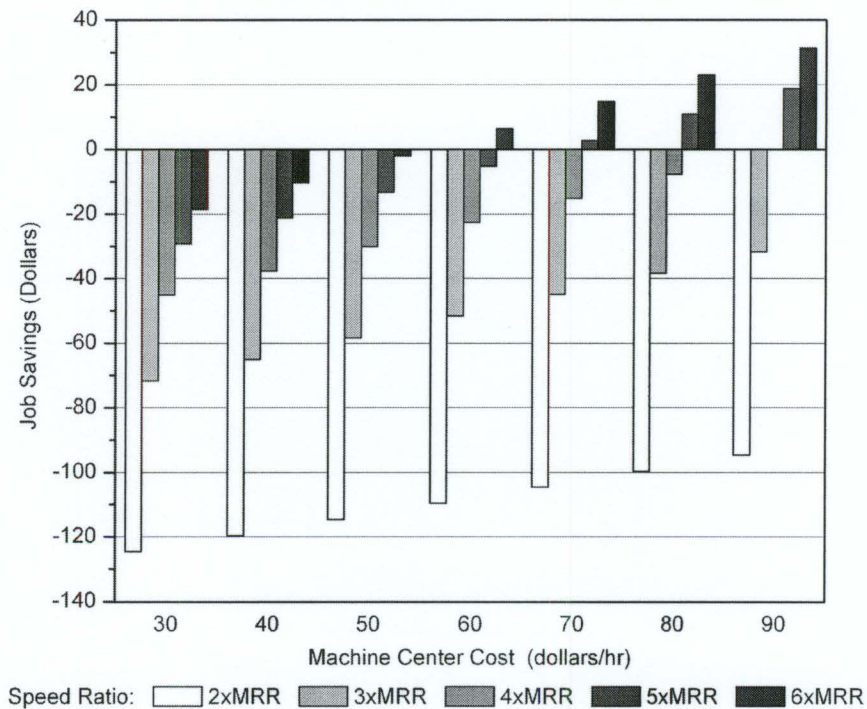


Figure 4.46: Job savings with abrasive wire at \$0.80/metre

Clearly, the use of AWEDM is not economical under most conditions at current wire costs. At high base machine costs however, the process does yield savings when the speed ratio is above four. To render the process more viable, a reduction in wire cost is required. This could be achieved either by replacing the diamonds abrasives with a less expensive material or by economies of scale, if wire demand increases substantially. Figure 4.47 shows the potential job savings if the wire cost is halved to \$0.40/metre.

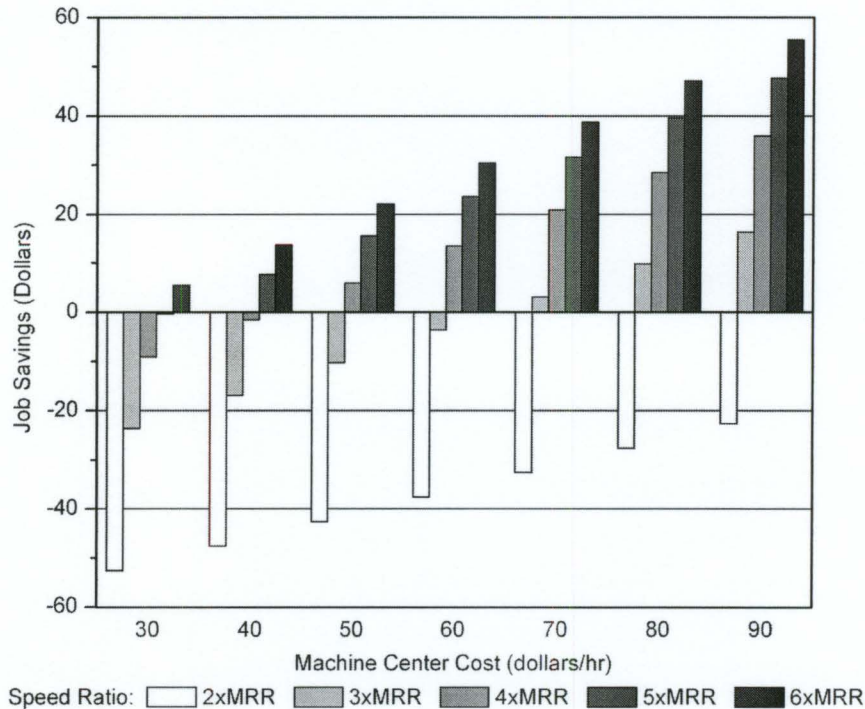


Figure 4.47: Job savings with abrasive wire at \$0.40/metre

Despite an over 30 times increase in cost from the base wire at \$0.012/m to the abrasive wire priced at \$0.40/m, AWEDM can become cost effective on a mid-level machine if 3 times the productivity achieved. Any further decrease in the abrasive wire cost would lead to dramatic savings especially on high-end machine centers.

In the preceding sections a simple geometric analysis has shown that the addition of abrasion can significantly improve upon even the highest removal rates obtainable today and that AWEDM may best lend itself to improving processes where material removal rates by WEDM are low such as in machining of metal matrix composites. Further, the benefit of the process is directly related to the wire speed as shown in Equation (4.18), which allows for drastic increases in MRR, if the added cost of the wire is not prohibitive. An economic analysis has shown that the increased cost of using an abrasive wire can be offset by the increase in

MRR. The potential benefits discussed here do not however take into account the reduction of the recast layer thickness, which would reduce or possibly eliminate the need for expensive, post-EDM polishing.

Through the experimental results and discussion presented in this Chapter, the concept of combining abrasion and WEDM has been proven. Analysis of material removal rates, cutting forces, recast layer, machining debris and machined surfaces have all testified to the simultaneous action of the two processes. A discussion based on the combined process and its economic feasibility has shown the process to be viable, and that substantial savings could be achieved if employed in a practical setting. The work presented here touches on the various aspects of the process that are critical to its success. A review and brief discussion of these results as well recommendations for areas of future research are presented in Chapter 5.

Chapter 5

Conclusions and Future Work

As a first work in the field of AWEDM, relevant literature, details of the process operation, design, and experimental work have been presented. A brief summary as well as conclusion on the contributions in this work are presented here with a discussion on some of the future work that might be conducted with respect to AWEDM.

5.1 Conclusions

The requirement for new approaches to improve upon machining performance has seen the development of various Hybrid Machining Processes. With only incremental improvements to WEDM over the past decade, a new approach was required. In order to improve upon both material removal rate and the quality of the machined surface, two responses that are typically mutually exclusive, the concept of an abrasion assisted WEDM process, termed AWEDM, has been presented. The process is realized by adopting the abrasive wire tool, used in fixed abrasive wire sawing, into the WEDM process. The current use of diamond grains is functional, in that the abrasives are electrically non-conducting, but not ideal. In terms of process economics, the use of a less expensive abrasive will help to render the process more viable. The replacement of diamond is likely acceptable even in machining of ultra-hard materials such as PCD, as the abrasives are engaged in machining a softened matrix material.

The experimental results presented in Chapter 4 indicate dramatic increases in material removal rates, as high as 1000%, due the addition of abrasion. The absolute values for the removal rate obtained in testing were however very low in comparison to those achievable on a dedicated WEDM machine tool. These comparably low values are a result of the

significant difference between generator designs used WEDM and die-sinker machines. Typical discharge durations used in WEDM are on the order of $0.5 \mu\text{s}$ with discharge currents as high as 1000 A. In contrast, the die-sinker used is capable of a max current of 72 A with a rise time of only $\sim 30 \text{ A}/\mu\text{s}$, requiring longer discharge durations to obtain reasonable cutting speeds.

The reduction of the recast layer is an additional benefit obtained due to the enhanced material removal rates. This reduction provides a distinct advantage over the conventional WEDM process that produced machined surfaces plagued with micro-cracks. This benefit alone opens up possible applications such as in the aerospace industry where surface quality is crucial or in the mould industry where the reduction of post-EDM polishing time provides significant savings.

In proving the concept of the process, the ability to control the proportion of EDM to abrasion was of key interest. By varying process parameters such as the servo-reference voltage and the discharge current, the process was shown to be consistent and easily controlled. An increase of either parameters results in a larger machining gap, thus reducing the abrasion component. The ability to control the process as such provides future users of the process the ability to tune the parameters such that their specific requirements are met.

The presence of machining forces in AWEDM is an important consideration when it comes to the accuracy of the process. Forces in the process were shown to vary with the extent of abrasion, and were measured to be as high as 2 N during aggressive machining. The application of forces to the wire during testing produced wire deflections that would be problematic when machining of contoured profiles. Adaptive control techniques as are used in WEDM could be employed with AWEDM to overcome this limitation. In practical use, the wire tension could also be higher than is typically used in WEDM, thereby reducing the wire bow.

Economics are extremely important to the manufacturing industry. As global markets continue to open and competition increases, the need for more economical manufacturing methods too increases. By examining the material removal mechanism in the hybrid process,

the overall material removal rates has been shown to be a superposition of the removal rates from the part processes. As removal rates due to WEDM increase, the benefit of abrasion becomes less significant. In using AWEDM for the machining of metal matrix composites such as PCD, however, has shown potential increases in material removal rates of approximately 250 %. An increase in the removal rates alone is not sufficient to deem process economical, as the cost of abrasive wire is high in comparison to conventional WEDM wire. For this, an economic analysis to determine whether the increased wire cost can be offset by improved machining rates has shown that, even with the present high cost of abrasive wire, the process could produce savings. If wire costs were reduced to half, dramatic savings could be achieved under even modest improvements in material removal. If AWEDM sees widespread use, wire costs should decrease dramatically due to both the use of a specially designed wire and economies of scale.

5.2 Future Work

As this is the first body of work relating the AWEDM, there remains a significant body of work to be completed. The development of a machine tool, either dedicated or modified, that is capable of accepting an abrasive wire and supplying electrical contact is critical to all future work in the field.

5.2.1 Practical Implementation

As discussed previously, the process could be employed on a conventional WEDM machine tool that has been modified to accept the use of abrasive wire. A review of some of the modifications that might be implemented is presented here.

In WEDM, the wire is positioned with respect to the workpiece and guided along its axis with the aid of stationary wire guides. It is also desirable in WEDM to supply the electrical power to the wire through electrical contacts in said guides. For implementation of AWEDM, the use of an abrasive wire will cause rapid deterioration of both the wire guides and the

electrical contacts due to severe abrasion. To overcome these limitations different solutions are possible.

To use existing wires, which are coated with abrasives along the entire periphery of the wire, the use of rollers as used on the experimental apparatus might be used. Figure 5.1 shows a schematic of this implementation.

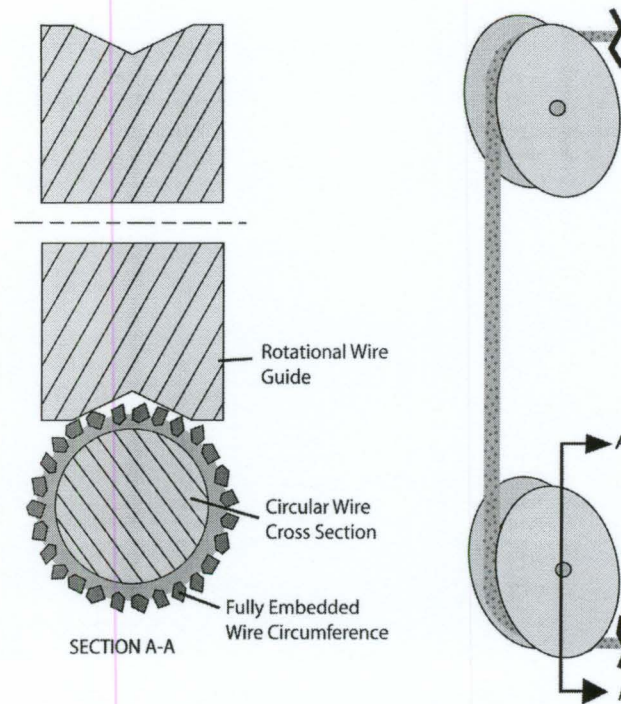


Figure 5.1: Schematic of current abrasive wire with rotational wire guides

By guiding the wire with rollers, relative motion between the wire and the guides is minimized. Rollers however, only provide guidance in the radial direction of the roller, thus requiring a more complex control system that orients either the wire guide or workpiece with respect to the cutting direction. The use of rollers does not provide a solution for making electrical contact with the wire. Just as the non-conductivity of the abrasives serves to isolate the core from the workpiece, they also isolate the wire core from the generator power. To overcome this, the application of electrical power may be accomplished by various means such

as the use of liquid-metal coupling (such as mercury or other low melting temperature metals), electrolytic coupling or conductive consumable brushes.

In an alternate solution, the development of a specially suited wire that would have abrasives only partially embedded along the wire circumference would be employed as shown in Figure 5.2. Further, the wire cross-section may be of circular, polygonal or semi-polygonal cross section. The sector of the wire that is free of abrasives can thus be used to supply electrical power to the wire core without abrading the electrical contacts. The polygonal shape is utilized to locate and guide the wire along its axis for improved precision.

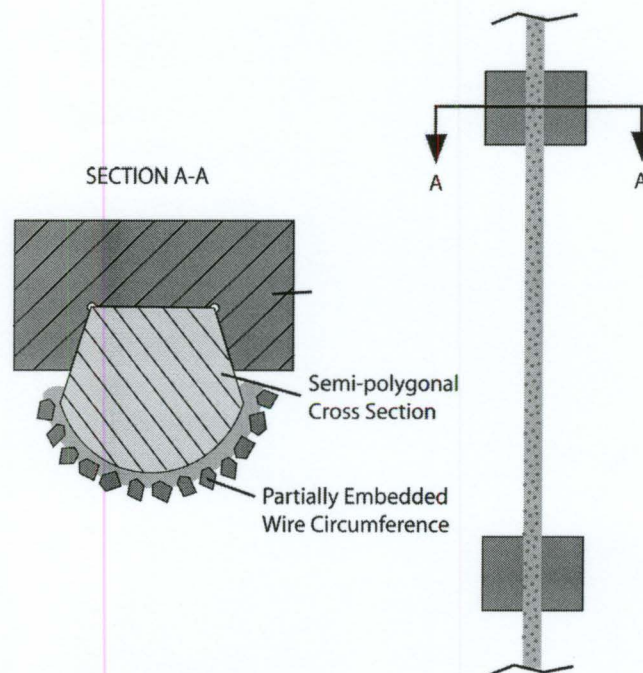


Figure 5.2: Schematic of partially coated wire with non-circular cross section and stationary wire guides

In implementing a specially designed wire with abrasives only partially embedded along the wire circumference, it is essential to orient the wire and the workpiece such that the machined surface or specifically, the instantaneous feed direction is normal to the sector of the wire that is embedded with abrasives. As with the rollers, this may be accomplished by various

means such as the addition of a rotary axis on the wire guides allowing them to be rotated to match the required feed direction.

The design of a suitable wire is discussed is of particular interest for various reasons. Apart from the rationale for a special wire as previously discussed, the use of higher wire tensions to minimize deflection under machining forces should be considered. If higher tensions are to be used, the wire must be capable of sustaining that tension. The wire currently used is sufficient in sustaining the wire tension, as it is comprised of a high strength steel core, though a wire that is specially designed for AWEDM should consider not only strength, but also the ability of the wire to withstand the EDM conditions. As was shown, the currently available wire becomes brittle after use, limiting the useable process parameters. Composite wires with high tensile strength cores, similar in design to those outlined by Kruth et al. [20] might provide the best results for use in AWEDM.

5.2.2 Areas for Future Research

There are numerous areas of both experimental and analytical research to be studied. Further experimental work on the effect of process parameters will help to understand the interactions in the process. Increasing the axial wire speed, for example, should provide an increase in material removal rate, but to what limit, and what effect does this have on the EDM aspect of the process? The effect of changing the EDM parameters too could have a great impact on the process as the degree of thermal softening is directly controlled by these parameters. A deeper analysis in this regard will provide a deeper understanding and make it possible to optimize the process for a given application.

The possible applications of the process are also key areas of interest. For example, for which materials will the process provide the greatest benefit? The machining of silicon wafers by EDM or wire sawing individually is a time consuming and expensive task, as both approaches have their limitations. In combining AWEDM to machine silicon wafers, a dramatic improvement may be possible.

The machining of PCD too has limitations when either grinding or EDM alone are applied. In grinding, very low G ratios are obtained, rendering the process expensive. Material removal rates in EDM are limited as the diamond particles in the cobalt matrix are non-conductive. By employing the hybrid process, both of these limitations can be overcome. The EDM component serves to ease the material removal by abrasion, while the abrasion component simultaneously improves upon EDM by removing the non-conducting diamond particles. This same principle may apply to the machining of all metal-matrix composites.

The desire to eliminate environmentally hazardous fluids from machining process has led to the development of Dry EDM and Dry WEDM [1,22,79]. These processes are currently limited in their effectiveness due to the increased electrical shorting because of wire vibration, and poor surface quality due to the re-adherence of EDM debris to the machined surface. The use of the hybrid process has the potential to solve both of these issues as the abrasive particles will serve to electrically isolate the workpiece and wire core, and the abrasive action will serve to remove the EDM debris and recast layer.

References

- [1] M. Kunieda, B. Lauwers et al, Advancing EDM through fundamental insight into the process, *Annals of the CIRP* 54(2) (2005) 599-622
- [2] K.H. Ho, S.T. Newman, State of the art in electrical discharge machining (EDM), *International Journal of Machine Tools and Manufacture* 43(13) (2003) 1287-1300
- [3] K.H. Ho, S.T. Newman et al, State of the art in wire electrical discharge machining (WEDM), *International Journal of Machine Tools and Manufacture* 44(12-13) (2004) 1247-1259
- [4] F. Han, J. Jiang, D. Yu, Influence of discharge current on machined surfaces by thermo-analysis in finish cut of WEDM, *International Journal of Machine Tools and Manufacture* 47(7-8) (2007) 1187-1196
- [5] J.P. Kruth, L. Stevens et al, Study of the white layer of a surface machined by die-sinking electro-discharge machining, *Annals of the CIRP* 44(1) (1995) 169-172
- [6] C.W. Hardin, J. Qu, A.J. Shih, Fixed abrasive diamond wire saw slicing of single-crystal silicon carbide wafers, *Materials and Manufacturing Processes* 19(2) (2004) 355-367
- [7] P. Dumitrescu, P. Koshy et al, High-power diode laser assisted hard turning of AISI D2 tool steel, *International Journal of Machine Tools and Manufacture* 46(15) (2006) 2009-2016
- [8] Cross Process Innovations, Columbia University. *Electronic Reference*. Retrieved 2-10-2007, from www.mrl.columbia.edu/ntm/CrossProcess/CrossProcessindex.htm
- [9] Trends in EDM, Moser, C. and Boehmert, B., MMS Online. *Electronic Reference*. Retrieved 2-10-2007, from www.mmsonline.com/articles/020001.html
- [10] B.M. Schumacher, After 60 years of EDM the discharge process remains still disputed, *Journal of Materials Processing Technology* 149(1-3) (2004) 376-381
- [11] T.H. Lee, T-F Theory of Electron Emission in High-Current Arcs, *Journal of Applied Physics* 30(2) (1959) 166-171

- [12] S. Hayakawa, M. Takahashi et al, Study on EDM phenomena with in-process measurement of gap distance, *Journal of Materials Processing Technology* 149(1-3) (2004) 250-255
- [13] D.K. Aspinwall, R.C. Dewes et al, Electrical discharge surface alloying of Ti and Fe workpiece materials using refractory powder compact electrodes and Cu wire, *Annals of the CIRP* 52(1) (2003) 151-156
- [14] A.B. Puri, B. Bhattacharyya, Modeling and analysis of white layer depth in a wire-cut EDM process through response surface methodology, *International Journal of Advanced Manufacturing Technology* 25(3-4) (2005) 301-307
- [15] H. Ramasawmy, L. Blunt, K.P. Rajurkar, Investigation of the relationship between the white layer thickness and 3D surface texture parameters in the die sinking EDM process, *Precision Engineering* 29(4) (2005) 479-490
- [16] G. Cusanelli, A. Hessler-Wyser et al, Microstructure at submicron scale of the white layer produced by EDM technique, *Journal of Materials Processing Technology* 149(1-3) (2004) 289-295
- [17] J. Simao, H.G. Lee et al, Workpiece surface modification using electrical discharge machining, *International Journal of Machine Tools and Manufacture* 43(2) (2003) 121-128
- [18] N.M. Abbas, D.G. Solomon, F. Bahari, A review on current research trends in electrical discharge machining (EDM), *International Journal of Machine Tools and Manufacture* 47(7-8) (2007) 1214-1228
- [19] D.F. Dauw, L. Albert, S.A. Meyrin, About the evolution of wire tool performance in wire EDM, *Annals of the CIRP* 41(1) (1992) 221-225
- [20] J.P. Kruth, B. Lauwers et al, Composite wires with high tensile core for wire EDM, *Annals of the CIRP* 53(1) (2004) 171-174
- [21] M. Kunieda, T. Takaya, S. Nakano, Improvement of dry EDM characteristics using piezoelectric actuator, *Annals of the CIRP* 53(1) (2004) 183-186
- [22] M. Kunieda, C. Furudate, High precision finish cutting by dry WEDM, *Annals of the CIRP* 50(1) (2001) 121-124

- [23] M. Kunieda, M. Yoshida, Electrical discharge machining in gas, *Annals of the CIRP* 46(1) (1997) 143-146
- [24] M. Kunieda, H. Muto, Development of Multi-spark EDM, *Annals of the CIRP* 49(1) (2000) 119-122
- [25] W.Y. Peng, Y.S. Liao, Study of electrical discharge machining technology for slicing silicon ingots, *Journal of Materials Processing Technology* 140(1-3) (2003) 274-279
- [26] W.I. Clark, A.J. Shih et al, Fixed abrasive diamond wire machining - part I: process monitoring and wire tension force, *International Journal of Machine Tools and Manufacture* 43(5) (2003) 523-532
- [27] Hardin, C. W., *Fixed Abrasive Diamond Wire Saw Slicing of Single Crystal SiC Wafers and Wood*, 2003, M.A.Sc. Thesis, North Carolina State University
- [28] J. Sugawara, H. Hara, A. Mizoguchi, Development of Fixed-Abrasive-Grain Wire Saw with Less Cutting Loss, *SEI Technical Review* 58 (2004) 7-11
- [29] H.J. Moller, Basic Mechanisms and Models of Multi-Wire Sawing, *Advanced Engineering Materials* 6(7) (2004) 501-513
- [30] M. Bhagavat, V. Prasad, I. Kao, Elasto-hydrodynamic interactions in the free abrasive wire slicing using a wire saw: Modelling and finite element analysis, *ASME Journal of Tribology* 122(2) (2000) 394-404
- [31] S. Wei, I. Kao, Vibration Analysis of Wire in Free Abrasive Machining of the Modern Wiresaw Manufacturing Process, *Journal of Sound and Vibration* 231 (2000) 1383-1395
- [32] L. Zhu, I. Kao, Galerkin-based modal analysis on the vibration of wire-slurry system in wafer slicing using a wiresaw, *Journal of Sounds and Vibration* 283 (2005) 589-620
- [33] F.Q. Yang, I. Kao, Free abrasive machining in slicing brittle materials with wiresaw, *Journal of Electronic Packaging* 123(3) (2001) 254-259
- [34] J. Sugawara, A. Yamakawa, A. Mizoguchi, Development of Fixed-Abrasive Grain Wire Saw, *SEI Technical Review* 157 (2000) 119

- [35] P.L. Tso, B.H. Yan, C.H. Lo, Study on thin diamond wire slicing with Taguchi method, *Materials Science Forum* 505-507 (2006) 1219-1224
- [36] D. Ide, Resin bond diamond wire for slicing ceramics, *Industrial Diamond Review* 67(613) (2007) 32-34
- [37] J. Ehrhardt, Composite electroplating by using brush technique, *Industrial & Engineering Chemistry Product Research and Development* 24(4) (1985) 575-578
- [38] Y. Chiba, Y. Tani et al, Development of a high-speed manufacturing method for electroplated diamond wire tools, *Annals of the CIRP* 52(1) (2003) 281-284
- [39] Y. Li, G. Li et al, New type of matrix material for the manufacture of electroplated diamond tools, *Industrial Diamond Review* 62(595) (2002) 259-262
- [40] W.I. Clark, A.J. Shih et al, Fixed abrasive diamond wire machining - part II: experiment design and results, *International Journal of Machine Tools and Manufacture* 43(5) (2003) 533-542
- [41] M. Mizuno, T. Iyama et al, Development of a Device for Measuring the Transverse Motion of a Saw-Wire, *Journal of Manufacturing Science and Engineering* 128(3) (2006) 826-834
- [42] H.K. Tonshoff, T. Friemuth, H. Hillmann-Apmann, Diamond wire sawing of steel components, *Industrial Diamond Review* 61(590) (2001) 203-208
- [43] G.L. Biasco, F. Barana, Robotwire Stone Profiling System, *Industrial Diamond Review* 51(546) (1991) 242-242
- [44] G.L. Biasco, Contouring with Diamond Wire, *Industrial Diamond Review* 54(562) (1994) 114-116
- [45] H. Gebhard, W. Macht, Innovative nickel stripping technique for diamond tools, *Industrial Diamond Review* 59(583) (1999) 303-303
- [46] P.T. Pajak, A.K.M. Desilva et al, Precision and efficiency of laser assisted jet electrochemical machining, *Precision Engineering* 30(3) (2006) 288-298

- [47] J. Kozak, K.E. Oczos, Selected problems of abrasive hybrid machining, *Journal of Materials Processing Technology* 109(3) (2001) 360-366
- [48] H. El-Hofy, *Advanced Machining Processes, Nontraditional and Hybrid Machining Processes*, McGraw-Hill, United States, 2005
- [49] K.P. Rajurkar, D. Zhu et al, New developments in electro-chemical machining, *Annals of the CIRP* 48(2) (1999) 567-579
- [50] B. Nowicki, R. Pierzynowski, S. Spadlo, The superficial layer of parts machined by brush electro-discharge mechanical machining (BEDMM), *Journal of Engineering Manufacture* 218(Pt. B) (2004) 9-15
- [51] R. Singh, J.S. Khamba, Ultrasonic machining of titanium and its alloys: A review, *Journal of Materials Processing Technology* 173(2) (2006) 125-135
- [52] E.P. DeGarmo, J.T. Black, R.A. Kohser, *Materials and Processes in Manufacturing*, 8th Ed., John Wiley & Sons, Inc., United States, 1999
- [53] D. Kremer, J.L. Lebrun et al, Effects of Ultrasonic Vibrations on the Performances in EDM, *Annals of the CIRP* 38(1) (1989)
- [54] Yan Cherng Lin, Machining characteristics of titanium alloy (Ti±6Al±4V) using a combination process of EDM with USM, *Journal of Materials Processing Technology* 104 (2000) 171-177
- [55] Y.C. Lin, B.H. Yan, Y.S. Chang, Machining characteristics of titanium alloy (Ti±6Al±4V) using a combination process of EDM with USM, *Journal of Materials Processing Technology* 104 (2000) 171-177
- [56] J. Kozak, Abrasive Electrodischarge Grinding (AEDG) of advanced materials, *Archives of Civil and Mechanical Engineering* 2(1-2) (2002) 83-101
- [57] E.Y. Grodzinskii, L.S. Zubatova, Electrochemical and Electrical-Discharge Abrasive Machining, *Soviet Engineering Research* 2(3) (1982) 90-92
- [58] P. Koshy, V.K. Jain, G.K. Lal, Mechanism of Material Removal in Electrical Discharge Diamond Grinding, *International Journal of Machine Tools and Manufacture* 36(10) (1996) 1173-1185

- [59] K. Suzuki, T. Uematsu, T. Nakagawa, On-machine Trueing/Dressing of Metal Bond Grinding Wheels by Electro-discharge Machining, *Annals of the CIRP* 36(1) (1987) 115-118
- [60] B.K. Rhoney, A.J. Shih et al, Wear mechanism of metal bond diamond wheels trued by wire electrical discharge machining, *Wear* 252(7-8) (2002) 644-653
- [61] N.K. Bezzubenko, *Cutting and Tooling*, Khar'kov Polytechnical Institute, Ukraine, 1974
- [62] E.Y. Grodzinskii, Grinding with electrical activation of the wheel cutting properties, *Machines and Tooling* 50(12) (1979) 10-13
- [63] P. Koshy, V.K. Jain, G.K. Lal, Grinding of cemented carbide with electrical spark assistance, *Journal of Materials Processing Technology* 72(1) (1997) 61-68
- [64] S.K. Choudhury, V.K. Jain, M. Gupta, Electrical Discharge Diamond Grinding of High Speed Steel, *Machining Science and Technology* 3(1) (1999) 91-105
- [65] K.M. Shu, G.C. Tu, Study of electrical discharge grinding using metal matrix composite electrodes, *International Journal of Machine Tools and Manufacture* 43(8) (2003) 845-854
- [66] V. Yadava, V.K. Jain, P.M. Dixit, Temperature distribution during electro-discharge abrasive grinding, *Machining Science and Technology* 6(1) (2002) 97-127
- [67] Z.N. Guo, M.Z. Chai et al, Study on Mechanical-electrochemical Machining with Wire-combined Tool, *Proceedings of the 15th International Symposium on Electromachining*, Pittsburgh PA USA, University of Nebraska-Lincoln (2007) 345-349
- [68] B. Stelter, EDM Apparatus and Method Incorporating Combined Electro-Erosion and Mechanical Sawing Features US Patent (6,737,602) (2004)
- [69] R. Snoeys, H. Cornelissen, K.U. Leuven, Correlation between Electro-Discharge Machining Data and Machining Settings, *Annals of the CIRP* 24(1) (1975) 83-88
- [70] J.A. Sanchez, L.N. Lopez de Lacalle et al, Study on gap variation in multi-stage planetary EDM, *International Journal of Machine Tools and Manufacture* 46(12-13) (2006) 1598-1603

- [71] R. Snoeys, F. van Dijck, Plasma Channel Diameter Growth Affects Stock Removal in EDM, *Annals of the CIRP* (1972) 39-40
- [72] H.-P. Schulze, R. Herms et al, Comparison of measured and simulated crater morphology for EDM, *Journal of Materials Processing Technology* 149(1-3) (2004) 316-322
- [73] G.N. Shah, A.C. Bell, S. Malkin, Quantitative characterization of abrasive surfaces using a new profile measuring system, *Wear* 41(2) (1977) 315-325
- [74] L. Blunt, S. Ebdon, The application of three-dimensional surface measurement techniques to characterizing grinding wheel topography, *International Journal of Machine Tools and Manufacture* 36(11) (1996) 1207-1226
- [75] J.F. Rahman, V. Radhakrishnan, Surface condition monitoring of grinding wheels by pneumatic back-pressure measurement, *Wear* 70(2) (1981) 219-226
- [76] D. Scott, On optimal and data-based histograms, *Biometrika* 66(3) (1979) 605-610
- [77] R.R. Hebbar, S. Chandrasekaar, T.N. Farris, Ceramic Grinding Temperatures, *Journal of the American Ceramic Society* 75(10) (1992) 2742-2748
- [78] G. Spur, S. Appel, Wire EDM cutting of PCD, *Industrial Diamond Review* 57(4) (1997) 124-130
- [79] Y.Z. Bo, M. Kunieda et al, High speed 3D milling by dry EDM, *Annals of the CIRP* 52(1) (2003) 147-150